Cell Stem Cell
Article

FoxO3 Regulates Neural Stem Cell Homeostasis

Valérie M. Renault,[1] Victoria A. Rafalski,[1,2] Alex A. Morgan,[3,6] Dervis A.M. Salih,[1] Jamie O. Brett,[1] Ashley E. Webb,[1] Saul A. Villeda,[1,2,7] Pramod U. Thekkat,[1] Camille Guillerey,[1] Nicholas C. Denko,[4] Theo D. Palmer,[5] Atul J. Butte,[3,6] and Anne Brunet[1,2,*]
[1]Department of Genetics
[2]Neurosciences Program
[3]Biomedical Informatics Program
[4]Department of Radiation Oncology
[5]Department of Neurosurgery
Stanford University, Stanford, CA 94305, USA
[6]Departments of Pediatrics and Medicine, Lucile Packard Children's Hospital, Stanford University, Stanford, CA 94304, USA
[7]Present address: 3801 Miranda Ave, VA Palo Alto, CA 94304
*Correspondence: anne.brunet@stanford.edu
DOI 10.1016/j.stem.2009.09.014

SUMMARY

In the nervous system, neural stem cells (NSCs) are necessary for the generation of new neurons and for cognitive function. Here we show that FoxO3, a member of a transcription factor family known to extend lifespan in invertebrates, regulates the NSC pool. We find that adult *FoxO3*$^{-/-}$ mice have fewer NSCs in vivo than wild-type counterparts. NSCs isolated from adult *FoxO3*$^{-/-}$ mice have decreased self-renewal and an impaired ability to generate different neural lineages. Identification of the FoxO3-dependent gene expression profile in NSCs suggests that FoxO3 regulates the NSC pool by inducing a program of genes that preserves quiescence, prevents premature differentiation, and controls oxygen metabolism. The ability of FoxO3 to prevent the premature depletion of NSCs might have important implications for counteracting brain aging in long-lived species.

INTRODUCTION

Neural stem cells (NSCs) can self-renew and generate all three neural lineages of the nervous system: neurons, astrocytes, and oligodendrocytes. During embryonic and postnatal development, NSCs give rise to rapidly amplifying neural progenitors, which are responsible for the proper formation of the nervous system. The adult mammalian brain contains two residual populations of relatively quiescent NSCs in the subgranular zone (SGZ) of the dentate gyrus (DG) in the hippocampus and in the subventricular zone (SVZ) of the cortex (Alvarez-Buylla and Temple, 1998; Zhao et al., 2008). In the adult brain, the generation of new neurons (neurogenesis) from NSCs is thought to play an important role in learning and memory, spatial pattern separation, and odor discrimination (Clelland et al., 2009; Gheusi et al., 2000; Imayoshi et al., 2008). Both the number of NSCs and neurogenesis decline with age and this age-dependent decline is correlated with a gradual loss of cognitive and sensory functions (Bondolfi et al., 2004; Kempermann et al., 1998; Tropepe et al., 1997). Conversely, the pool of NSCs, neurogenesis, and cognitive performance in adults are preserved in a strain of long-lived mutant mice (Kinney et al., 2001; Sun et al., 2005). Thus, an intact pool of functional NSCs may be crucial for preserving cognitive functions throughout life.

The polycomb family member Bmi-1 has been recently found to play an important role in NSC self-renewal by negatively regulating the cell cycle inhibitor $p21^{CIP1}$ in embryonic NSCs (Fasano et al., 2007), and $p16^{INK4a}$ and $p19^{ARF}$ in adult NSCs (Molofsky et al., 2005, 2006). TLX, a nuclear receptor, also regulates NSC self-renewal during development and adulthood in a cell-autonomous manner (Zhang et al., 2008). Other mechanisms to regulate the self-renewal and multipotency of NSCs throughout life remain largely unknown, but one intriguing possibility is that genes that regulate lifespan in invertebrates may have evolved to control stem cell pools in mammals.

FoxO transcription factors are necessary for the extreme longevity of mutants of the insulin pathway in invertebrates (Kenyon, 2005). In humans, single-nucleotide polymorphisms in one of the four FoxO genes, *FoxO3*, have recently been associated with extreme longevity (Flachsbart et al., 2009; Willcox et al., 2008), raising the possibility that FoxO3 also regulates lifespan in mammals. FoxO factors can elicit a variety of cellular responses, including cell cycle arrest, differentiation, resistance to oxidative stress, and apoptosis (Salih and Brunet, 2008). FoxO factors have recently been found to regulate the self-renewal of adult hematopoietic stem cells (HSCs), primarily by providing resistance to oxidative stress (Miyamoto et al., 2007; Tothova et al., 2007). Whether and how FoxO transcription factors regulate NSCs is unknown.

FoxO transcription factors are inactivated in response to insulin or growth factors by phosphorylation by the protein kinase Akt, which results in their nuclear export (Salih and Brunet, 2008). Activation of the PI3K-Akt pathway, for example by ablation of the gene encoding the PTEN phosphatase, promotes the self-renewal of neural progenitor cells (Groszer et al., 2006; Li et al., 2002; Sinor and Lillien, 2004). However, the role of the PI3K-Akt pathway in the NSC pool in vivo has not been examined and the PI3K-Akt pathway has many other downstream targets in addition to FoxO factors.

Here we show that the transcription factor FoxO3, a member of a gene family that extends lifespan in invertebrates, is necessary for the regulation of the NSC pool in mice. We also identify

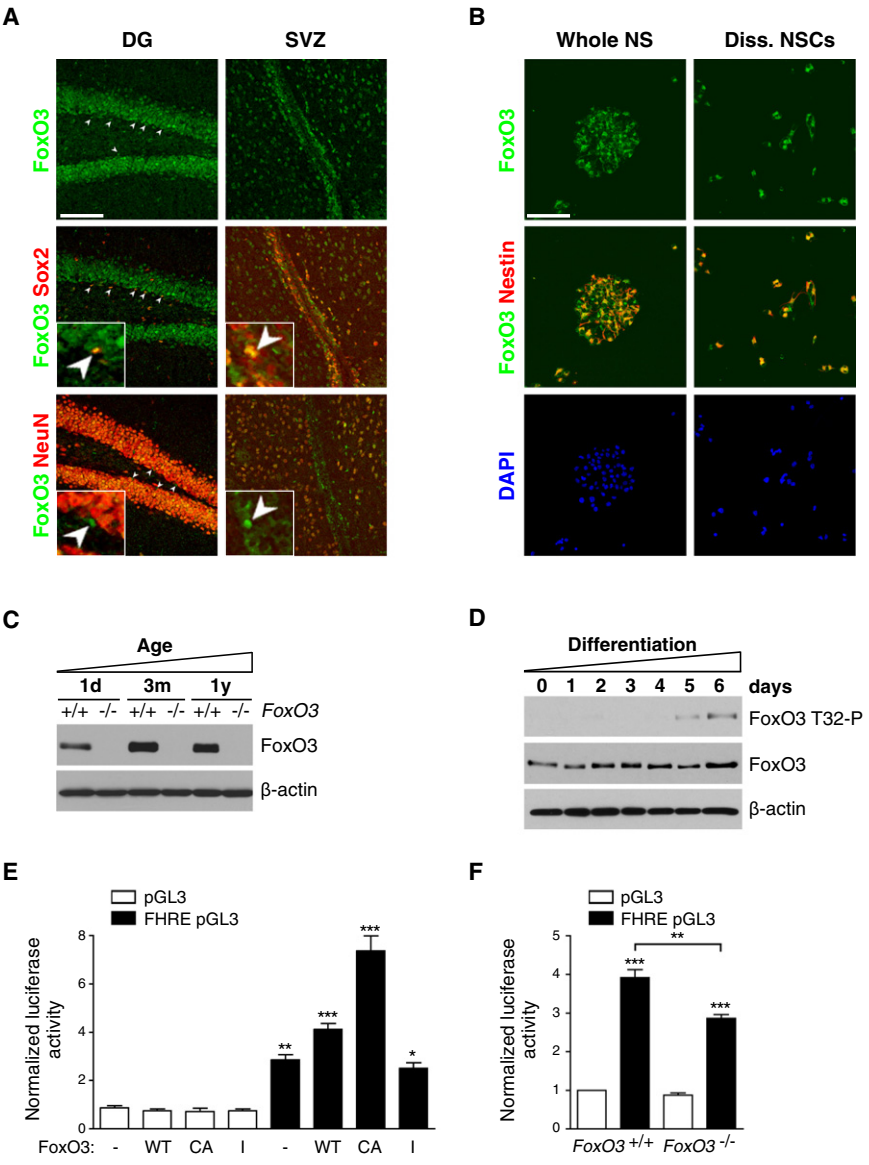

Figure 1. FoxO3 Is Expressed and Active in NSCs

(A) FoxO3 is expressed in adult NSCs in vivo. Immunohistochemistry on brain sections of 3-month-old mice with antibodies to FoxO3 ("Ct"), Sox2, and NeuN in the dentate gyrus (DG) of the hippocampus and in the subventricular zone (SVZ) of Sox2-positive/FoxO3-positive and NeuN-negative/FoxO3-positive nuclei are shown by white arrowheads. Higher magnification images are included. Scale bar represents 100 μm.

(B) FoxO3 is expressed in purified NSCs in culture. Immunocytochemistry on NSCs isolated from 3-month-old mice with antibodies to FoxO3 ("Ct") and to Nestin. DAPI was used to stain nuclei. NSCs were either grown as neurospheres (whole NS) (left) or freshly dissociated NSCs (Diss. NSCs) (right). Scale bar represents 100 μm.

(C) FoxO3 expression in NSCs at different ages. Western blots of protein lysates from secondary neurospheres in self-renewing conditions from *FoxO3*$^{+/+}$ and *FoxO3*$^{-/-}$ littermates at three different ages, 1-day-old (1d), 3-month-old (3m), and 1-year-old (1y), probed with antibodies to FoxO3 ("NFL") and to β-actin. The data presented are representative of three independent experiments.

(D) FoxO3 phosphorylation is increased in differentiated progeny. Western blots of protein lysates of dissociated wild-type adult NSCs in self-renewing conditions (day 0) or in differentiation conditions for increasing lengths of time (days 1–6) (Figure S3B). Western blots were probed with antibodies to FoxO3 ("NFL"), to Phospho-T32 (FoxO3 T32-P) and to β-actin. Blots representative of three independent experiments.

(E) A FoxO-dependent reporter gene is responsive to FoxO3 in NSCs. Luciferase assays in wild-type adult NSCs with a promoter containing three FoxO binding sites driving the luciferase reporter gene (FHRE pGL3) or a control promoter (pGL3) and FoxO3 expression vectors (minus sign, empty vector; WT, wild-type; CA, constitutively active; I, inactive). Values represent mean ± SEM from three independent experiments. One-way ANOVA, Bonferroni posttests, *$p < 0.05$, **$p < 0.01$, ***$p < 0.001$.

(F) Endogenous FoxO3 is active in self-renewing NSCs. Luciferase assays in *FoxO3*$^{+/+}$ and *FoxO3*$^{-/-}$ adult NSCs with FHRE pGL3 or control pGL3 as in (E). Values were normalized to the first column. Values represent mean ± SEM from three independent experiments. One-way ANOVA, Bonferroni posttests, **$p < 0.01$, ***$p < 0.001$.

the program of genes regulated by FoxO3 in NSCs. Our findings suggest that FoxO3 regulates the NSC pool by inducing a program that promotes quiescence, prevents premature differentiation, and controls oxygen metabolism. FoxO3's ability to regulate NSC homeostasis may protect normal cognitive function in organisms that live to an advanced age.

RESULTS

FoxO3 Is Expressed in Adult NSCs/Neural Progenitors In Vivo and In Vitro

To determine whether FoxO3 protein is expressed in NSC niches in the adult mouse brain, we used an antibody that recognized FoxO3 but did not significantly detect FoxO1, FoxO4, or FoxO6 in cells (Figures S1A–S1C available online). We stained brain sections of adult *FoxO3*$^{+/+}$ and *FoxO3*$^{-/-}$ mice with this antibody and found that FoxO3 is expressed in both the SGZ and the SVZ (Figure S2A). Western blotting experiments confirmed that FoxO3 is highly expressed in NSC niches in vivo (Figure S2B).

NSC niches contain NSCs, committed progenitors, and differentiated progeny. To determine whether FoxO3 is expressed in NSCs in vivo, we stained brain sections with antibodies to FoxO3 and to Sox2, a marker of NSCs/neural progenitors, or to NeuN, a marker of neurons (Figure 1A). These experiments revealed that FoxO3 is expressed in Sox2-positive cells in the SGZ and the SVZ (Figure 1A). FoxO3 is expressed in a subset of NeuN-negative cells (Figure 1A, bottom, white arrows) and in

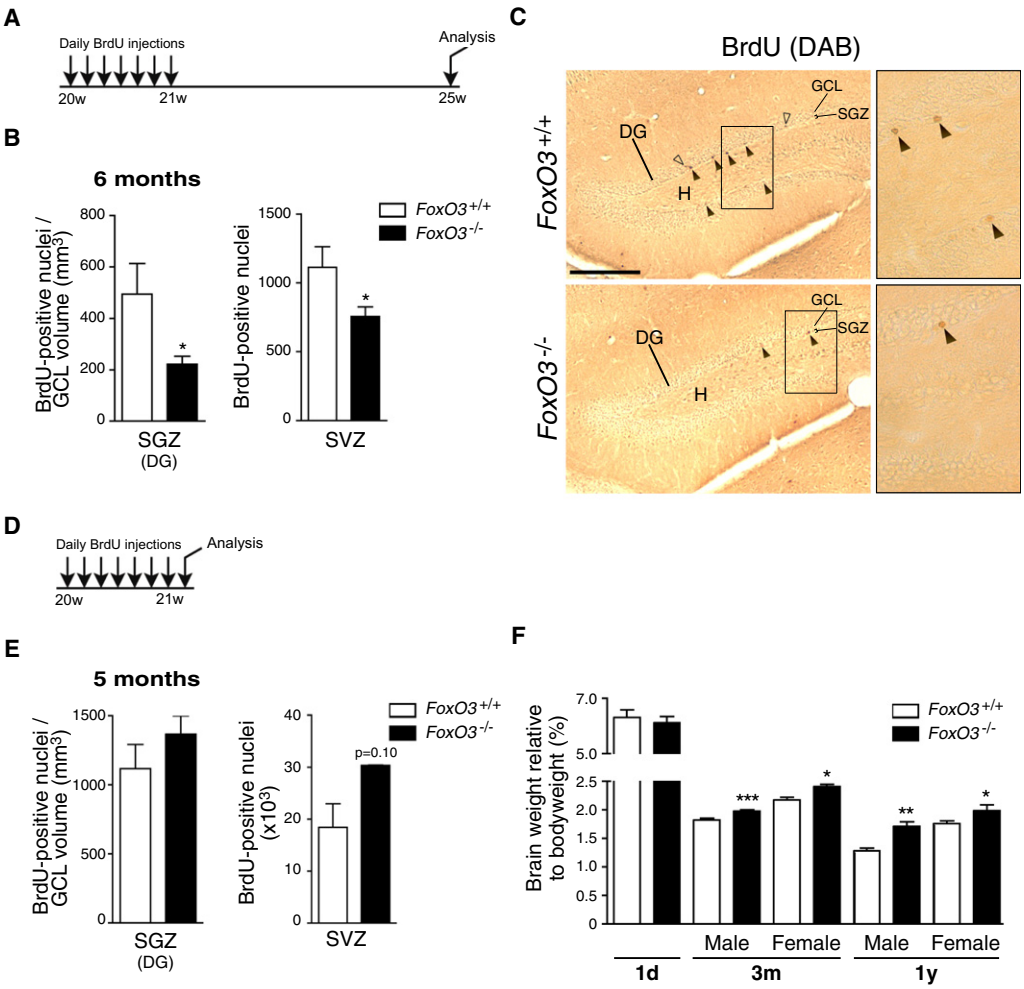

Figure 2. The Ablation of FoxO3 Results in a Decrease in NSC Number In Vivo

(A) Experimental design for the quantification of NSCs in vivo. 5-month-old *FoxO3*$^{+/+}$ and *FoxO3*$^{-/-}$ littermates were injected daily with BrdU for 7 days and sacrificed 1 month after the last BrdU injection.

(B) Quantification of label-retaining NSCs in vivo. Number of BrdU-positive cells 1 month after 7 days of daily BrdU injection in SGZ of the DG (left) and the SVZ (right, Figure S4A). The number of BrdU-positive cells in the SGZ was normalized to the volume of the granular cell layer (GCL) (Figure S4C). Values represent mean ± SEM (left) and mean ± SD (right) from five animals for *FoxO3*$^{+/+}$ and four animals for *FoxO3*$^{-/-}$ mice. Mann-Whitney test, *p < 0.05.

(C) Examples of label-retaining NSCs in the DG of *FoxO3*$^{+/+}$ and *FoxO3*$^{-/-}$ mice. Coronal sections of adult *FoxO3*$^{+/+}$ and *FoxO3*$^{-/-}$ mouse brains showing BrdU-positive nuclei in the SGZ 1 month after 7 days of daily BrdU injection. Filled arrowhead: label-retaining NSCs. Empty arrowhead: BrdU-positive cells that have migrated into the GCL. DG, dentate gyrus; H, hilus. Scale bar represents 200 μm. Right panels represent higher magnifications of the rectangles in the left panels.

(D) Experimental design for the quantification of proliferating NSCs and neural progenitors in vivo. 5-month-old *FoxO3*$^{+/+}$ and *FoxO3*$^{-/-}$ littermates were injected daily with BrdU for 7 days and sacrificed 1 day after the last BrdU injection.

(E) Quantification of proliferating NSCs and neural progenitors in vivo. Number of BrdU-positive cells in the SGZ (left) and in the SVZ (right) 1 day after 7 days of daily BrdU injection. The number of BrdU-positive cells in the SGZ was normalized to the GCL volume (Figure S4D). Values represent mean ± SEM (left) and mean ± SD (right) from three animals for each genotype. Mann-Whitney test, p = 0.40 (left) and p = 0.10 (right).

(F) Brain weight is increased in adult *FoxO3*$^{-/-}$ mice compared to *FoxO3*$^{+/+}$ littermates. Brain weights were measured for *FoxO3*$^{-/-}$ and *FoxO3*$^{+/+}$ animals in mice at different ages (1-day-old [1d], 3-month-old [3m], and 1-year-old [1y]). Values represent mean ± SEM from 4–6 mice (1d), 20–23 males and 6–9 females (3m), and 4–7 males and females (1y). Mann-Whitney test, *p < 0.05; **p < 0.01; ***p < 0.001.

bromodeoxyuridine (BrdU)-positive label-retaining cells, which are thought to be NSCs (Figure S2C; see Figure 2). These results indicate that FoxO3 is expressed in adult NSCs, as well as in other cells in the NSC niches. The fact that FoxO3 staining overlaps with the nuclear staining of Sox2 and BrdU further suggests that FoxO3 is nuclear in adult NSCs and therefore likely to be active in these cells (Figure 1A; Figure S2C).

To confirm that FoxO3 is expressed in NSCs, we isolated NSCs from both the DG and the SVZ regions of the postnatal or adult mouse brain. Mouse NSCs form clonal spheres called neurospheres, which are composed of NSCs and more committed neural progenitors (Reynolds and Weiss, 1992). Immunostaining experiments on whole neurospheres or on dissociated NSCs revealed that FoxO3 is expressed in

NSCs/progenitors derived from both postnatal and adult animals and is coexpressed with Nestin, a NSC/progenitor marker (Figure 1B; Figure S3A).

To quantify the levels of FoxO3 in NSCs as a function of age, we used western blotting on protein extracts of neurospheres from NSCs isolated from mice at three different age milestones: birth (1-day-old), adulthood (3-month-old), and middle age (1-year-old). These experiments confirmed that FoxO3 is expressed in NSCs from mice at all ages (Figure 1C). FoxO3 protein expression is lower in NSCs from neonates than in NSCs from adults, but there was no significant change in FoxO3 expression in NSCs from young versus middle-aged adults (Figure 1C). Thus, FoxO3 is expressed in NSCs/progenitors from both developing and adult mice, with higher expression in adult NSCs.

FoxO3 Activity Is Higher in Self-Renewing NSCs than in Differentiated Progeny

To assess FoxO3 activity in NSCs, we compared the phosphorylation status of FoxO3 in self-renewing versus differentiating adult NSCs via western blotting with phospho-specific antibodies to Threonine 32 (T32), one of the three sites of FoxO3 phosphorylated by Akt (Brunet et al., 1999). A larger percentage of FoxO3 was phosphorylated at T32 in differentiated progeny than in self-renewing NSCs (Figure 1D; Figure S3B). As T32 phosphorylation is correlated with FoxO3 inactivation (Brunet et al., 1999), these results suggest that FoxO3 is more active in self-renewing NSCs than in their differentiated progeny.

To quantify FoxO3 activity in NSCs, we performed luciferase assays by using a luciferase reporter gene under the control of three Forkhead binding sites (Brunet et al., 1999). We first verified that this FoxO reporter gene was responsive to FoxO3 in NSCs by transfecting wild-type adult NSCs with active or inactive forms of FoxO3 (Figure 1E). We next tested the activity of endogenous FoxO3 in NSCs and found that this FoxO reporter gene was active in adult *FoxO3*$^{+/+}$ NSCs and that its activity was significantly decreased in *FoxO3*$^{-/-}$ NSCs (Figure 1F). The remainder of the activity of the FoxO reporter gene in *FoxO3*$^{-/-}$ NSCs is likely due to partial compensation by other FoxO family members. Taken together, these findings indicate that FoxO3 is active in self-renewing NSCs.

The Ablation of FoxO3 Results in a Decrease in NSC Number In Vivo

To determine whether FoxO3 regulates the NSC pool in vivo, we performed BrdU injection experiments in adult *FoxO3*$^{-/-}$ and *FoxO3*$^{+/+}$ mice (Figure 2). *FoxO3*$^{-/-}$ mice are viable and normal in outward appearance, though they are prone to cancer and die at around 1 to 1.5 years of age (data not shown; Paik et al., 2007). BrdU was injected daily into adult *FoxO3*$^{-/-}$ and *FoxO3*$^{+/+}$ littermates for 7 days and the mice were sacrificed either 1 month (Figure 2A) or 1 day (Figure 2D) after the last BrdU injection. We counted BrdU-positive cells in the NSC niches 1 month after the last BrdU injection (Figures 2B and 2C; Figure S4A). These label-retaining cells are thought to be the relatively quiescent NSCs that remain in NSC niches whereas neural progenitors and differentiated cells migrate away from NSC niches (Bondolfi et al., 2004). *FoxO3*$^{-/-}$ mice displayed a significant reduction in the number of label-retaining NSCs compared to *FoxO3*$^{+/+}$ mice in both the SGZ (Figure 2B, left) and the SVZ (Figures 2B, right, and Figure S4A). This result suggests that in the absence of FoxO3, adult mice have fewer NSCs. In contrast, when mice were sacrificed 1 day after the BrdU injections (Figure 2D), *FoxO3*$^{-/-}$ mice tended to have more BrdU-positive cells than *FoxO3*$^{+/+}$ mice in the SGZ ($p = 0.40$) and the SVZ ($p = 0.10$) (Figure 2E). BrdU-positive cells in the short-term BrdU paradigm are mostly neural progenitors, so these results indicate that in *FoxO3*$^{-/-}$ mice, the number of progenitors is not decreased and may even be slightly increased. Consistent with this finding, brains from adult *FoxO3*$^{-/-}$ mice were significantly heavier than brains from wild-type counterparts. In contrast, brains from *FoxO3*$^{-/-}$ mice had similar weight as wild-type counterparts at birth (Figure 2F). Together, these results suggest that *FoxO3* loss may lead to the short-term amplification of progenitors, resulting in the exhaustion of the NSC pool over time.

The Absence of FoxO3 Leads to the Depletion of NSCs in Adult Mice

To independently test whether FoxO3 prevents the progressive depletion of NSCs in vivo, we isolated NSCs from adult *FoxO3*$^{-/-}$ and *FoxO3*$^{+/+}$ mice and tested the ability of these cells to form primary neurospheres. The frequency of primary neurospheres formed at low cell density from freshly isolated NSCs can be used as an estimate of the pool size of NSCs in the brain and indirectly as a measure of self-renewal (Kippin et al., 2005). We found that NSCs from adult *FoxO3*$^{-/-}$ mice formed primary neurospheres at a significantly lower frequency than NSCs from *FoxO3*$^{+/+}$ littermates (Figure 3A). Although neurospheres can fuse, which can limit the interpretation of these experiments (Reynolds and Rietze, 2005), these results confirm that FoxO3 regulates the NSC pool. These findings are also consistent with the possibility that FoxO3 is necessary for NSC self-renewal.

To compare the ability of FoxO3 to regulate the NSC pool at different ages, we isolated NSCs from *FoxO3*$^{-/-}$ and *FoxO3*$^{+/+}$ mice at different ages. *FoxO3*$^{-/-}$ NSCs isolated from embryos (data not shown) or from 1-day-old mice (Figure 3B; Figure S5A) formed primary neurospheres with the same frequency as *FoxO3*$^{+/+}$ NSCs. In contrast, *FoxO3*$^{-/-}$ NSCs isolated from both young adult mice and middle-aged mice formed neurospheres at a significantly lower frequency than *FoxO3*$^{+/+}$ NSCs (Figure 3B; Figure S5B). These results indicate that the absence of FoxO3 leads to defects in the NSC pool that are evident only in adult mice. Because *FoxO3* is constitutively deleted in *FoxO3*$^{-/-}$ mice, it is not possible to distinguish whether FoxO3 regulates the NSC pool only in adults or whether FoxO3 also acts in NSCs during embryonic and/or postnatal development. As previously reported (Molofsky et al., 2006), the frequency of primary neurospheres formed in culture decreased significantly with the age of the mice (Figure 3B). The absence of FoxO3 did not have a greater impact on NSCs from middle-aged mice than in NSCs from young adult mice (Figure 3B), which might be due to a progressive inactivation of FoxO3 function during aging.

FoxO3 Is Necessary for NSC Self-Renewal

We tested whether FoxO3 is necessary for NSC self-renewal. Primary neurospheres can be dissociated to generate secondary

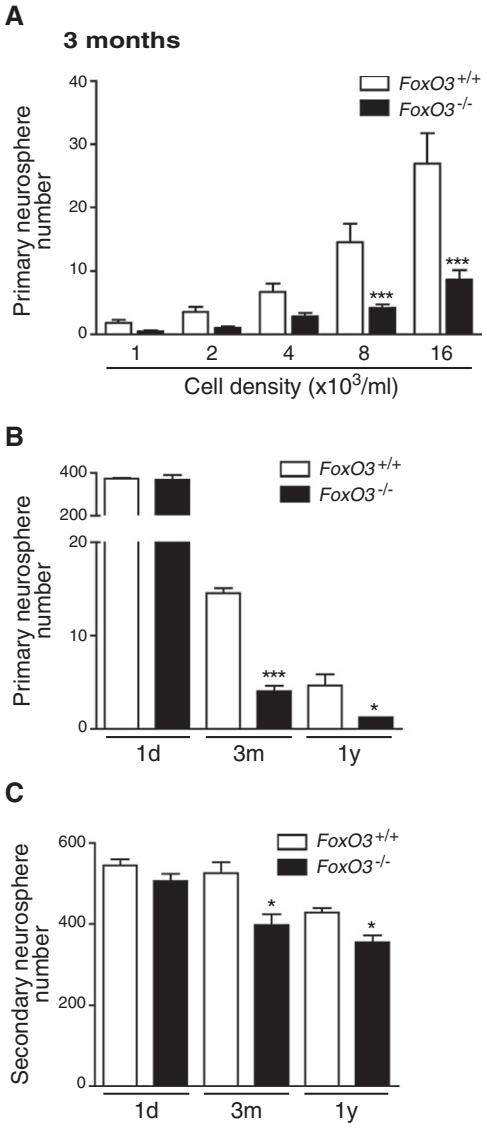

Figure 3. FoxO3 Regulates the NSC Pool and NSC Self-Renewal in Adult Mice, but Not in Neonates

(A) *FoxO3*$^{-/-}$ NSCs from adult mice display a defect in primary neurosphere formation. NSCs isolated from 3-month-old *FoxO3*$^{+/+}$ or *FoxO3*$^{-/-}$ littermates were seeded at the indicated cell densities. The number of neurospheres formed after 1 week was counted. Values represent mean ± SEM from seven independent experiments performed with five littermates for each genotype. Two-way ANOVA ($p < 0.0001$ for the genotype variable), Bonferroni posttests, ***$p < 0.001$.

(B) *FoxO3*$^{-/-}$ NSCs from adult mice, but not from neonates, display a defect in primary neurosphere formation. Frequency of primary neurospheres formed from NSCs at low density (8000 cells/ml) from mice at different ages (1-day-old [1d], 3-month-old [3m], 1-year-old [1y]). Values represent mean ± SEM from two independent experiments with two littermates (1d), seven independent experiments with five littermates (3m), and three independent experiments with three to five littermates (1y) for each genotype. Two-way ANOVA with Bonferroni posttests, *$p < 0.05$; ***$p < 0.001$.

(C) *FoxO3*$^{-/-}$ NSCs from adult mice, but not from neonates, display a defect in secondary neurosphere formation. Dissociated cells from primary neurospheres from *FoxO3*$^{+/+}$ or *FoxO3*$^{-/-}$ littermates were seeded at 4000 cells/ml. The number of secondary neurospheres formed after 1 week was counted. Values represent mean ± SEM from two independent experiments with two littermates (1d), four independent experiments with five littermates (3m), and four independent experiments with three to five littermates for each genotype (1y) for each genotype. Two-way ANOVA with Bonferroni posttests, *$p < 0.05$.

neurospheres, and the number of secondary neurospheres formed can serve as a measure of NSC self-renewal (Kippin et al., 2005). We dissociated *FoxO3*$^{-/-}$ and *FoxO3*$^{+/+}$ primary neurospheres and tested the ability of the dissociated cells to form secondary neurospheres. Whereas *FoxO3*$^{-/-}$ NSCs from neonates formed secondary neurospheres at the same frequency as *FoxO3*$^{+/+}$ NSCs, *FoxO3*$^{-/-}$ NSCs isolated from young and middle-aged adults generated fewer secondary neurospheres than *FoxO3*$^{+/+}$ NSCs (Figure 3C; Figures S5C–S5E). This result suggests that FoxO3 regulates NSC self-renewal. The ability of adult *FoxO3*$^{-/-}$ NSCs to form neurospheres at later passages in vitro was not significantly different from that of *FoxO3*$^{+/+}$ NSCs (Figure S5F), perhaps because other FoxO family members compensate for the lack of FoxO3 after several passages in culture. Concomitant deletion of FoxO1, FoxO3, and FoxO4 results in defects in neurosphere formation upon serial passage in culture (Paik et al., 2009 [this issue]), confirming the functional redundancy among FoxO family members in cultured NSCs. These results suggest that FoxO3 prevents the premature exhaustion of NSCs by preserving their self-renewal capacity.

The Ability of NSCs to Generate Different Neural Lineages Is Defective in the Absence of FoxO3

NSCs give rise to three types of progeny (neurons, astrocytes, and oligodendrocytes), and the proper balance between the three fates is pivotal for the functionality of the NSC pool. The ability of NSCs to generate progeny can be measured by assessing cellular fates in secondary neurospheres, because each neurosphere derives from a single NSC (Kippin et al., 2005). We examined the progeny of *FoxO3*$^{-/-}$ and *FoxO3*$^{+/+}$ secondary neurospheres after 7 days in differentiation conditions. Neurospheres generated from adult NSCs contained mainly astrocytes (GFAP positive), as well as fewer numbers of immature neurons (Tuj1 positive) or immature oligodendrocytes (O4 positive) (Figure 4A), indicating that these neurospheres arose from at least bipotent NSCs. To measure NSC functionality, we scored the number of differentiated secondary neurospheres formed at low cell density that contain at least one immature neuron (Tuj1 positive) or one immature oligodendrocyte (O4 positive) in addition to astrocytes. We found that NSCs isolated from neonate *FoxO3*$^{-/-}$ and *FoxO3*$^{+/+}$ mice formed similar numbers of bipotent neurospheres (Figures 4B and 4C). In contrast, NSCs isolated from young or middle-aged adult *FoxO3*$^{-/-}$ mice formed significantly fewer secondary neurospheres containing oligodendrocytes than those isolated from *FoxO3*$^{+/+}$ mice (Figure 4B). *FoxO3*$^{-/-}$ NSCs from middle-aged mice tended to form fewer neurospheres containing both neurons and astrocytes and more neurospheres containing only astrocytes compared to *FoxO3*$^{+/+}$ NSCs (Figures 4C and 4D). Similar results were obtained when differentiated neurospheres were stained for all three cell fates simultaneously (Figure S6). These findings indicate that *FoxO3* loss results in a deficiency in the ability of NSCs to generate different neural lineages that is evident only in adulthood. Our observations further suggest that in the

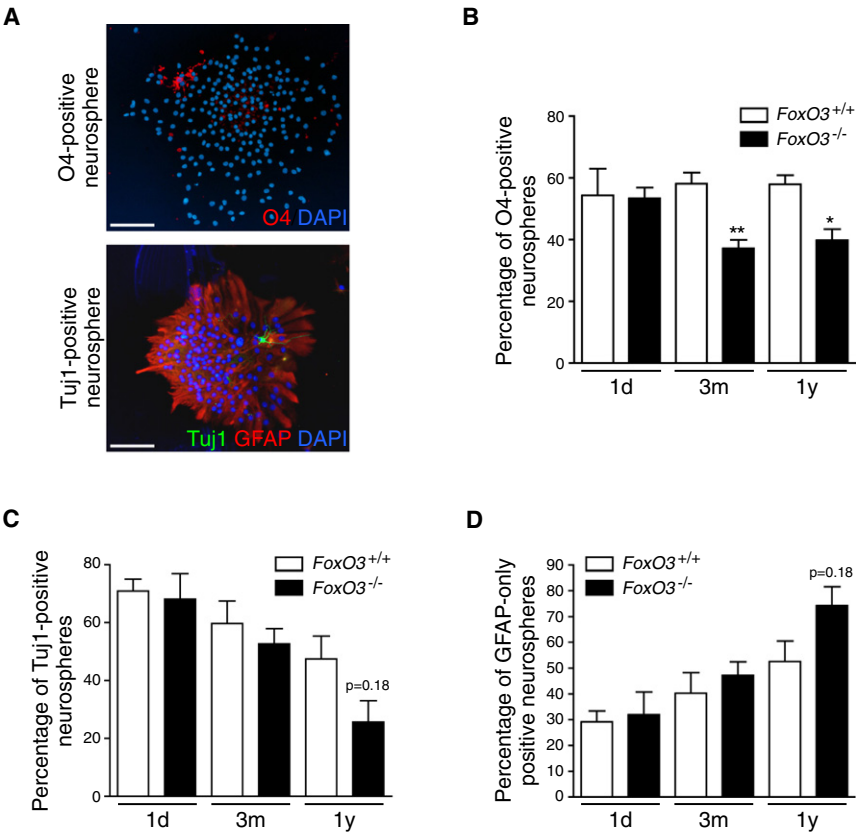

Figure 4. FoxO3 Controls the Ability of Adult NSCs to Give Rise to Different Lineages

(A) Adult NSCs give rise to at least bipotent neurospheres. Astrocytes, neurons, and oligodendrocytes present in whole neurospheres after 7 days of differentiation were stained with antibodies to GFAP, Tuj1, and O4, respectively. Scale bars represent 100 μm.

(B) *FoxO3*$^{-/-}$ NSCs from adult mice, but not from neonates, give rise to fewer oligodendrocyte-containing neurospheres than *FoxO3*$^{+/+}$ NSCs. *FoxO3*$^{+/+}$ and *FoxO3*$^{-/-}$ NSCs from mice at different ages (1-day-old [1d], 3-month-old [3m], 1-year-old [1y]) were grown as secondary neurospheres at low density. The neurospheres were differentiated for a week and stained with antibodies to O4. Neurospheres that contained oligodendrocytes were counted. Values represent mean ± SEM from two independent experiments with two littermates (1d), five littermates (3m), and three to five littermates (1y) for each genotype. Student's t test, *$p < 0.05$; **$p < 0.01$.

(C and D) *FoxO3*$^{-/-}$ NSCs from middle-aged mice tend to give rise to fewer neuron-containing neurospheres than *FoxO3*$^{+/+}$ NSCs. Neurospheres were grown as described in (B) and stained with antibodies to Tuj1 and GFAP. Neurospheres that contained neurons and astrocytes were counted. Values represent mean ± SEM from two independent experiments with two littermates (1d), five littermates (3m), and three to five littermates (1y) for each genotype. Student's t test, $p = 0.18$.

(C) Neurospheres containing at least one Tuj-1-positive cell.

(D) Neurospheres containing only GFAP-positive cells.

absence of FoxO3, NSCs become more similar to progenitors (i.e., less able to self-renew and more committed to a specific lineage). NSCs lacking FoxO3 also resemble NSCs from older animals, which are less able to self-renew and more skewed toward astrocytes (Bondolfi et al., 2004).

FoxO3 Acts in the Nervous System to Regulate the NSC Pool

FoxO3 is expressed in a number of tissues, raising the question of whether FoxO3 regulates the NSC pool by acting in the brain or in other tissues, which could in turn affect NSCs. To address this question, we crossed *FoxO3*$^{lox/lox}$ mice with *Nestin-Cre* transgenic mice, which express the Cre recombinase in NSCs/progenitors from embryonic day 10.5 (Tronche et al., 1999). As expected, *FoxO3*$^{lox/lox}$;*Nestin-Cre* mice displayed an ablation of the FoxO3 protein in the brain, but not in the majority of other tissues (Figure 5A). Interestingly, young and middle-aged adult *FoxO3*$^{lox/lox}$;*Nestin-Cre* mice had significantly heavier brains than their control siblings (Figure 5B). These results suggest that FoxO3 regulates brain weight by acting in the nervous system, rather than in other tissues.

To test whether FoxO3 regulates the NSC pool by acting in the nervous system, we performed BrdU long-term retention experiments in vivo in *FoxO3*$^{lox/lox}$;*Nestin-Cre* mice and *FoxO3*$^{lox/lox}$ siblings (Figure 5C). We found that young adult *FoxO3*$^{lox/lox}$; *Nestin-Cre* mice tended to have fewer label-retaining NSCs in the SVZ and in the SGZ than control siblings, though this did not reach statistical significance (Figure 5C). The effects of *FoxO3* loss in vivo were less pronounced in *FoxO3*$^{lox/lox}$; *Nestin-Cre* mice than in *FoxO3*$^{-/-}$ mice, which could suggest that FoxO3 regulates NSCs in part by acting in tissues other than the nervous system. However, the difference in magnitude in long-term BrdU retention between *FoxO3*$^{lox/lox}$;*Nestin-Cre* and *FoxO3*$^{-/-}$ mice is likely due to the different genetic backgrounds of these mice and/or to the different ages of the mice when the NSC pools were examined.

To independently test whether FoxO3 acts in the nervous system to regulate NSCs, we isolated NSCs from *FoxO3*$^{lox/lox}$; *Nestin-Cre* mice and control mice and assessed their ability to form primary neurospheres. NSCs isolated from *FoxO3*$^{lox/lox}$; *Nestin-Cre* mice had no FoxO3 protein expression for up to four passages (Figure 5D), indicating that the deletion of the *FoxO3* gene was efficient. Interestingly, NSCs isolated from 9-month-old *FoxO3*$^{lox/lox}$;*Nestin-Cre* mice displayed significant defects in their ability to form primary neurospheres compared to NSCs isolated from control *FoxO3*$^{lox/lox}$ littermates (Figure 5E). Together, these results suggest that FoxO3 acts in the nervous system to regulate adult brain weight and NSC homeostasis in vivo. Because FoxO3 is deleted from embryonic day 10.5 in *FoxO3*$^{lox/lox}$;*Nestin-Cre* mice, the effects of *FoxO3* loss on brain weight and NSCs may be a result of FoxO3's action in the embryonic and/or postnatal brain. It is also possible that

FoxO3 regulates NSCs in part by acting in other tissues, e.g., blood vessels that form the NSC niche or metabolic tissues that would then affect the systemic milieu. However, two independent ways of deleting FoxO factors in the nervous system—*Nestin-Cre* (this study) or *GFAP-cre* (Paik et al., 2009 [this issue])—both result in similar NSC phenotypes, supporting the notion that FoxO factors act in the nervous system to regulate NSCs.

FoxO3 Regulates the Quiescence and Survival of NSCs

To determine the cellular mechanisms by which FoxO3 regulates NSCs, we tested whether the absence of FoxO3 affects cell proliferation in neurospheres. Cells dissociated from secondary neurospheres from young adult *FoxO3*$^{-/-}$ mice displayed a significant increase in BrdU incorporation in culture compared to cells from *FoxO3*$^{+/+}$ mice (Figure 6A). There was no difference in the proportion of cells in G2/M phases between *FoxO3*$^{+/+}$ and *FoxO3*$^{-/-}$ NSCs (data not shown), suggesting that the primary effect of FoxO3 loss is at the G1/S transition. Thus, the absence of FoxO3 leads to the proliferation of NSCs/progenitors cells in neurospheres. Without FoxO3, NSCs may lose their ability to re-enter a state of relative quiescence after they divide, which may lead to the amplification of progenitors and the exhaustion of the pool of NSCs in vivo.

We also quantified apoptotic cell death in *FoxO3*$^{-/-}$ and *FoxO3*$^{+/+}$ NSCs. Freshly isolated NSCs from adult *FoxO3*$^{-/-}$ mice displayed an increased number of cleaved caspase 3-positive cells compared to *FoxO3*$^{+/+}$ NSCs (Figure 6B, left), which might contribute to the decreased self-renewal of *FoxO3*$^{-/-}$ NSCs. In contrast, the level of apoptosis for cells dissociated from secondary *FoxO3*$^{-/-}$ neurospheres was lower than for cells dissociated from *FoxO3*$^{+/+}$ neurospheres (Figure 6B, right). These findings, coupled with the observation that *FoxO3*$^{-/-}$ mice have increased brain weight compared to *FoxO3*$^{+/+}$ littermates (Figure 2F), suggests that cell death is not a major consequence of FoxO3 loss and that loss of quiescence may play a more important role in the depletion of NSCs in vivo in *FoxO3*$^{-/-}$ mice.

FoxO3 Coordinates the Expression of a Specific Program of Genes in NSCs

To gain insight into the molecular mechanisms by which FoxO3 regulates NSCs, we determined the program of genes regulated by FoxO3 in NSCs. We performed a genome-wide microarray analysis on RNA isolated from two independent biological replicates, each in duplicate, of *FoxO3*$^{-/-}$ and *FoxO3*$^{+/+}$ secondary neurospheres from young adult mice. We used secondary neurospheres because *FoxO3*$^{-/-}$ and *FoxO3*$^{+/+}$ neurospheres displayed a significant difference in self-renewal ability. Analysis of the microarray data revealed that the expression of a specific subset of genes is decreased in *FoxO3*$^{-/-}$ neurospheres compared to *FoxO3*$^{+/+}$ neurospheres (Figures 7A and 7B; Table S1). The changes in expression levels of a number of these genes were validated by reverse transcription followed by quantitative PCR (Figure S7).

The analysis of our microarray data revealed that FoxO3 is required for the expression of genes involved in cell quiescence, as was previously shown in other cell types (Salih and Brunet, 2008). For example, FoxO3 is necessary for the expression of *p27*^{KIP1} and *Cyclin G2* (Figure 7A; Figure S7). The comparison of our microarray data with available molecular signatures revealed that FoxO3-regulated genes were significantly enriched for genes that form a molecular signature for quiescence (Figure 7C; Figures S8A and S8B). These results support the notion that FoxO3 regulates the homeostasis of the NSC pool by preventing the premature overproliferation of progenitors and preserving the relative quiescence of NSCs. We also found that FoxO3 was necessary for the expression of genes involved in oxidative stress resistance (e.g., *selenbp1*) (Figure 7A; Figure S7) and in glucose metabolism and transport (e.g., *Pdk1, Slc2a3*) (Figures 7A and 7C; Figure S7), consistent with the known role of the FoxO family in stress resistance and cellular metabolism (Accili and Arden, 2004). The ability of FoxO3 to coordinate a program maintaining quiescence, stress resistance, and glucose metabolism in adult NSCs may be critical for preserving the stemness of these cells.

Interestingly, we also identified genes that were not previously known to be upregulated by FoxO factors. First, FoxO3 was necessary for the upregulation of genes involved in early neurogenesis (e.g., *Otx2*) (Figure 7A; Figure S7), which may contribute to the defect in multipotency of *FoxO3*$^{-/-}$ neurospheres (Figure S6). Surprisingly, the comparison between our microarray data and publicly available molecular signatures revealed that FoxO3 was necessary for the expression of genes upregulated in hypoxic brains and other hypoxic tissues, including *Ddit4*, *Ndrg1, Ero1l,* and *Vegfa* (Figures 7A and 7C; Figures S7, S8C, and S8D; Table S1). These findings raise the possibility that FoxO3 is necessary for the response of NSCs to low oxygen. The ability of FoxO3 to control oxygen metabolism in NSCs may participate in the regulation of NSCs in vivo.

FoxO3 is also required for the repression of specific genes in neurospheres (Figure 7B). For example, genes expressed in mature oligodendrocytes, including *Myelin Basic Protein*, *Plp1,* and *Apod*, were upregulated in *FoxO3*$^{-/-}$ NSCs compared to *FoxO3*$^{+/+}$ NSCs (Figure 7B; Figure S7; Table S1). These results suggest that FoxO3 normally prevents premature oligodendrocyte differentiation. Consistent with these findings, we observed that the corpus callosum area, a brain structure that contains mature oligodendrocytes, is increased in adult *FoxO3*$^{-/-}$ mice compared to *FoxO3*$^{+/+}$ littermates (Figure S9). The inhibition of the premature differentiation of NSCs by FoxO3 may contribute to the functionality of NSCs in vivo.

Finally, the comparison of our microarray data with genes that are known to change during aging in human and mouse brains revealed a correlation between FoxO3-regulated genes and genes that are regulated during aging in the brain (Figure 7C; Figures S8E and S8F). These observations are consistent with the possibility that FoxO3, a gene that belongs to a family that promotes longevity in invertebrates, also regulates genes that are important to counteract the aging process in mammalian adult stem cells.

Identification of FoxO3 Direct Targets in NSCs

FoxO3-regulated genes are enriched for the presence of a FoxO binding motif in their regulatory regions (Figure 7A; Table S1), raising the possibility that a subset of FoxO3-regulated genes might be direct FoxO3 target genes in NSCs. To identify direct targets of FoxO3, we performed electrophoretic mobility shift

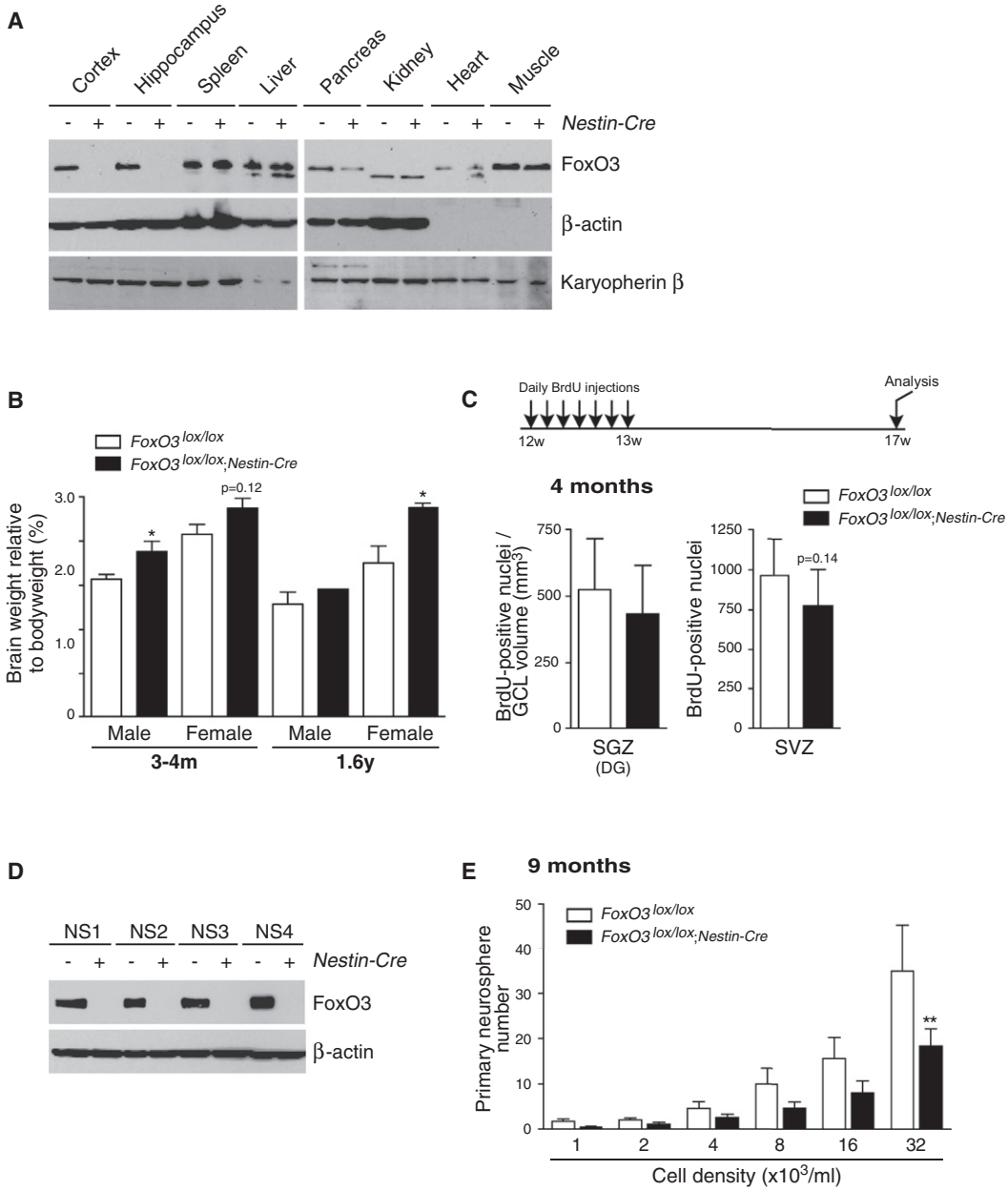

Figure 5. Consequences of *FoxO3* Loss in the Nervous System on Brain Weight and the NSC Pool

(A) Expression of FoxO3 in the tissues of *FoxO3*$^{lox/lox}$*;Nestin-Cre* mice. FoxO3 expression in different tissues of 2-month-old *FoxO3*$^{lox/lox}$*;Nestin-Cre* mice was determined by western blot with antibodies to FoxO3 ("NFL") and antibodies to β-actin and karyopherin β. Note that FoxO3 was partially deleted in the pancreas.

(B) Brain weights of *FoxO3*$^{lox/lox}$*;Nestin-Cre* and *FoxO3*$^{lox/lox}$ mice. Brain weights were measured after perfusion in 3- to 4-month-old mice (3–4m) and 1.6-year-old mice (1.6y). Values represent mean ± SEM from nine to ten males and nine to ten females (3–4m), and one to three males and five to eight females (1.6y). One male and two females (3–4m) and three females (1.6y) of the *FoxO3*$^{lox/+}$ genotype were included in the control group (*FoxO3*$^{lox/lox}$).

(C) Quantification of label-retaining NSCs in *FoxO3*$^{lox/lox}$*;Nestin-Cre* and *FoxO3*$^{lox/lox}$ animals in vivo. Number of BrdU-positive cells in the SGZ (left) and the SVZ (right) in 3-month-old *FoxO3*$^{lox/lox}$*;Nestin-Cre* and *FoxO3*$^{lox/lox}$ littermates injected daily with BrdU for 7 days and sacrificed 1 month after the last BrdU injection. The number of BrdU-positive cells in the SGZ was normalized to the volume of the granular cell layer (GCL). Values represent mean ± SEM (left) and mean ± SD (right) from 8 *FoxO3*$^{lox/lox}$*;Nestin-Cre* mice and 11 *FoxO3*$^{lox/lox}$ control littermates. Two *FoxO3*$^{lox/+}$ littermates were included in the control group (*FoxO3*$^{lox/lox}$). Mann-Whitney test, p = 0.27 (left) and p = 0.14 (right).

(D) Ablation of the FoxO3 protein in NSCs from *FoxO3*$^{lox/lox}$*;Nestin-Cre* mice. FoxO3 expression in NSCs isolated from 3-month-old *FoxO3*$^{lox/lox}$ mice (–) or *FoxO3*$^{lox/lox}$*;Nestin-Cre* mice (+) 7 days after isolation (NS1) or at three consecutive passages (NS2 to 4) was determined by western blot with antibodies to FoxO3 ("NFL") and antibodies to β-actin.

(E) Ablation of FoxO3 in the brain impairs primary neurosphere formation. NSCs isolated from 9-month-old *FoxO3*$^{lox/lox}$ mice (control) or *FoxO3*$^{lox/lox}$*;Nestin-Cre* mice were seeded at low density. The number of neurospheres formed after 1 week was counted. Values represent mean ± SEM from triplicates from four independent experiments conducted with three littermates for each genotype. Two-way ANOVA, $p < 0.01$ for the genotype variable, Bonferroni posttests, $^{**}p < 0.01$.

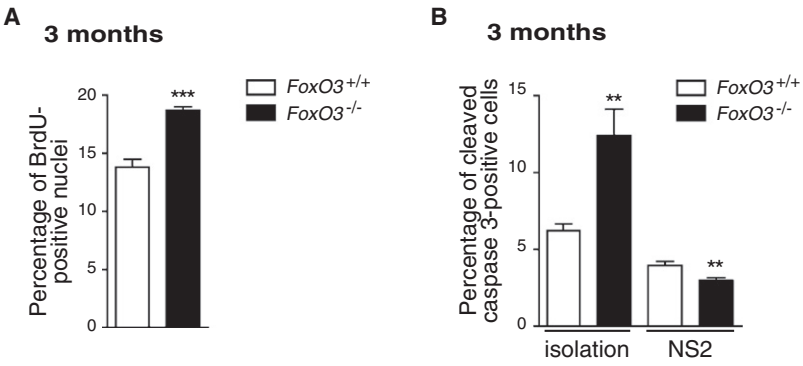

Figure 6. FoxO3 Is Necessary for Maintaining NSCs/Neural Progenitor Quiescence

(A) Increased cell proliferation in *FoxO3*$^{-/-}$ neurospheres. Cells dissociated from secondary neurospheres from 3-month-old *FoxO3*$^{+/+}$ or *FoxO3*$^{-/-}$ mice were plated on poly-D-lysine and incubated for 1 hr with BrdU. Cells were immunostained with antibodies to BrdU. BrdU-positive nuclei were counted. Values represent mean ± SEM from two independent experiments with five littermates for each genotype. Student's t test, ***p < 0.001.

(B) Apoptosis in *FoxO3*$^{-/-}$ NSCs compared to *FoxO3*$^{+/+}$ NSCs. Freshly isolated NSCs or cells dissociated from secondary neurospheres isolated from 3-month-old *FoxO3*$^{+/+}$ or *FoxO3*$^{-/-}$ mice were stained with antibodies to cleaved caspase 3. Cleaved caspase 3-positive cells were counted. Values represent mean ± SEM from two independent experiments with five littermates for each genotype. Student's t test, **p < 0.01.

assays (EMSA) and chromatin immunoprecipitation (ChIP) in NSCs. EMSA experiments revealed that FoxO3 could bind in vitro to FoxO binding sites present in the regulatory regions of the *Ddit4*, *Ndrg1*, and *Otx2*, suggesting that these genes are direct targets of FoxO3 (Figures S10A and S10B). ChIP experiments revealed that FoxO3 is recruited to the FoxO binding sites in the promoters of the *p27*^{KIP1} and *Ddit4* genes (Figure 7D; Figure S10C). These results indicate that *p27*^{KIP1}, a cell cycle inhibitor involved in cell quiescence and *Ddit4*, a known target of hypoxia-inducible factor 1 (HIF1), are direct target genes of FoxO3 in NSCs. In contrast, FoxO3 was not bound at the promoters of *Otx2* and *Ndrg1* by ChIP (data not shown), suggesting that these two genes may not be direct FoxO3 targets in NSCs.

The Response of *FoxO3*$^{-/-}$ NSCs to Low Oxygen Is Impaired In Vitro

Because a subset of FoxO3-regulated genes is involved in the cellular response to hypoxia, we compared the ability of *FoxO3*$^{+/+}$ and *FoxO3*$^{-/-}$ NSCs to form neurospheres in low-oxygen (2%) versus atmospheric oxygen (20%) conditions (Figure 7E). Consistent with published findings for embryonic NSCs/progenitors (Studer et al., 2000), adult NSCs showed an increased ability to form neurospheres in low oxygen compared to atmospheric oxygen (Figure 7E). In contrast, *FoxO3*$^{-/-}$ NSCs did not display an increased ability to form neurospheres in low-oxygen compared to atmospheric oxygen conditions (Figure 7E). These results suggest that the response of *FoxO3*$^{-/-}$ NSCs to low oxygen is impaired in vitro. It is also possible that 2% oxygen, which mimics in vivo physiological oxygen concentrations in the mammalian brain (Zhu et al., 2005), helps reveal differences between *FoxO3*$^{-/-}$ and *FoxO3*$^{+/+}$ NSCs. Together, these results indicate that FoxO3 is necessary for the expression of a program of genes that coordinate cell quiescence, inhibition of premature differentiation, and oxygen metabolism, which may all contribute to the ability of FoxO3 to regulate the homeostasis of the NSC pool.

DISCUSSION

Our results indicate that FoxO3 regulates processes and pathways relevant to NSC homeostasis both in vitro and in vivo. In the absence of FoxO3, NSCs display a decreased ability to self-renew and to give rise to different neural lineages, which may result in the depletion of NSCs in vivo. Our findings also suggest that FoxO3 regulates NSC homeostasis by controlling a program of genes that precisely governs cell cycle re-entry and promotes a state of glucose and oxygen metabolism compatible with optimal self-renewal. Because the NSC pool is a limited reserve that needs to be maintained throughout life, preserving this pool may be an important factor in the healthspan of long-lived organisms.

The effects of *FoxO3* loss on NSCs manifest themselves only in adult animals. This observation raises the possibility that FoxO3 plays a more important role in adult NSCs than in embryonic or neonatal NSCs. It is also possible that FoxO3 acts to alter embryonic or postnatal NSC biology or the NSC niche, which would ultimately result in the depletion of adult NSCs later in life. Alternatively, FoxO3 loss may be better compensated by other FoxO family members in embryonic and postnatal NSCs than in adult NSCs. Precisely studying the timing of action of FoxO3 in NSCs will require crossing *FoxO3*$^{lox/lox}$ mice with mice expressing a tamoxifen-inducible form of Cre (CreER) driven from promoters that are active in NSCs, such as *Nestin, GFAP, Glast*, or *TLX* (Johnson et al., 2009).

Our experiments indicate that FoxO3 exerts at least part of its action in the nervous system to regulate brain weight and the NSC pool. FoxO3 may also act in part in the stem cell niche or systemically to regulate NSCs. FoxO3 is expressed in neurons, astrocytes, and oligodendrocytes, as well as in endothelial cells of the vasculature, all of which may contribute to the NSC niche. Because FoxO3 has been shown to play an important role in specific endothelial cells (Paik et al., 2007), a portion of the defect observed in the brain of *FoxO3*$^{-/-}$ mice might come from FoxO3 loss in blood vessels. A rigorous demonstration of the cell autonomy of FoxO3 will require the generation of mouse models in which FoxO3 is specifically deleted in NSCs. Nevertheless, the observation that *FoxO3*$^{lox/lox}$;*Nestin-Cre* mice (this study) and *FoxO1/3/4*$^{lox/lox}$;*GFAP-Cre* mice (Paik et al., 2009 [this issue]), which both lead to *FoxO* deletion in NSCs, have similar NSC phenotypes both in vivo and in vitro, suggests that FoxO factors act cell autonomously in NSCs. This notion is further supported by the observation that in vitro deletion of FoxO in NSCs leads

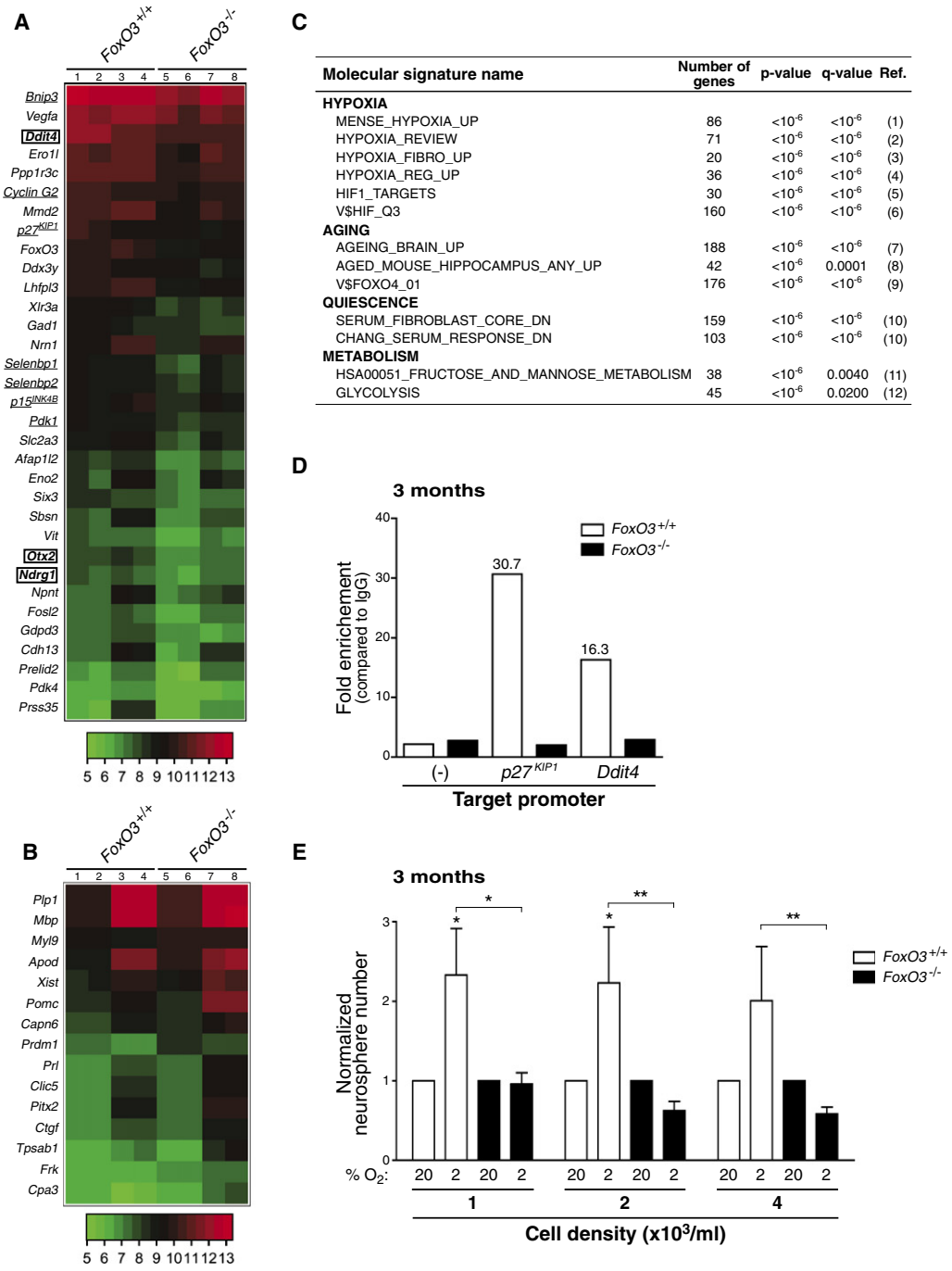

Molecular signature name	Number of genes	p-value	q-value	Ref.
HYPOXIA				
MENSE_HYPOXIA_UP	86	$<10^{-6}$	$<10^{-6}$	(1)
HYPOXIA_REVIEW	71	$<10^{-6}$	$<10^{-6}$	(2)
HYPOXIA_FIBRO_UP	20	$<10^{-6}$	$<10^{-6}$	(3)
HYPOXIA_REG_UP	36	$<10^{-6}$	$<10^{-6}$	(4)
HIF1_TARGETS	30	$<10^{-6}$	$<10^{-6}$	(5)
V$HIF_Q3	160	$<10^{-6}$	$<10^{-6}$	(6)
AGING				
AGEING_BRAIN_UP	188	$<10^{-6}$	$<10^{-6}$	(7)
AGED_MOUSE_HIPPOCAMPUS_ANY_UP	42	$<10^{-6}$	0.0001	(8)
V$FOXO4_01	176	$<10^{-6}$	$<10^{-6}$	(9)
QUIESCENCE				
SERUM_FIBROBLAST_CORE_DN	159	$<10^{-6}$	$<10^{-6}$	(10)
CHANG_SERUM_RESPONSE_DN	103	$<10^{-6}$	$<10^{-6}$	(10)
METABOLISM				
HSA00051_FRUCTOSE_AND_MANNOSE_METABOLISM	38	$<10^{-6}$	0.0040	(11)
GLYCOLYSIS	45	$<10^{-6}$	0.0200	(12)

Figure 7. FoxO3 Is Necessary for the Expression of a Program of Genes that Coordinately Regulates NSC Homeostasis

(A and B) Differentially regulated genes in *FoxO3*$^{-/-}$ NSCs compared to *FoxO3*$^{+/+}$ NSCs. Whole-genome microarray data obtained from two independent biological replicates of RNA from duplicates of *FoxO3*$^{-/-}$ and *FoxO3*$^{+/+}$ secondary neurospheres isolated from 3-month-old mice (five littermates for each genotype). Heat-map of selected genes downregulated (A) and upregulated (B) more than 1.5-fold in *FoxO3*$^{-/-}$ NSCs compared to *FoxO3*$^{+/+}$ NSCs with a false discovery rate less than 5%. Lanes 1–2 and 5–6: duplicates from one experiment. Lanes 3–4 and 7–8: duplicates from a second independent experiment. Underlined: known FoxO target genes. Surrounded by a square: genes containing FoxO binding motifs in their regulatory regions (Table S1).

(C) FoxO3-regulated genes in NSCs are involved in quiescence, hypoxia, aging, and glucose metabolism. Selected publicly available molecular signatures highly enriched for genes downregulated in *FoxO3*$^{-/-}$ NSCs as provided by GSEA (gene set enrichment analysis). See Supplemental Data for references (Ref.) 1–12.

(D) FoxO3 is recruited to the promoters of *p27*^{KIP1} and *Ddit4* in NSCs. ChIP of FoxO3 from NSCs isolated from 3-month-old mice shows significant recruitment of FoxO3 at the promoters of *p27*^{KIP1} and *Ddit4*. FoxO3 recruitment was not found at control regions that did not have FoxO binding sites (–) and did not occur in *FoxO3*$^{-/-}$ neurospheres. Depicted is a representative ChIP analysis. Similar results were obtained in independent experiments (Figure S10C).

to self-renewal defects and by the functional validation of direct FoxO targets in NSCs (Paik et al., 2009). FoxO factors may in fact provide a pivotal link between extrinsic and intrinsic signals by integrating a variety of external stimuli, including growth factors and oxidative stress (Salih and Brunet, 2008).

FoxO factors are necessary for the maintenance and self-renewal of adult hematopoietic stem cells (HSCs) (Miyamoto et al., 2007; Tothova et al., 2007). HSCs continuously regenerate the hematopoietic tissue whereas NSCs have lower regenerative capacity. Interestingly, the program of genes controlled by FoxO3 in NSCs reveals little overlap with the program of genes controlled by FoxO factors in HSCs (Miyamoto et al., 2007; Tothova et al., 2007). FoxO factors may regulate different stem cell types by inducing specific gene expression programs tailored for the unique biology of these types of stem cells. Identifying the programs induced by FoxO3 in different types of stem cells should help uncover differences between stem cells from rapidly regenerating versus slowly regenerating tissues.

FoxO factors are inhibited by the PI3K-Akt pathway and activated by the PTEN phosphatase. Increased PI3K-Akt signaling promotes the self-renewal of cortical progenitors and adult SVZ cells (Groszer et al., 2006; Li et al., 2002; Sinor and Lillien, 2004). Whether increased PI3K-Akt signaling promotes the short-term expansion of progenitors at the expense of the NSC pool in vivo is unknown. The deletion of the *PTEN* gene in HSCs leads to the long-term depletion of HSCs, which is rescued by rapamycin, an mTOR inhibitor (Yilmaz et al., 2006). It will be interesting to determine the importance of the PI3K-Akt pathway and downstream pathways (FoxO versus mTOR) in the long-term regulation of the NSC pool.

Our findings suggest that FoxO3 is necessary for the expression of hypoxia-dependent genes in NSCs, several of which are known to be targets of the hypoxia-inducible factor HIF1. In *C. elegans,* the FoxO transcription factor DAF-16 and HIF1 also share common target genes (McElwee et al., 2004). However, in other mammalian cells, FoxO3 inhibits hypoxia-dependent genes in an indirect manner (Bakker et al., 2007; Emerling et al., 2008). Thus, FoxO3 may both directly regulate some HIF1 target genes and indirectly inhibit HIF1-dependent transcription. The balance between these two functions of FoxO3 could be altered by variations in the levels of oxygen. Alternatively, the regulation of the hypoxic program may differ, depending on the types of cells or tissues. The finding that FoxO3 is required for the expression of genes that mediate the response to hypoxia in NSCs is consistent with the observation that hypoxia and HIF1 promote self-renewal and multipotency in stem cells (Keith and Simon, 2007). NSCs are located in close proximity to blood vessels in vivo and may be subjected to varying levels of oxygen (Mirzadeh et al., 2008; Shen et al., 2008; Tavazoie et al., 2008), so the ability of FoxO3 to regulate oxygen metabolism in NSCs might also play a role in the protection of these cells in vivo.

In conclusion, our findings suggest that a gene identified based on its function in regulating lifespan in invertebrates may have evolved to play a critical role in regulating NSC homeostasis in mammals. Because NSCs have been shown to be important for learning, memory, and mood regulation, our findings could give insight into the decline in cognitive function that occurs during aging.

EXPERIMENTAL PROCEDURES

Materials and other experimental procedures are described in the Supplemental Data.

Animals

FoxO3$^{-/-}$ and *FoxO3*$^{lox/lox}$ mice in the FVB/N background were generously provided by Dr. Ron DePinho (Dana Farber Cancer, Boston). *Nestin-Cre* mice in the C57/Bl6 background were purchased from Jackson Laboratories. All care and procedures were in accordance with the Guide for the Care and Use of Laboratory Animals. All animal experiments were approved by Stanford's Administrative Panel on Laboratory Animal Care (APLAC) and in accordance with institutional and national guidelines.

Quantification of BrdU-Positive NSCs and Progenitors In Vivo

Mice were injected intraperitoneally with 50 mg/kg of BrdU (EMD Biosciences) once a day for 7 days and sacrificed either 1 day or 1 month later. Mice were anesthetized and perfused transcardially with PBS containing 5 U/ml of heparin, then with 4% paraformaldehyde (PFA). Brains were fixed in 4% PFA for 4 hr at 4°C, then in 30% sucrose/4% PFA overnight at 4°C, and embedded in Tissue-Tek (Sakura) at −80°C. Coronal sections (40 μm) were cut with a microtome. Sections were incubated in 3% H_2O_2 for 30 min, in 2 N HCl solution for 30 min at 37°C, followed by washes in boric acid buffer (pH 8.4). Sections were incubated with the BrdU antibody (AbD serotec, 1:500) overnight at 4°C, and then with the secondary antibody (biotinylated donkey anti-rat, Jackson ImmunoResearch, 1:500) overnight at 4°C. The sections were then incubated in the ABC solution (Vector Laboratories) for 90 min, and with DAB (Sigma, 0.05%) containing 0.15% H_2O_2 for 2–10 min. The sections were dried, dehydrated on slides, and mounted with Permount (Fisher Scientific). BrdU staining and quantification was performed on every sixth section from Bregma +1.54 mm to −1.34 mm (SVZ) and from Bregma −0.94 mm to −3.88 mm (DG). BrdU-positive cells were counted in a blinded manner. The total number of BrdU-positive cells in each region was obtained by multiplying the number of BrdU-positive nuclei by 6. In the DG, the number of BrdU-positive cells was normalized by the granular cell layer (GCL) volume (in mm^3). The GCL volume was quantified on every sixth section by calculating the area of the GCL on both sides via Metamorph (Molecular Devices). The total GCL volume was estimated by multiplying these areas by 6 and then by 40 μm.

Mouse NSC Cultures

Isolation of mouse NSCs/progenitors was done as described previously (Palmer et al., 1997). In brief, the brains were dissected to remove the olfactory bulbs, cerebellum, and brainstem. The forebrains were finely minced; digested for 30 min at 37°C in HBSS media containing 2.5 U/ml Papain (Worthington), 1 U/ml Dispase (Roche), and 250 U/ml DNase I (Sigma); and mechanically dissociated. NSCs/progenitors were purified with two Percoll gradients (25% then 65%) (Amersham) and plated at a density of 10^5 cells/cm^2 in Neuro-Basal-A medium with penicillin-streptomycin-glutamine (Invitrogen), B27 supplement (Invitrogen, 2%), bFGF (Peprotech, 20 ng/ml), and EGF (Peprotech, 20 ng/ml) (self-renewal/proliferation media). Cells were incubated at 37°C in 5% CO_2 and 20% oxygen at 95% humidity.

(E) *FoxO3*$^{-/-}$ NSCs form fewer neurospheres than *FoxO3*$^{+/+}$ NSCs in low-oxygen conditions. Normalized frequency of neurospheres formed from NSCs at low density in 20% oxygen (20) or in 2% oxygen (2). NSCs were dissociated from secondary neurospheres generated from 3-month-old *FoxO3*$^{-/-}$ and *FoxO3*$^{+/+}$ mice. Values represent mean ± SEM from four independent experiments with three to five littermates for each genotype. The normalization was done by dividing the triplicate average from each experiment in 2% oxygen by the triplicate average from the same experiment in 20% oxygen. Two-way ANOVA, Bonferroni post-tests, *$p < 0.05$; **$p < 0.01$.

Primary and Secondary Neurosphere Assays

At isolation, NSCs were plated in triplicate at low density (1 to 32,000 cells/ml) into a 24-well plate in self-renewal/proliferation media and the number of primary neurospheres formed was assessed in a blinded manner after 7 days. Primary neurospheres were dissociated with Accutase (Chemicon) and plated in triplicate at low density (1 to 4000 cells/ml) into a 24-well plate in self-renewal/proliferation media and the number of secondary neurospheres formed was assessed after 7 days. For moderate hypoxia (2%), cell culture dishes were placed into an Invivo$_2$ humidified hypoxia workstation (Ruskinn Technologies, Bridgend, UK).

NSC Ability to Generate Different Neural Lineages

Secondary neurospheres from self-renewal assays were plated onto acid-treated glass coverslips (Bellco) coated with poly-D-lysine (Sigma, 50 μg/ml) and incubated in differentiation media (NeuroBasal-A medium supplemented with penicillin-streptomycin-glutamine, B27 supplement, and 1% fetal bovine serum [Invitrogen]). Differentiated neurospheres were fixed in 4% PFA and then stained with antibodies to Tuj1 (Covance, 1:1000) or to GFAP (guinea pig, Advanced Immunochemicals Inc., 1:1000). Alternatively, neurospheres were incubated with the antibody to O4 (a gift from Ben Barres, 1:1 in 10% goat serum/1% BSA/0.1 M L-lysine) before fixation. Secondary antibodies (Molecular Probes) were used at a dilution of 1:400. For quantification, three coverslips containing 50 whole neurospheres per coverslip were counted in a blinded manner.

Microarray Analysis

FoxO3$^{-/-}$ and *FoxO3*$^{+/+}$ secondary neurospheres were collected 6 days after initial plating at 5 × 10^4 cells/ml. Total RNA was extracted with the mirVana kit (Ambion). Microarray hybridization was performed at the Stanford Protein and Nucleic Acid facility with oligonucleotide arrays (Affymetrix, Mouse Genome 430 2.0 Array). Background adjustment and normalization with RMA (robust multiarray analysis) was performed. The RankProd implementation of the method of Rank Products was used to determine the differentially expressed probes.

ACCESSION NUMBERS

Microarray data were deposited at the Gene Expression Omnibus (GEO) database under the accession number GSE18326.

SUPPLEMENTAL DATA

Supplemental Data include Supplemental Experimental Procedures, 10 figures, and 1 table and can be found with this article online at http://www.cell.com/immunity/supplemental/S1934-5909(09)00510-4.

ACKNOWLEDGMENTS

Work supported by an NIH/NIA grant R01 AG026648, a CIRM grant, a Brain Tumor Society grant, a Klingenstein Fellowship, and an AFAR grant (A.B.), a Stanford University Dean's fellowship (V.M.R.), an NSF graduate fellowship (V.A.R.), an NIH/NRSA 5T32 CA09302 (A.E.W.), the Lucile Packard Foundation for Children's Health and NLM grant R01 LM009719 (A.J.B.), and NLM grant T15 LM007033 (A.A.M.). We thank Kimmi Hoang for help with mouse colony management, Michael Stadler for help with Luxol blue staining, Ben Barres for the generous gift of the O4 antibody, Brandon Cord (T.D.P.'s lab) for help in NSC cultures, and Nathan Woodling (Katrin Andreasson's lab) for help with the BrdU protocol. We thank Ioanna Papandreou (N.C.D.'s lab) for her help with low-oxygen experiments. We thank Ron DePinho for the generous gift of the *FoxO3*$^{-/-}$ and *FoxO3*$^{lox/lox}$ mice and for discussing results prepublication. We thank Steve Artandi, Michael Greenberg, Tom Rando, Julien Sage, and members of the Brunet lab for critically reading the manuscript.

Received: September 29, 2008
Revised: June 26, 2009
Accepted: September 28, 2009
Published: November 5, 2009

REFERENCES

Accili, D., and Arden, K.C. (2004). FoxOs at the crossroads of cellular metabolism, differentiation, and transformation. Cell *117*, 421–426.

Alvarez-Buylla, A., and Temple, S. (1998). Stem cells in the developing and adult nervous system. J. Neurobiol. *36*, 105–110.

Bakker, W.J., Harris, I.S., and Mak, T.W. (2007). FOXO3a is activated in response to hypoxic stress and inhibits HIF1-induced apoptosis via regulation of CITED2. Mol. Cell *28*, 941–953.

Bondolfi, L., Ermini, F., Long, J.M., Ingram, D.K., and Jucker, M. (2004). Impact of age and caloric restriction on neurogenesis in the dentate gyrus of C57BL/6 mice. Neurobiol. Aging *25*, 333–340.

Brunet, A., Bonni, A., Zigmond, M.J., Lin, M.Z., Juo, P., Hu, L.S., Anderson, M.J., Arden, K.C., Blenis, J., and Greenberg, M.E. (1999). Akt promotes cell survival by phosphorylating and inhibiting a Forkhead transcription factor. Cell *96*, 857–868.

Clelland, C.D., Choi, M., Romberg, C., Clemenson, G.D., Jr., Fragniere, A., Tyers, P., Jessberger, S., Saksida, L.M., Barker, R.A., Gage, F.H., et al. (2009). A functional role for adult hippocampal neurogenesis in spatial pattern separation. Science *325*, 210–213.

Emerling, B.M., Weinberg, F., Liu, J.L., Mak, T.W., and Chandel, N.S. (2008). PTEN regulates p300-dependent hypoxia-inducible factor 1 transcriptional activity through Forkhead transcription factor 3a (FOXO3a). Proc. Natl. Acad. Sci. USA *105*, 2622–2627.

Fasano, C.A., Dimos, J.T., Ivanova, N.B., Lowry, N., Lemischka, I.R., and Temple, S. (2007). shRNA knockdown of Bmi-1 reveals a critical role for p21-Rb pathway in NSC self-renewal during development. Cell Stem Cell *1*, 87–99.

Flachsbart, F., Caliebe, A., Kleindorp, R., Blanche, H., von Eller-Eberstein, H., Nikolaus, S., Schreiber, S., and Nebel, A. (2009). Association of FOXO3A variation with human longevity confirmed in German centenarians. Proc. Natl. Acad. Sci. USA *106*, 2700–2705.

Gheusi, G., Cremer, H., McLean, H., Chazal, G., Vincent, J.D., and Lledo, P.M. (2000). Importance of newly generated neurons in the adult olfactory bulb for odor discrimination. Proc. Natl. Acad. Sci. USA *97*, 1823–1828.

Groszer, M., Erickson, R., Scripture-Adams, D.D., Dougherty, J.D., Le Belle, J., Zack, J.A., Geschwind, D.H., Liu, X., Kornblum, H.I., and Wu, H. (2006). PTEN negatively regulates neural stem cell self-renewal by modulating G0–G1 cell cycle entry. Proc. Natl. Acad. Sci. USA *103*, 111–116.

Imayoshi, I., Sakamoto, M., Ohtsuka, T., Takao, K., Miyakawa, T., Yamaguchi, M., Mori, K., Ikeda, T., Itohara, S., and Kageyama, R. (2008). Roles of continuous neurogenesis in the structural and functional integrity of the adult forebrain. Nat. Neurosci. *11*, 1153–1161.

Johnson, M.A., Ables, J.L., and Eisch, A.J. (2009). Cell-intrinsic signals that regulate adult neurogenesis in vivo: Insights from inducible approaches. BMB Rep. *42*, 245–259.

Keith, B., and Simon, M.C. (2007). Hypoxia-inducible factors, stem cells, and cancer. Cell *129*, 465–472.

Kempermann, G., Kuhn, H.G., and Gage, F.H. (1998). Experience-induced neurogenesis in the senescent dentate gyrus. J. Neurosci. *18*, 3206–3212.

Kenyon, C. (2005). The plasticity of aging: Insights from long-lived mutants. Cell *120*, 449–460.

Kinney, B.A., Meliska, C.J., Steger, R.W., and Bartke, A. (2001). Evidence that Ames dwarf mice age differently from their normal siblings in behavioral and learning and memory parameters. Horm. Behav. *39*, 277–284.

Kippin, T.E., Martens, D.J., and van der Kooy, D. (2005). p21 loss compromises the relative quiescence of forebrain stem cell proliferation leading to exhaustion of their proliferation capacity. Genes Dev. *19*, 756–767.

Li, L., Liu, F., Salmonsen, R.A., Turner, T.K., Litofsky, N.S., Di Cristofano, A., Pandolfi, P.P., Jones, S.N., Recht, L.D., and Ross, A.H. (2002). PTEN in neural precursor cells: regulation of migration, apoptosis, and proliferation. Mol. Cell. Neurosci. *20*, 21–29.

McElwee, J.J., Schuster, E., Blanc, E., Thomas, J.H., and Gems, D. (2004). Shared transcriptional signature in *Caenorhabditis elegans* Dauer larvae and

long-lived daf-2 mutants implicates detoxification system in longevity assurance. J. Biol. Chem. *279*, 44533–44543.

Mirzadeh, Z., Merkle, F.T., Soriano-Navarro, M., Garcia-Verdugo, J.M., and Alvarez-Buylla, A. (2008). Neural stem cells confer unique pinwheel architecture to the ventricular surface in neurogenic regions of the adult brain. Cell Stem Cell *3*, 265–278.

Miyamoto, K., Araki, K.A., Naka, K., Arai, F., Takubo, K., Yamazaki, S., Matsuoka, S., Miyamoto, T., Ito, K., Ohmura, M., et al. (2007). Foxo3a is essential for maintenance of the hematopoietic stem cell pool. Cell Stem Cell *1*, 101–112.

Molofsky, A.V., He, S., Bydon, M., Morrison, S.J., and Pardal, R. (2005). Bmi-1 promotes neural stem cell self-renewal and neural development but not mouse growth and survival by repressing the p16Ink4a and p19Arf senescence pathways. Genes Dev. *19*, 1432–1437.

Molofsky, A.V., Slutsky, S.G., Joseph, N.M., He, S., Pardal, R., Krishnamurthy, J., Sharpless, N.E., and Morrison, S.J. (2006). Increasing p16INK4a expression decreases forebrain progenitors and neurogenesis during ageing. Nature *443*, 448–452.

Paik, J.H., Kollipara, R., Chu, G., Ji, H., Xiao, Y., Ding, Z., Miao, L., Tothova, Z., Horner, J.W., Carrasco, D.R., et al. (2007). FoxOs are lineage-restricted redundant tumor suppressors and regulate endothelial cell homeostasis. Cell *128*, 309–323.

Paik, J.-h., Ding, Z., Narurkar, R., Ramkissoon, S., Muller, F., Kamoun, W.S., Chae, S.-S., Zheng, H., Ying, H., Mahoney, J., et al. (2009). FoxOs cooperatively regulate diverse pathways governing neural stem cell homeostasis. Cell Stem Cell *5*, this issue, 540–553.

Palmer, T.D., Takahashi, J., and Gage, F.H. (1997). The adult rat hippocampus contains primordial neural stem cells. Mol. Cell. Neurosci. *8*, 389–404.

Reynolds, B.A., and Rietze, R.L. (2005). Neural stem cells and neurospheres—re-evaluating the relationship. Nat. Methods *2*, 333–336.

Reynolds, B.A., and Weiss, S. (1992). Generation of neurons and astrocytes from isolated cells of the adult mammalian central nervous system. Science *255*, 1707–1710.

Salih, D.A., and Brunet, A. (2008). FoxO transcription factors in the maintenance of cellular homeostasis during aging. Curr. Opin. Cell Biol. *20*, 126–136.

Shen, Q., Wang, Y., Kokovay, E., Lin, G., Chuang, S.M., Goderie, S.K., Roysam, B., and Temple, S. (2008). Adult SVZ stem cells lie in a vascular niche: A quantitative analysis of niche cell-cell interactions. Cell Stem Cell *3*, 289–300.

Sinor, A.D., and Lillien, L. (2004). Akt-1 expression level regulates CNS precursors. J. Neurosci. *24*, 8531–8541.

Studer, L., Csete, M., Lee, S.H., Kabbani, N., Walikonis, J., Wold, B., and McKay, R. (2000). Enhanced proliferation, survival, and dopaminergic differentiation of CNS precursors in lowered oxygen. J. Neurosci. *20*, 7377–7383.

Sun, L.Y., Evans, M.S., Hsieh, J., Panici, J., and Bartke, A. (2005). Increased neurogenesis in dentate gyrus of long-lived Ames dwarf mice. Endocrinology *146*, 1138–1144.

Tavazoie, M., Van der Veken, L., Silva-Vargas, V., Louissaint, M., Colonna, L., Zaidi, B., Garcia-Verdugo, J.M., and Doetsch, F. (2008). A specialized vascular niche for adult neural stem cells. Cell Stem Cell *3*, 279–288.

Tothova, Z., Kollipara, R., Huntly, B.J., Lee, B.H., Castrillon, D.H., Cullen, D.E., McDowell, E.P., Lazo-Kallanian, S., Williams, I.R., Sears, C., et al. (2007). FoxOs are critical mediators of hematopoietic stem cell resistance to physiologic oxidative stress. Cell *128*, 325–339.

Tronche, F., Kellendonk, C., Kretz, O., Gass, P., Anlag, K., Orban, P.C., Bock, R., Klein, R., and Schutz, G. (1999). Disruption of the glucocorticoid receptor gene in the nervous system results in reduced anxiety. Nat. Genet. *23*, 99–103.

Tropepe, V., Craig, C.G., Morshead, C.M., and van der Kooy, D. (1997). Transforming growth factor-alpha null and senescent mice show decreased neural progenitor cell proliferation in the forebrain subependyma. J. Neurosci. *17*, 7850–7859.

Willcox, B.J., Donlon, T.A., He, Q., Chen, R., Grove, J.S., Yano, K., Makaki, K.H., Willcox, D.C., Rodriguez, B., and Curb, J.D. (2008). FOXO3A genotype is strongly associated with human longevity. Proc. Natl. Acad. Sci. USA *105*, 13987–13992.

Yilmaz, O.H., Valdez, R., Theisen, B.K., Guo, W., Ferguson, D.O., Wu, H., and Morrison, S.J. (2006). Pten dependence distinguishes haematopoietic stem cells from leukaemia-initiating cells. Nature *441*, 475–482.

Zhang, C.L., Zou, Y., He, W., Gage, F.H., and Evans, R.M. (2008). A role for adult TLX-positive neural stem cells in learning and behaviour. Nature *451*, 1004–1007.

Zhao, C., Deng, W., and Gage, F.H. (2008). Mechanisms and functional implications of adult neurogenesis. Cell *132*, 645–660.

Zhu, L.L., Wu, L.Y., Yew, D.T., and Fan, M. (2005). Effects of hypoxia on the proliferation and differentiation of NSCs. Mol. Neurobiol. *31*, 231–242.

Cell Stem Cell, Volume *5*

Supplemental Data

FoxO3 Regulates Neural Stem Cell Homeostasis

Valérie M. Renault, Victoria A. Rafalski, Alex A. Morgan, Dervis A.M. Salih, Jamie O. Brett, Ashley E. Webb, Saul A. Villeda, Pramod U. Thekkat, Camille Guillerey, Nicholas C. Denko, Theo D. Palmer, Atul J. Butte, and Anne Brunet

Supplemental Experimental Procedures

Antibodies

Antibodies to β-actin, GAPDH, and karyopherin β were obtained from Novus Biological, Abcam, and Santa Cruz Biotechnology respectively. Antibodies to GFAP were obtained from Dako, antibodies to CNPase and Sox2 (Y-17) were purchased from Santa Cruz, and antibodies to NeuN were purchased from Millipore. The antibody to myc (9E10) was purchased from Calbiochem and the antibody to BrdU was from AbD serotec. Antibodies to Nestin and cleaved caspase 3 were obtained from BD Pharmingen and Cell Signaling Technology respectively. Antibodies to phospho-T32 and to FoxO3 ('NFL' and 'Ct') were described previously (Brunet et al., 1999; Greer et al., 2007). 'NFL' is directed to full length human FoxO3. 'Ct' is directed to amino-acids 497 to 601 of mouse FoxO3.

Immunohistochemistry on mouse brain sections

Mice were anesthetized and perfused transcardially with PBS containing 5 U/ml of Heparin, then by 4% paraformaldehyde (PFA). Brains were fixed in 4% PFA

for 4 hours at 4ºC, then in 30% Sucrose/4% PFA overnight at 4ºC, and embedded in Tissue-Tek (Sakura) at -80ºC. Coronal sections (40 µm) were obtained using a microtome (MICROM). The antigens were retrieved by a 30-min incubation in Sodium Citrate 10 mM pH 6.0/Triton 0.05% at 80ºC. Sections were incubated with primary antibodies (FoxO3 'Ct', 1:500; NeuN, 1:600; Sox2, 1:200; BrdU, 1:500) overnight at 4ºC, with secondary antibodies (biotinylated donkey anti-rabbit, 1:400; Texas Red donkey anti-mouse, anti-goat, or anti-rat, 1:400, Jackson ImmunoResearch) overnight at 4ºC, and then with Fluorescein-DFAT streptavidin (1:500, Jackson ImmunoResearch) overnight at 4ºC. Fluorescent images were taken with a Leica confocal with LCS Leica Confocal Software (Cell Sciences Imaging Facility, Stanford University).

Western blotting

NSC protein extracts were obtained by lysing NSC in lysis buffer (Tris HCl pH 8.0 (50 mM), NaCl (100 mM), EGTA (2 mM), NaF (10 mM), β-glycerophosphate (40 mM), Triton-X100 (0.4%), aprotinin (10 µg/ml), phenylmethylsulfonyl fluoride (PMSF, 1 mM)). Tissue protein extracts were obtained by lysing tissues in RIPA buffer (Tris-HCl pH 8.0 (50 mM), NaCl (150 mM), EDTA (1 mM), NP-40 (1%), Na-deoxycholate (0.25%), PMSF (10 mM), Aprotinin (10 µg/ml), NaF (10 mM), β-glycerophosphate (40 mM)). Thirty µg of proteins was resolved on SDS-PAGE (10%) and transferred onto nitrocellulose membranes. The membranes were incubated with primary antibodies and the primary antibody was visualized using

HRP-conjugated anti-mouse or anti-rabbit secondary antibodies and enhanced chemiluminescence (ECL, Amersham).

Luciferase assays

NSC at early passages were seeded at 10^5 cells/ml in poly-D-lysine-coated 24-well plates. The next day, NSC were transfected using Lipofectamine (Invitrogen) with 200 ng of a luciferase reporter construct driven by three tandem repeats of the FoxO binding element contained in the FasL promoter (FHRE pGL3) (Brunet et al., 1999), 200 ng of a *Renilla* luciferase reporter construct (pRL0), and for the positive controls, 200 ng of FoxO3 constructs in pECE plasmids (Brunet et al., 1999). Forty-eight hours after transfection, cells were lysed and luciferase and renilla luciferase activities were measured using the Dual Luciferase Reporter Assay System (Promega) according to the manufacturer's protocol.

BrdU and cleaved caspase 3 immunocytochemistry

Freshly dissociated NSC were plated onto acid-treated glass coverslips (Bellco) coated with poly-D-lysine (Sigma, 50 μg/ml) at a density of 5 x 10^4 cells/ml in 24-well dishes. Twenty-four hours later, BrdU (10 μM) was added for 1 hr and the cells were fixed in 4% PFA and permeabilized in 0.4%Triton for 30 min. Coverslips were incubated with 2N HCl for 30 min, and washed extensively with PBS. Coverslips were incubated with primary antibodies (BrdU, 1:500) and with secondary antibodies (Alexa 488 goat anti-rat, 1:400, Molecular Probes). For

quantification, at least 1,000 cells per coverslip on three different coverslips from two independent experiments were counted in a blinded manner.

For cleaved caspase 3 staining, twenty-four hours after plating, cells were fixed in 4% PFA and permeabilized with 0.1% Triton X-100 for 30 min. Coverslips were incubated with antibodies to cleaved caspase 3 (1:400) and with the Alexa 555 goat anti-rabbit antibodies (1:400, Molecular Probes). Cleaved caspase 3-positive nuclei were quantified in a blinded manner from a total of more than 1,000 nuclei on three coverslips.

References for GSEA analysis (Figure 7C)

(1): (Mense et al., 2006);

(2): (Harris, 2002);

(3): (Kim et al., 2003);

(4): (Leonard et al., 2003);

(5): (Semenza, 2001);

(6): http://www.broad.mit.edu/gsea/msigdb/cards/V$HIF1_Q3.html;

(7): (Lu et al., 2004);

(8): (Carter et al., 2005);

(9): http://www.broad.mit.edu/gsea/msigdb/cards/V$FOXO4_01.html;

(10): (Chang et al., 2004);

(11): (Kanehisa et al., 2008);

(12): http://wikipathways.org/index.php/Pathway:WP534.

Chromatin Immunoprecipitation

NSC from 3 month-old mice were plated at a density of 1 x 10^5 cells/ml. Twenty four hours later, dissociated NSC were switched to medium without EGF and bFGF for 4 hours and treated with 20 μM LY294002 (Calbiochem) for 1 hour to activate endogenous FoxO3 (Brunet et al., 1999). Cells were crosslinked with 1% PFA for 10 min. Crosslinking was stopped with 0.125 M glycine for 5 min. NSC were resuspended in swelling buffer (HEPES pH 7.8 (10 mM), $MgCl_2$ (1.5 mM), KCl (10 mM), NP-40 (0.1%), DTT (1 mM), PMSF (0.5 mM)), and incubated on ice for 15 min, and then dounced 25 times. Nuclei were pelleted and resuspended in RIPA buffer (10% NP-40, 10% sodium deoxycholate, 10% SDS in PBS, with protease inhibitor tablet [Roche]). Chromatin was sheared by sonication with a Vibra-Cell Sonicator VC130 (Sonics) six times for 30 s at 60% amplitude. Chromatin was cleared by centrifugation at 14,000 rpm for 15 min at 4°C. Immunoprecipitation was done as described (Mortazavi et al., 2006). Briefly, 5 μg of IgG antibody (Zymed) or 2.5 μg each of anti-FoxO3 'NFL' and H-144 (Santa Cruz Biotechnology) was coupled to sheep anti-rabbit IgG Dynabeads (Invitrogen). Chromatin from 5-8 x10^6 NSC was incubated with antibody-coupled beads. Beads were washed with solutions from Upstate Biotechnology (1 x low salt buffer, 2 x high salt buffer, 3 x LiCl Buffer, 2 x TE) and chromatin was eluted (NaHCO3 (0.1M), SDS (1%)) at 65°C for 1 hr. Crosslinks were reversed by an overnight incubation at 65°C. DNA was purified and concentrated with the PCR purification kit (Qiagen). For quantification of the ChIP products, real-time PCR was performed using a BioRad CFX96 Real Time System and C1000 Thermal

Cycler. The following primers were used with the following conditions: 0.5x SYBR Green (BioRad), 0.5 mM forward primer, 0.5 mM reverse primer, 2.5 μl DNA using the following program: 94°C for 3 minutes, then 40 cycles of 95°C for 20 seconds, 57°C for 30 seconds, 72°C for 30 seconds:

p27^{KIP1} (forward): 5' TTTTTACGCATCGCTGCTACT 3',

p27^{KIP1} (reverse): 5' GCTTAGCCGACCTCACTACG 3',

Ddit4 (forward): 5' CTTTCAGCAGCTGCCAAGGTC 3',

Ddit4 (reverse): 5' CAGAAGCTAGGGGTACCTTTCTC 3',

negative control (forward) 5' GGGGGATAATGATTGCAAAA 3'

negative control (reverse): 5' GCGTGGACAGAGATGTAGGC 3'.

Standard curves were calculated for each primer set using a serial dilution of the input, and were in turn used to determine fold enrichment relative to the IgG control ChIP.

FoxO3 antibody specificity

HEK293T cells were transfected with empty vector or with myc-tagged mouse FoxO family members (FoxO1, FoxO3, FoxO4 and FoxO6 in pcDNA4.1). Briefly, 2.5 μg of DNA was transfected in each well of a 12-well plate (350,000 cells per well) using the calcium phosphate method. Forty eight hours after plating, cells were fixed in 4% PFA and permeabilized with 0.1% Triton X-100 for 30 min. Coverslips were incubated with antibodies to FoxO3 ('Ct'; 1:500) or to myc (1:500) for 2 hours and washed with PBS. Cells were then incubated for 1 hr with Texas Red goat anti-rabbit antibodies or FITC goat anti-mouse antibodies (1:400,

Molecular Probes). Coverslips were mounted in Vectashield containing DAPI. Pictures were taken randomly using a fluorescent microscope and AxioVision 4 software (Zeiss).

Multipotency assay

After 7 days in a neurosphere assay (low cell plating density, 1 to 4,000 cells/ml), secondary or tertiary neurospheres were collected and transferred onto acid-treated glass coverslips coated with poly-D-lysine (50 µg/ml) in 24-well plate. Neurosphere differentiation was induced by incubation in differentiation medium (NeuroBasal-A medium supplemented with penicillin-streptomycin-glutamine, B27 supplement (2%) and 1% Fetal Bovine Serum (FBS)) for 7 days. Differentiation medium was changed every other day for a week. To simultaneously determine the ability of neurospheres to differentiate into astrocytes, neurons and oligodendrocytes, unfixed differentiated neurospheres were incubated with the antibody to O4 (1:1 in 10% goat serum/1% BSA/0.1M L-lysine) for 2 hrs at room temperature before fixation using 4% PFA for 15 min. Neurospheres were the incubated with secondary antibodies (biotinylated donkey anti-mouse, 1:400, Jackson Immunologicals) for 1 hr at room temperature, followed by an incubation with the ABC system (Vector Laboratories) for 30 min at room temperature, and the reaction with the DAB solution (Sigma, 0.05%) containing 0.015% H_2O_2 for 10 min. Differentiated neurospheres were next stained with antibodies to Tuj1 (1:1,000) and GFAP (guinea pig, 1:1,000). Secondary antibodies (Alexa 488 goat anti-rabbit and goat anti-guinea pig,

Molecular Probes) were used at a dilution of 1:400. The coverslips were mounted on slides using Vectashield containing DAPI (Vector laboratories) and examined under epifluorescent illumination using a Zeiss microscope digital camera with AxioVision 4 software. For quantification, 20 to 50 whole neurospheres were counted in a blinded manner.

Reverse-transcription followed by quantitative PCR

The expression of mouse transcripts was determined by reverse transcription of total RNA followed by quantitative PCR analysis (RT-qPCR). After a DNAse treatment, 2 µg of total RNA was reverse transcribed (High Capacity Reverse Transcription kit, Applied Biosystems) according to the manufacturer's protocol. Real-time PCR was performed on a Bio-rad iCycler using iQ SYBR Green mix (BioRad) with the following primers:

Cyclin G2: 5' TCTTGGCCCTTATGAAGGTGA 3' (forward) and

5' CATTTACACTGACTGATGCGGAT 3' (reverse),

Ero1l: 5' TCAAACCCTGCCATTCTGATG 3' (forward) and

5' TCAGCTTGCTCACATTCTTCAA 3' (reverse),

Mbp: 5' GGGCATCCTTGACTCCATCG 3' (forward) and

5' GCTCTGCTTTAGCCAGGGT 3' (reverse),

Myelin (plp1): 5' TGAGCGCAACGGTAACAGG 3' (forward) and

5' GGGAGAACACCATACATTCTGG 3' (reverse),

Otx2: 5' TATCTAAAGCAACCGCCTTACG 3' (forward) and

5' AAGTCCATACCCGAAGTGGTC 3' (reverse),

p27^{KIP1}: 5’ CAGAGTTTGCCTGAGACCCAA 3’ (forward) and

5’ GCAGGAGAGCCAGGATGTCA 3’ (reverse),

Pdk1: 5” GGACTTCGGGTCAGTGAATGC 3’ (forward) and

5’ TCCTGAGAAGATTGTCGGGGA 3’ (reverse),

Selenbp1: 5’ ATGGCTACAAAATGCACAAAGTG 3’ (forward) and

5’ CCTGTGTTCCGGTAAATGCAG 3’ (reverse),

Slc2a3: 5’ ATGGGGACAACGAAGGTGAC 3’ (forward) and

5’ GTCTCAGGTGCATTGATGACTC 3’ (reverse),

Vegfa: 5’ GTACCCCGACGAGATAGAGT 3’ (forward) and

5’ ATGATCTGCATGGTGATGTTG 3’ (reverse),

Xlr3a: 5’ TTGATGCTGGTAGGGAGGACA 3’ (forward) and

5’ AGAACTTTGTTAGGTGGCTCTTC 3’ (reverse),

β-actin: 5’ TGTTACCAACTGGGACGACA 3’ (forward) and

5’ CTCTCAGCTGTGGTGGTGAA 3’ (reverse).

The experiments were conducted in triplicate and the results were expressed as $2^{-(\text{Gene of interest Ct-}\beta\text{-actin Ct})}$. Control PCR reactions were also performed on total RNA that had not been reverse-transcribed to test for the presence of genomic DNA in the RNA preparation.

Histopathology

Histopathology was performed on 3 month-old *FoxO3*$^{-/-}$ and *FoxO3*$^{+/+}$ mice using the Luxol Fast Blue staining method. Briefly, 30 µm coronal brain sections were mounted on slides and were dehydrated and immersed in Luxol Fast Blue

solution (Sigma) overnight at 60ºC. Slides were rinsed in 95% ethanol for 5 min, in distilled water for 5 min, and then in 0.05% lithium carbonate, in 70% ethanol, and in distilled water. Slides were dehydrated and mounted using Permount (Fisher Scientific). The corpus callosa of *FoxO3*$^{-/-}$ and *FoxO3*$^{+/+}$ brains were measured at Bregma -1.34 mm by light microscopy and normalized by the brain section area.

Electrophoretic Mobility Shift Assay

Electrophoretic mobility shift assays were performed as described (Greer et al., 2007). Briefly, the forward and reverse oligonucleotides surrounding FoxO canonical binding sites in the promoters of specific genes were annealed and labeled with polynucleotide kinase in the presence of [γ-^{32}P] ATP for 30 min. The following oligonucleotides containing FoxO canonical binding sites (underlined) were used:

FoxO3_01 (*Otx2*): 5' CGGACAGTGTTA<u>AATAAACAAGGG</u>TCTCTTTAAAAT 3' (forward) and 5' ATTTTAAAGAGA<u>CCCTTGTTTATTT</u>AACACTGTCCG 3' (reverse),

FoxO4_01 (*Ddit4*): 5' GGATCAAGGAAA<u>GACTTGTTTATTAT</u>AGGGGCGCG 3' (forward) and 5' CGCGCCCCT<u>ATAATAAACAAGTC</u>TTTCCTTGATCC 3' (reverse),

FoxO3_01 (*Ndrg1*): 5' GTAGCCTGGCAAGGTTTGTTTATGTCCGTGCGTGCGT AGGGC 3' (forward) and 5' GCCCTACGCACGCACGGACATAAACAAACCTTG CCAGGCTAC 3' (reverse)

The double-stranded probes were purified from a 15% native gel. 10,000 cpm of labeled probes were incubated for 20 min at room temperature with 100–500 ng of recombinant GST-FoxO3 protein and 6 μg of salmon sperm DNA in electrophoretic mobility shift assay binding buffer (Tris-HCl, pH 7.5 (50 mM), KCl (250 mM), dithiothreitol (5 mM), $MgCl_2$ (25 mM), glycerol (50%), and Nonidet P-40 (0.25%)). The reactions were then resolved by electrophoresis on 4% native acrylamide gels. Gels were dried and autoradiographed.

Author contributions

V.M.R. designed, performed and analyzed all experiments, except the ones indicated below, and supervised J.O.B and C.G. V.A.R. designed, performed and analyzed NSC differentiation markers by Western blot and self-renewal assays in low oxygen conditions. A.M. analyzed the microarray data. D.A.S. helped characterize *FoxO3*$^{lox/lox}$;*Nestin-Cre* mice, measure mouse brain weight, and stain corpus callosum. J.O.B. performed and analyzed RT-qPCR and EMSA experiments. A.E.W. designed, performed, and analyzed ChIP experiments. S.A.V. initiated a similar project in rat NSC and provided ideas. P.U.T. helped with Western blotting, immunocytochemistry, and the mouse colony. C.G. performed and analyzed luciferase experiments. N.C.D. helped with low oxygen experiments and provided ideas. T.D.P helped set up NSC cultures and provided ideas. A.J.B. supervised A.M., helped analyze the microarray data and provided ideas. A.B. helped design and analyze the experiments. V.M.R. and A.B. wrote the paper, with the help of V.A.R., J.O.B., A.E.W., and A.M..

Supplemental References

Brunet, A., Bonni, A., Zigmond, M.J., Lin, M.Z., Juo, P., Hu, L.S., Anderson, M.J., Arden, K.C., Blenis, J., and Greenberg, M.E. (1999). Akt promotes cell survival by phosphorylating and inhibiting a Forkhead transcription factor. Cell *96*, 857-868.

Carter, T.A., Greenhall, J.A., Yoshida, S., Fuchs, S., Helton, R., Swaroop, A., Lockhart, D.J., and Barlow, C. (2005). Mechanisms of aging in senescence-accelerated mice. Genome Biol *6*, R48.

Chang, H.Y., Sneddon, J.B., Alizadeh, A.A., Sood, R., West, R.B., Montgomery, K., Chi, J.T., van de Rijn, M., Botstein, D., and Brown, P.O. (2004). Gene expression signature of fibroblast serum response predicts human cancer progression: similarities between tumors and wounds. PLoS biology *2*, E7.

Greer, E.L., Oskoui, P.R., Banko, M.R., Maniar, J.M., Gygi, M.P., Gygi, S.P., and Brunet, A. (2007). The energy sensor AMP-activated protein kinase directly regulates the mammalian FOXO3 transcription factor. J Biol Chem *282*, 30107-30119.

Harris, A.L. (2002). Hypoxia--a key regulatory factor in tumour growth. Nat Rev Cancer *2*, 38-47.

Kanehisa, M., Araki, M., Goto, S., Hattori, M., Hirakawa, M., Itoh, M., Katayama, T., Kawashima, S., Okuda, S., Tokimatsu, T.*, et al.* (2008). KEGG for linking genomes to life and the environment. Nucleic Acids Res *36*, D480-484.

Kim, H., Lee, D.K., Choi, J.W., Kim, J.S., Park, S.C., and Youn, H.D. (2003). Analysis of the effect of aging on the response to hypoxia by cDNA microarray. Mech Ageing and Dev *124*, 941-949.

Leonard, M.O., Cottell, D.C., Godson, C., Brady, H.R., and Taylor, C.T. (2003). The role of HIF-1 alpha in transcriptional regulation of the proximal tubular epithelial cell response to hypoxia. J Biol Chem *278*, 40296-40304.

Lu, T., Pan, Y., Kao, S.Y., Li, C., Kohane, I., Chan, J., and Yankner, B.A. (2004). Gene regulation and DNA damage in the ageing human brain. Nature *429*, 883-891.

Mense, S.M., Sengupta, A., Zhou, M., Lan, C., Bentsman, G., Volsky, D.J., and Zhang, L. (2006). Gene expression profiling reveals the profound upregulation of hypoxia-responsive genes in primary human astrocytes. Physiol Genomics *25*, 435-449.

Mortazavi, A., Leeper Thompson, E.C., Garcia, S.T., Myers, R.M., and Wold, B. (2006). Comparative genomics modeling of the NRSF/REST repressor network: from single conserved sites to genome-wide repertoire. Genome Res *16*, 1208-1221.

Semenza, G.L. (2001). Hypoxia-inducible factor 1: oxygen homeostasis and disease pathophysiology. Trends Mol Med *7*, 345-350.

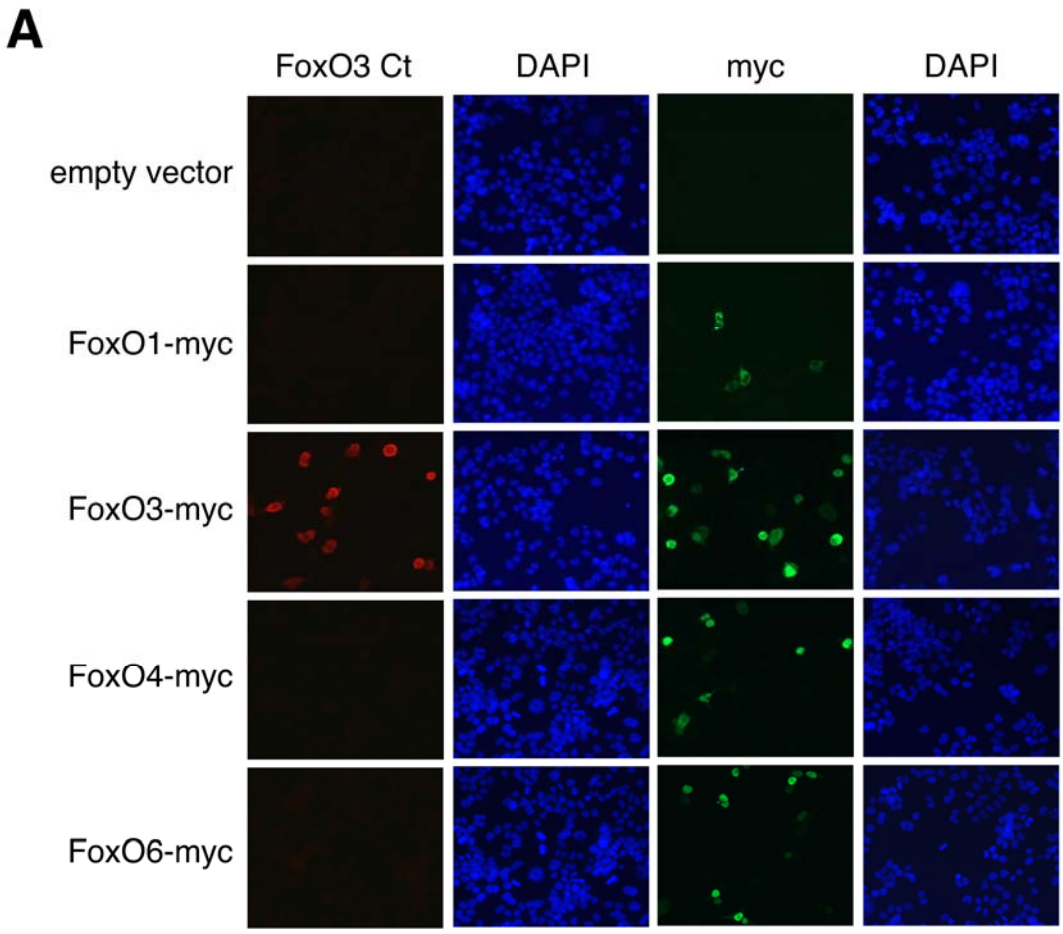
A
FoxO3 Ct
DAPI
myc
DAPI
empty vector
FoxO1-myc
FoxO3-myc
FoxO4-myc
FoxO6-myc

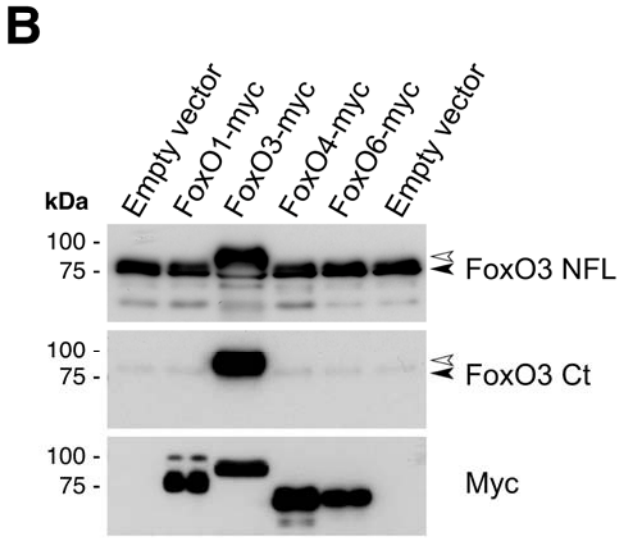
B
kDa
Empty vector
FoxO1-myc
FoxO3-myc
FoxO4-myc
FoxO6-myc
Empty vector
100 -
75 -
FoxO3 NFL
100 -
75 -
FoxO3 Ct
100 -
75 -
Myc

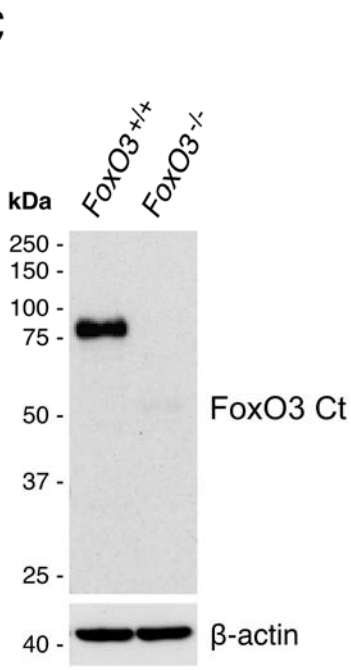
C
kDa
FoxO3+/+
FoxO3-/-
250 -
150 -
100 -
75 -
50 -
37 -
25 -
FoxO3 Ct
40 -
β-actin

Figure S1. Specificity of the antibodies to FoxO3
(A) Specificity of the 'Ct' antibody to FoxO3 by immunocytochemistry. HEK293T cells expressing myc-tagged forms of mouse FoxO1, FoxO3, FoxO4, and FoxO6 were immunostained with antibodies to FoxO3 'Ct' and to the myc epitope. Cell nuclei were stained with DAPI. **(B-C)** Specificity of the 'NFL' and 'Ct' antibodies to FoxO3 by Western blotting. **(B)** Western blotting of protein extracts of 293T cells expressing myc-tagged forms of mouse FoxO1, FoxO3, FoxO4, and FoxO6 using antibodies to FoxO3 ('NFL' or 'Ct') and to the myc epitope. Empty arrowhead: Overexpressed myc-FoxO3. Filled arrowhead: endogenous FoxO3. **(C)** Western blots of protein lysates from secondary neurospheres in self-renewal conditions from 3 month-old *FoxO3*$^{+/+}$ and *FoxO3*$^{-/-}$ littermates probed with antibodies to FoxO3 ('Ct') and to β-actin as a loading control. Molecular weights are indicated in kDa.

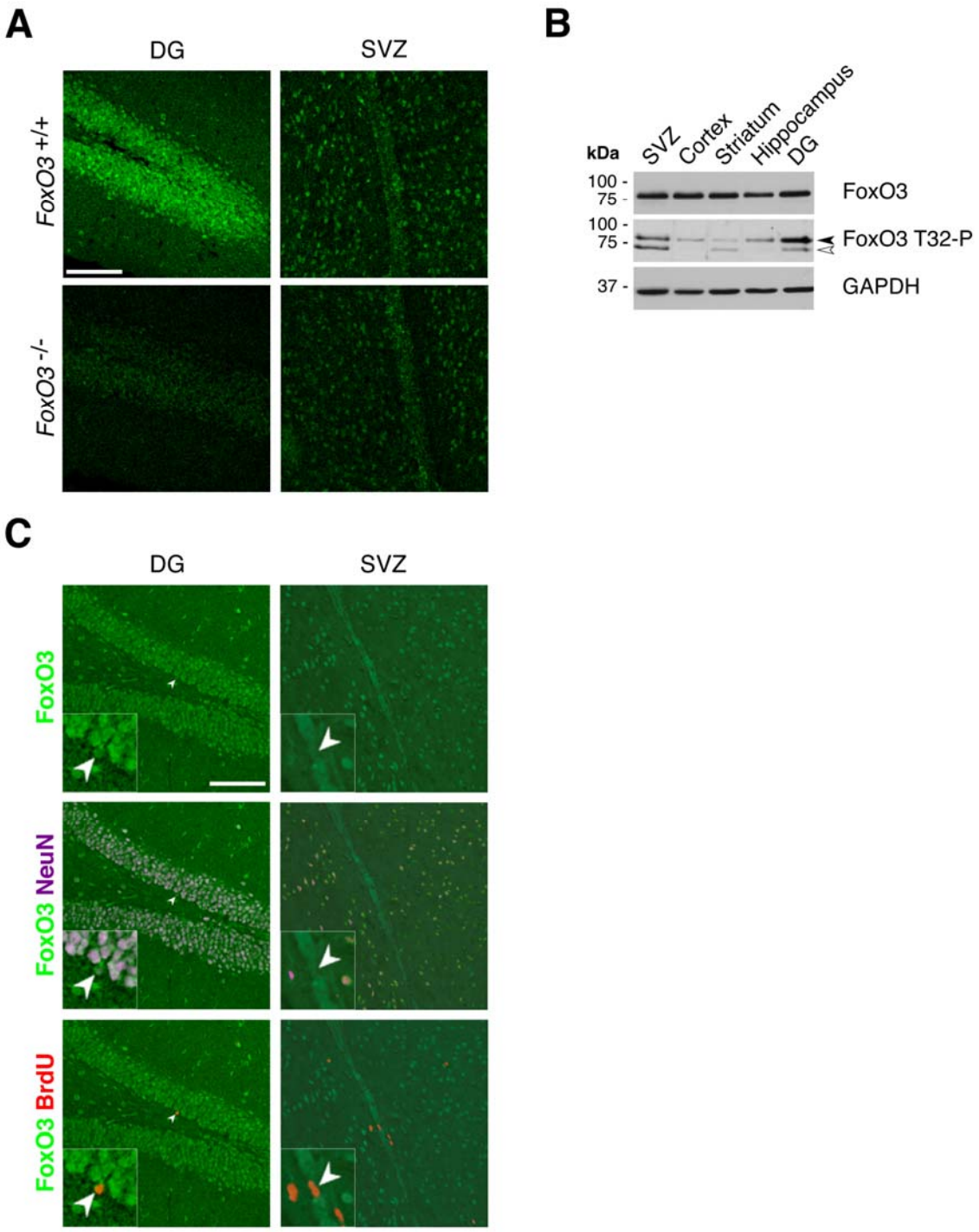

Figure S2. FoxO3 is expressed in NSC niches *in vivo*
(A) FoxO3 expression in NSC niches *in vivo*. Immunohistochemistry of FoxO3 in the DG and the SVZ of adult *FoxO3*$^{+/+}$ and *FoxO3*$^{-/-}$ brains, showing the specificity of the FoxO3 antibody ('Ct'). Note that there is remaining staining in *FoxO3*$^{-/-}$ brain sections that is likely background staining. Scale bar: 50 μm. (B) FoxO3 expression in adult brain regions. Western blots of lysates from the SVZ,

DG, and cortex isolated from adult wild-type brain probed with antibodies to FoxO3 ('NFL'), to phospho-Threonine 32 (FoxO3 T32-P: filled arrowhead), and to GAPDH as a loading control. The T32-P antibodies recognize a band of lower molecular weight in these brain tissues, which likely corresponds to another FoxO family member (empty arrowhead), as this phosphorylation site and the surrounding amino-acids are conserved in other FoxO family members and as this band is still seen in *FoxO3*$^{-/-}$ extracts (data not shown). Note that in protein extracts from dissected brain regions, it is not possible to distinguish NSC from progenitors and differentiating progeny. (C) FoxO3 is expressed in BrdU-positive label-retaining NSC *in vivo*. Immunohistochemistry with antibodies to FoxO3 ('Ct'), to NeuN, and to BrdU in the DG and SVZ of 3 month-old mice one month after 7 days of daily BrdU injections. BrdU-positive/NeuN-negative/FoxO3-positive nuclei in the SGZ and in the SVZ are shown by white arrowheads. Scale bar: 100 µm.

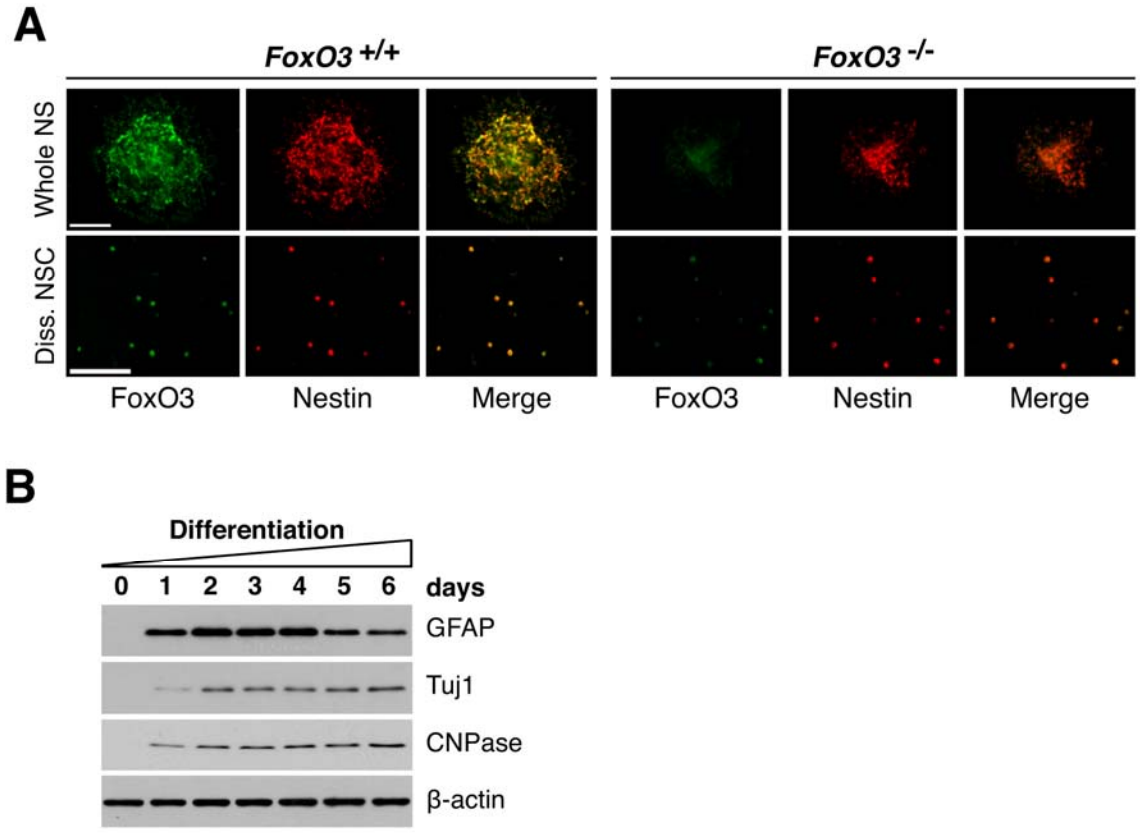

Figure S3. FoxO3 is expressed in NSC *in vitro*
(A) FoxO3 is expressed in NSC in culture. Immunocytochemistry on NSC isolated from 3 month-old *FoxO3*$^{+/+}$ and *FoxO3*$^{-/-}$ littermate neonate mice with antibodies to FoxO3 ('NFL') and to Nestin (NSC/progenitor marker). NSC were either grown as neurospheres (whole NS) (top panels) or freshly dissociated NSC (Diss. NSC) (bottom panels). Note that there is remaining staining in *FoxO3*$^{-/-}$ NSC that is likely background staining. Similar results were obtained with adult NSC. Scale bars: 200 μm. (B) Differentiation marker expression during NSC differentiation. Western blots of protein lysates of dissociated wild-type NSC in self-renewal conditions (day 0) or in differentiation conditions for increasing lengths of time (day 1-6). Western blots were probed with antibodies to Tuj1 (neurons), GFAP (astrocytes), CNPase (oligodendrocytes), and β-actin as a loading control, to verify that NSC differentiated under these conditions.

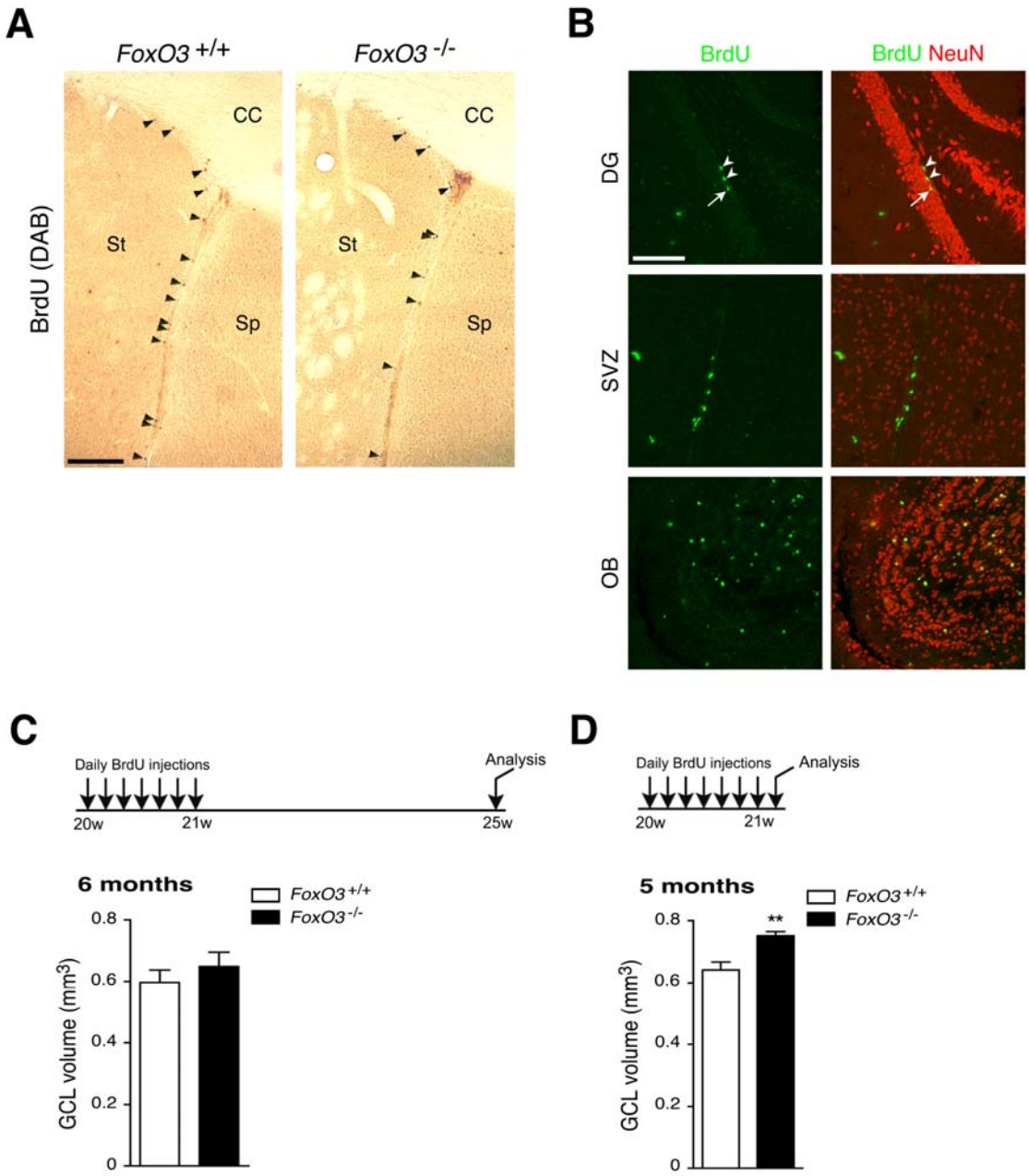

Figure S4. Quantification of label-retaining NSC in *FoxO3*$^{+/+}$ and *FoxO3*$^{-/-}$ brains *in vivo*

(A) Label-retaining NSC in the SVZ of *FoxO3*$^{+/+}$ and *FoxO3*$^{-/-}$ mice. Coronal sections of adult *FoxO3*$^{+/+}$ and *FoxO3*$^{-/-}$ mouse brains showing BrdU-positive nuclei in the SVZ one month after 7 days of daily BrdU injections. Label-retaining NSC are indicated by a filled arrowhead. St: striatum, Sp: septum, CC: corpus callosum. Scale bar: 200 µm. (B) Label-retaining cells are NeuN-negative in the SGZ and the SVZ. Immunohistochemistry of BrdU and NeuN (neuronal marker) in the SVZ and the DG one month after 7 days of daily BrdU injection. BrdU-

positive nuclei were negatively labeled for NeuN in the SGZ (arrowhead) and in the SVZ, while BrdU-positive nuclei were positively labeled for NeuN in the granular cell layer (GCL, arrow) and in the olfactory bulb (OB). Scale bar: 100 μm. (C) Volume of the granule cell layer in 6 month-old adult *FoxO3*$^{+/+}$ and *FoxO3*$^{-/-}$ littermates 4 weeks after 7 daily BrdU injections. Quantification of the granular cell layer (GCL) area of the DG in 10-12 coronal sections using Metamorph. Values represent mean ± SD of 5 animals for *FoxO3*$^{+/+}$ and 4 animals for *FoxO3*$^{-/-}$ mice. Mann-Whitney test, p=0.11. (D) Volume of the granule cell layer in 5 month-old adult *FoxO3*$^{+/+}$ and *FoxO3*$^{-/-}$ littermates one day after 7 daily BrdU injections. Quantification of the granular cell layer (GCL) area of the DG in 10-12 coronal sections using Metamorph. Values represent mean ± SD of 3 animals for *FoxO3*$^{+/+}$ and 3 animals for *FoxO3*$^{-/-}$ mice. Mann-Whitney test, **: $p<0.01$.

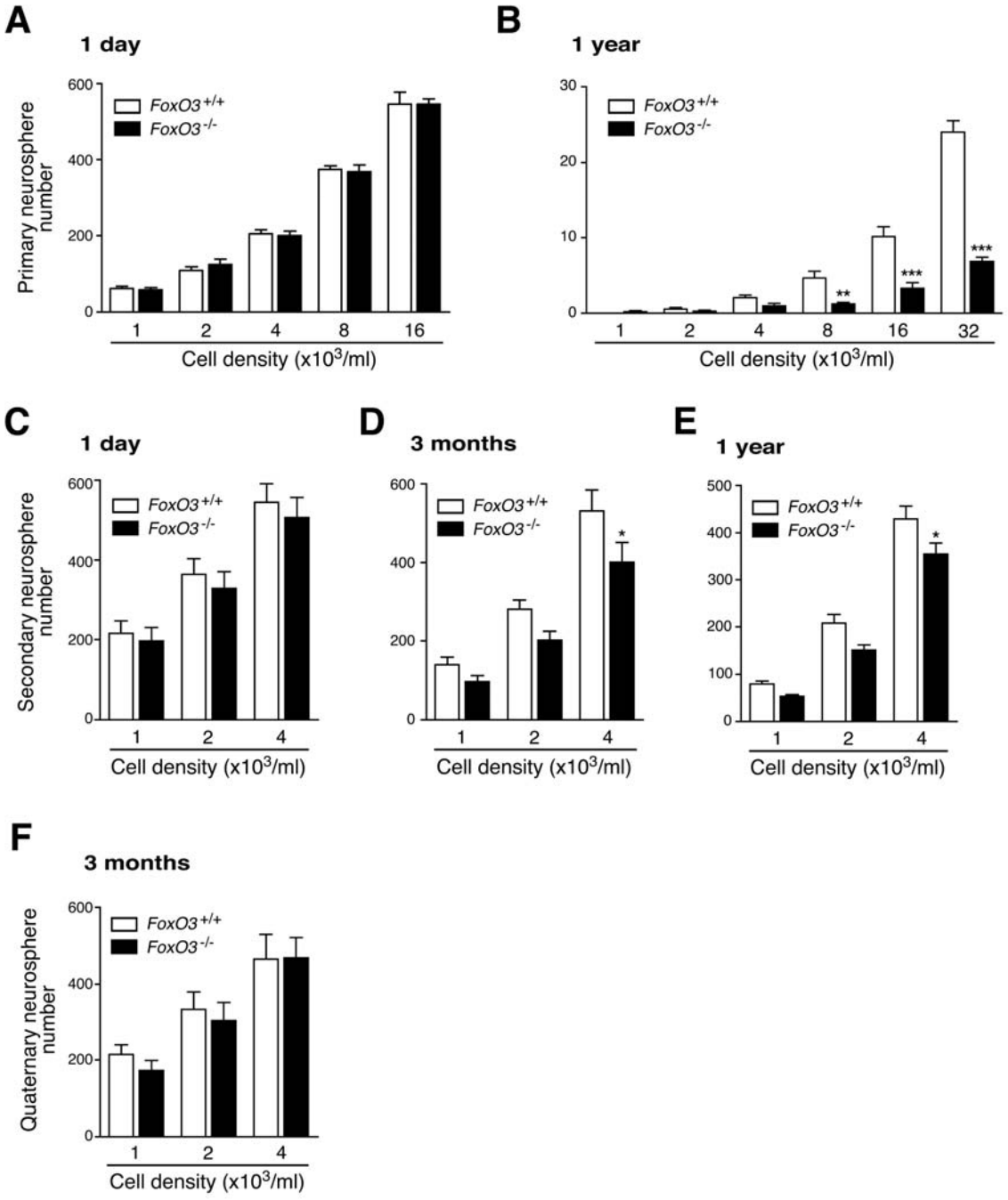

Figure S5. Quantification of the neurosphere-forming ability of *FoxO3*$^{+/+}$ and *FoxO3*$^{-/-}$ NSC

(A-B) *FoxO3*$^{-/-}$ NSC from middle-aged adult mice, but not from neonate mice, display a defect in primary neurosphere formation. NSC freshly isolated from *FoxO3*$^{+/+}$ or *FoxO3*$^{-/-}$ littermates at two different ages were seeded in triplicate at a density of 1,000 to 32,000 cells/ml and the number of neurospheres formed

after one week was counted. (A) 1 day-old. Values represent mean ± SD of 2 independent experiments conducted with two littermates for each genotype. Two-way ANOVA, p=0.9766 for the genotype variable; (B) 1 year-old. Values represent mean ± SD of 3 independent experiments conducted with 3 to 5 littermates for each genotype. Two-way ANOVA, p<0.0001 for the genotype variable, Bonferroni post-tests, **: p<0.01; ***: p<0.001. (C-E) Adult *FoxO3*$^{-/-}$ NSC display a defect in secondary neurosphere formation. Dissociated primary neurospheres formed after NSC isolation from *FoxO3*$^{+/+}$ or *FoxO3*$^{-/-}$ littermates at 3 different ages (1 day-old, C; 3 month-old, D; 1 year-old, E), were seeded at 1,000 to 4,000 cells/ml and the number of secondary neurospheres formed after one week was counted. Values represent mean ± SEM of 2 independent experiments with two littermates (C), 4 independent experiments with 5 littermates (D), and 4 independent experiments with 3-5 littermates (E) for each genotype. Two-way ANOVA, p=0.3587 (C), p=0.0028 (D), and p=0.0004 (E) for the genotype variable, Bonferroni post-tests, *: p<0.05. (F) Self-renewal is not affected at later passages in *FoxO3*$^{-/-}$ NSC versus *FoxO3*$^{+/+}$ NSC. NSC from 3 month-old *FoxO3*$^{+/+}$ or *FoxO3*$^{-/-}$ littermates were seeded at a density of 1,000 to 4,000 cells/ml, and the number of neurospheres formed after one week was counted. Values represent mean ± SEM of 2 independent experiments conducted with 5 littermates for each genotype. Two-way ANOVA, p=0.5501 for the genotype variable.

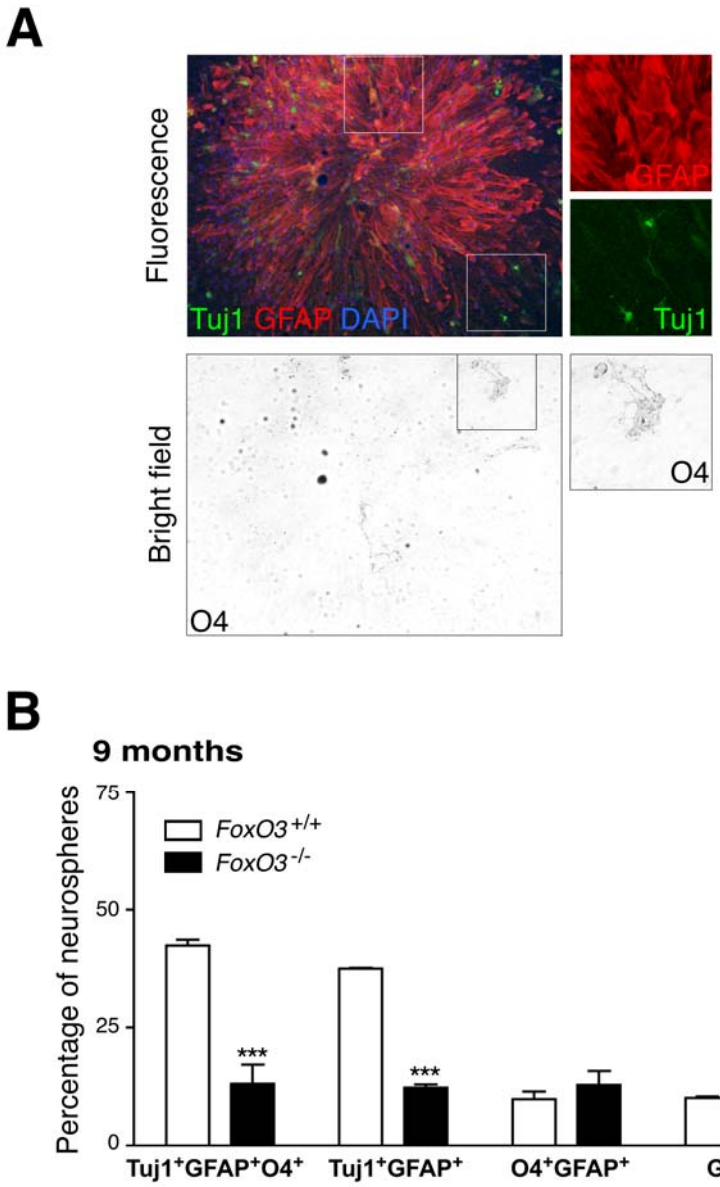

Figure S6. *FoxO3*$^{-/-}$ NSC from adult mice have defects in multipotency compared to *FoxO3*$^{+/+}$ NSC

(A) *FoxO3*$^{+/+}$ and *FoxO3*$^{-/-}$ NSC from 9 month-old mice were grown as secondary or tertiary neurospheres at low density and placed in differentiation medium for 7 days. Neurospheres were stained simultaneously with antibodies to Tuj1 (neurons), GFAP (astrocytes), and O4 (oligodendrocytes). A multipotent neurosphere (Tuj1-positive/GFAP-positive/O4-positive) is shown. (B) Neurospheres that contained all three types of progeny (Tuj1+/GFAP+/O4+), two types of progeny (Tuj1+/GFAP+ or O4+/GFAP+), or just one progeny (GFAP+) were counted in a blinded manner as a percentage of the total number of neurospheres. Values represent mean ± SEM of two independent experiments (secondary and tertiary neurospheres) on 2 littermates for each genotype. Two-

way ANOVA, Bonferroni post-tests, ***: $p<0.001$. Note that in Figure 4, the O4-positive neurospheres that were counted correspond to the sum of the Tuj1-positive/GFAP-positive/O4-positive and the GFAP-positive/O4-positive neurospheres.

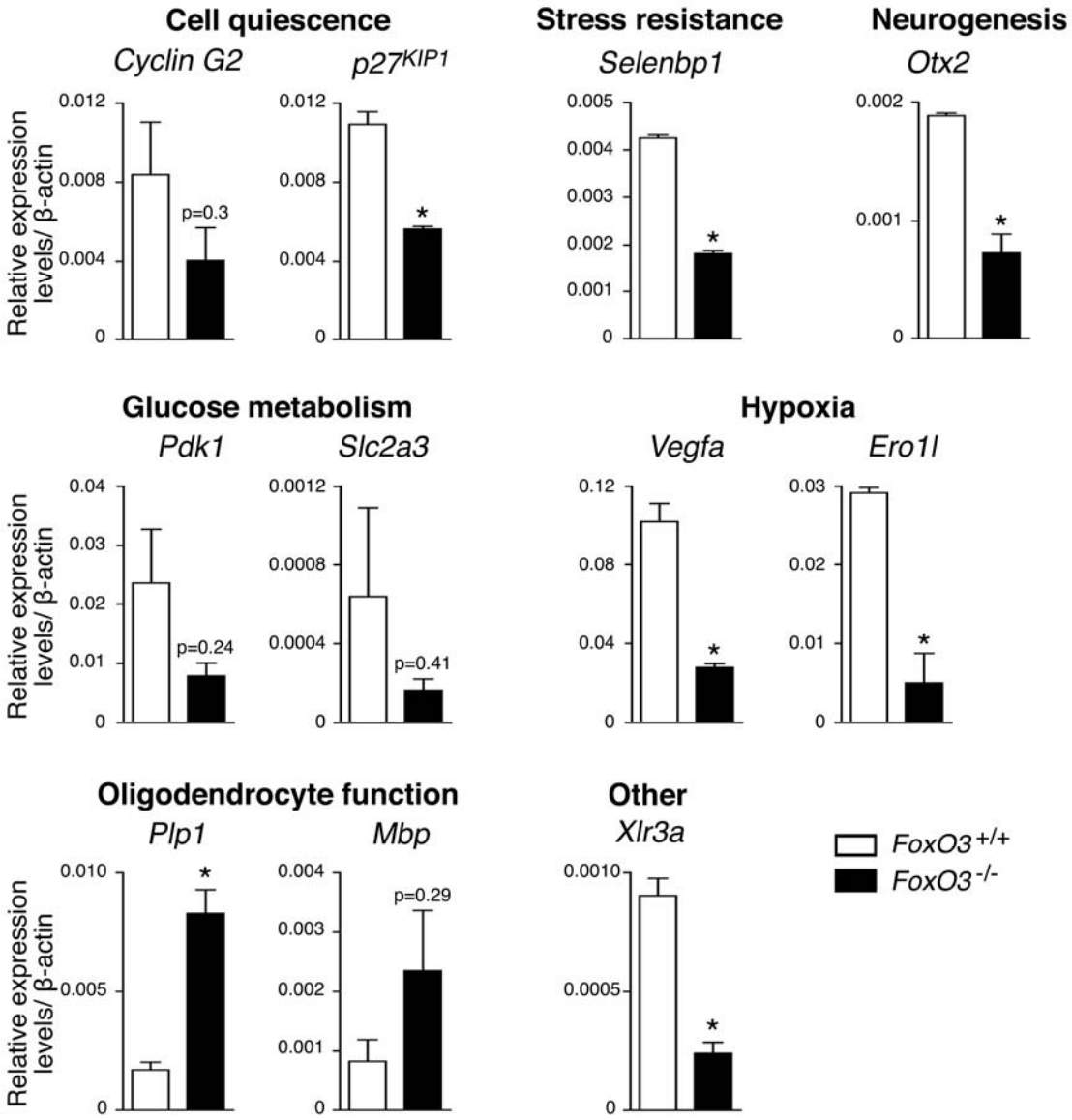

Figure S7. Validation of the differences in gene expression for selected genes differentially regulated between *FoxO3*$^{-/-}$ and *FoxO3*$^{+/+}$ NSC
RT-qPCR analysis of RNA from *FoxO3*$^{-/-}$ and *FoxO3*$^{+/+}$ secondary neurospheres from 3 month-old mice with primers to specific genes. The results are normalized by β-actin expression. Values represent mean ± SEM of two independent samples conducted in triplicate. These results were also observed in an independent experiment. Student's t-test, *: $p<0.05$.

A

B

Gene Title	Symbol
selenium binding protein 1	Selenbp1
Max interacting protein 1	Mxi1
cyclin G2	Ccng2
gelsolin	Gsn
myelin basic protein	Mbp
apolipoprotein D	Apod

C

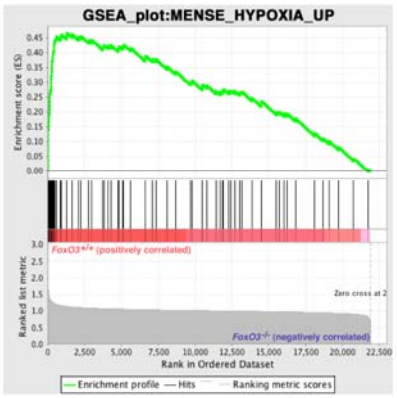

D

Gene Title	Symbol
solute carrier family 2 (facilitated glucose transporter), member 3	Slc2a3
N-myc downstream regulated gene 1	Ndrg1
ERO1-like (S. cerevisiae)	Ero1l
enolase 2, gamma neuronal	Eno2
protein phosphatase 1, regulatory (inhibitor) subunit 3C	Ppp1r3c
pyruvate dehydrogenase kinase, isoenzyme 1	Pdk1
ankyrin repeat domain 37	Ankrd37
BCL2/adenovirus E1B interacting protein 3	Bnip3
procollagen-proline, 2-oxoglutarate 4-dioxygenase (proline 4-hydroxylase), alpha II polypeptide	P4ha2
glucan (1,4-alpha-), branching enzyme 1	Gbe1
adrenomedullin	Adm
6-phosphofructo-2-kinase/fructose-2,6-biphosphatase 3	Pfkfb3
Max interacting protein 1	Mxi1
thymic stromal lymphopoietin	Tslp
procollagen-proline, 2-oxoglutarate 4-dioxygenase (proline 4-hydroxylase), alpha 1 polypeptide	P4ha1
insulin induced gene 2	Insig2

E

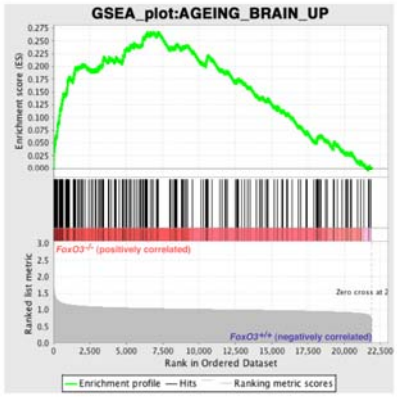

F

Gene Title	Symbol
DNA-damage-inducible transcript 4	Ddit4
N-myc downstream regulated gene 1	Ndrg1
PDZ and LIM domain 3	Pdlim3
caveolin, caveolae protein 1	Cav1
WD repeat domain, phosphoinositide interacting 1	Wipi1
regulator of G-protein signaling 20	Rgs20
spondin 1, (f-spondin) extracellular matrix protein	Spon1
caveolin 2	Cav2
angiotensinogen (serpin peptidase inhibitor, clade A, member 8)	Agt
apolipoprotein D	Apod
proteolipid protein (myelin) 1	Plp1
cytochrome P450, family 1, subfamily b, polypeptide 1	Cyp1b1

Figure S8. FoxO3-regulated genes are enriched for genes expressed in cell quiescence, hypoxia, and aging

(A) Gene set enrichment analysis plot for FoxO3-regulated genes and genes expressed in quiescent cells (Chang et al., 2004). (B) List of genes enriched for high levels of expression in quiescent cells and in *FoxO3*$^{+/+}$ NSC compared to *FoxO3*$^{-/-}$ NSC. (C) Gene set enrichment analysis plot for FoxO3-regulated genes

and genes expressed in hypoxic astrocytes and HeLa cells (Mense et al., 2006). (D) List of genes enriched for high levels of expression in hypoxic astrocytes and HeLa cells and in *FoxO3*$^{+/+}$ NSC compared to *FoxO3*$^{-/-}$ NSC. (E) Gene set enrichment analysis plot for FoxO3-regulated genes and genes expressed in human aging brains (Lu et al., 2004). (F) List of genes enriched for high levels of expression in human aging brains and in *FoxO3*$^{+/+}$ NSC compared to *FoxO3*$^{-/-}$ NSC.

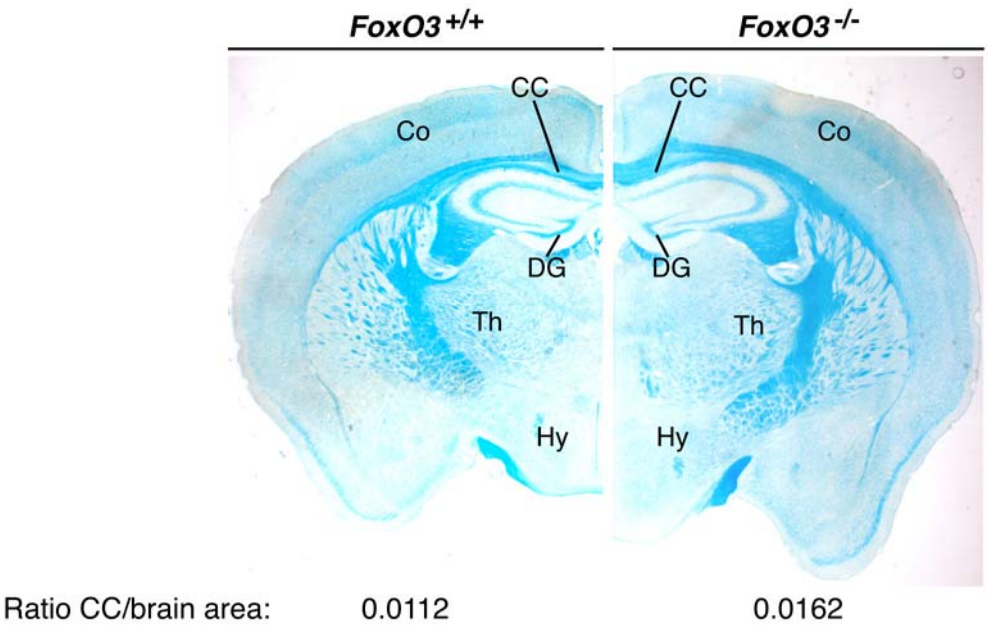

Figure S9. The corpus callosum area is increased relative to the brain area in adult *FoxO3*$^{-/-}$ mice compared to *FoxO3*$^{+/+}$ littermates
Histopathology of sections of 3 month-old *FoxO3*$^{-/-}$ and *FoxO3*$^{+/+}$ male brains using Luxol Fast Blue staining. Representative sections are shown. Co: cortex; DG: dentate gyrus; CC: corpus callosum; Th: thalamus; Hy: hypothalamus.

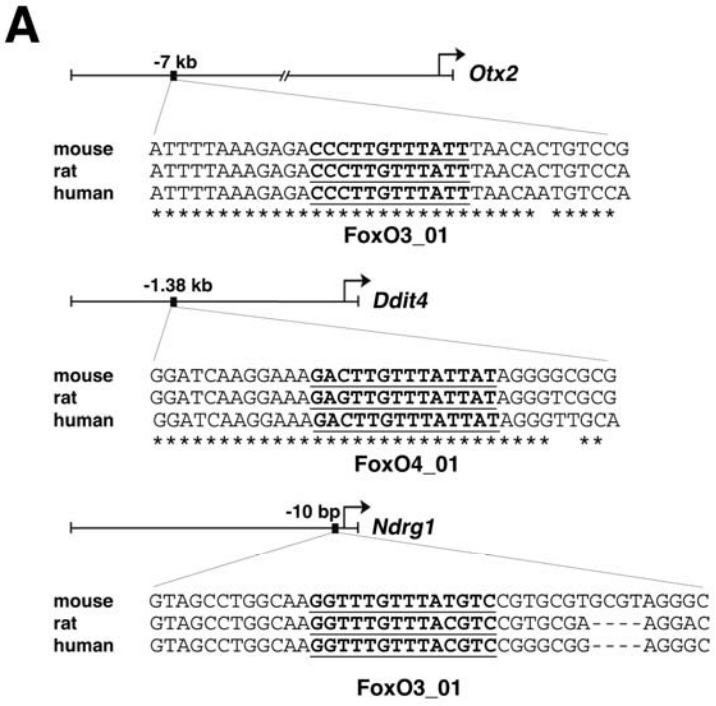

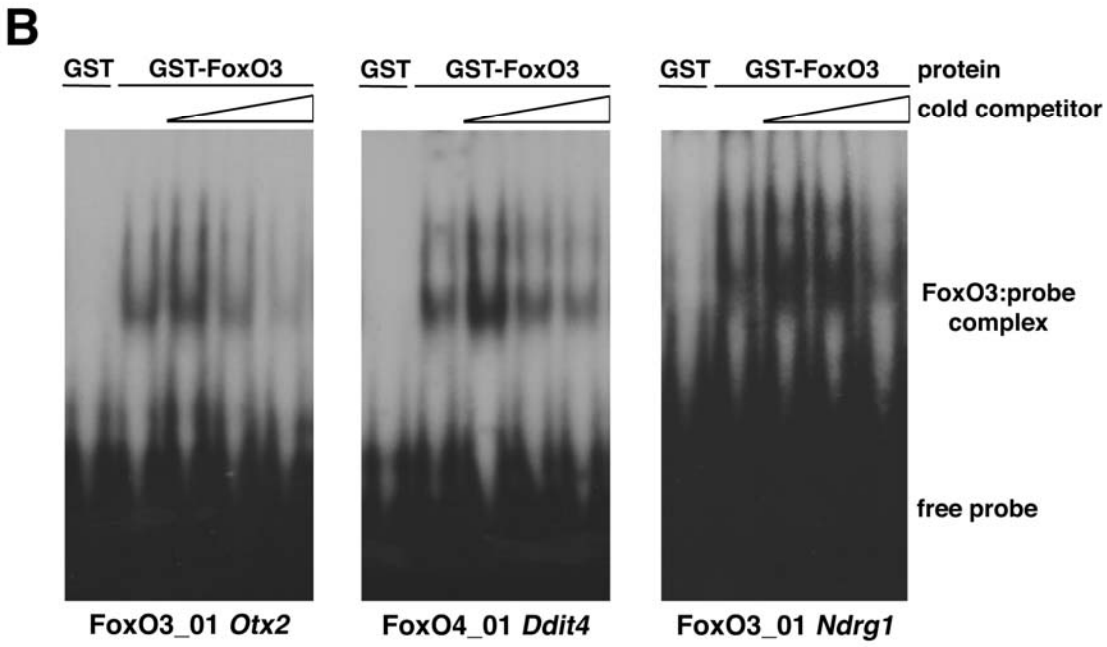

C

	Fold enrichement (compared to IgG)			
	Experiment #1		Experiment #2	
Target promoter	*FoxO3*$^{+/+}$	*FoxO3*$^{-/-}$	*FoxO3*$^{+/+}$	*FoxO3*$^{-/-}$
(-)	2.17	2.75	0.79	1.70
p27^{KIP1}	30.67	2.00	5.01	1.09
Ddit4	16.30	2.90	19.11	1.43

Figure S10. FoxO3 binds to FoxO binding sites in the regulatory regions of target genes

(A) Location of conserved FoxO binding sites in the regulatory regions of *Otx2, Ddit4,* and *Ndrg1* genes. Alignment of human, mouse, and rat sequences are shown. FoxO binding sites are bold and underlined. *: conserved nucleotides in the human, mouse, and rat sequences. (B) FoxO3 binds to FoxO binding sites in the regulatory regions of the genes encoding *Otx2, Ddit4,* and *Ndrg1.* Electrophoretic mobility shift assays (EMSA) using probes corresponding to FoxO binding sites in the regulatory regions of the *Otx2, Ddit4*, and *Ndrg1* genes and a purified form of human FoxO3 (GST-FoxO3). (C) Chromatin Immunoprecipitation (ChIP) of FoxO3 from adult NSC shows significant recruitment of FoxO3 at the promoters of $p27^{KIP1}$ and *Ddit4*. This enrichment of FoxO3 was not found at control regions that did not have FoxO binding sites and did not occur in $FoxO3^{-/-}$ neurospheres. The values presented correspond to the fold enrichment of ChIP with the FoxO3 antibodies over ChIP with control IgG in two independent experiments.

Table S1

Symbol	GeneID	Name	Probe	Fold Change (*FoxO3*$^{-/-}$ over *FoxO3*$^{+/+}$)	q-value	MENSE_HYPOXIA_UP	HYPOXIA_REVIEW	HYPOXIA_FIBRO_UP	HYPOXIA_REG_UP	HIF1_TARGETS	SERUM_FIBROBLAST_CORE_DN	V$_HIF1_Q3	AGEING_BRAIN_UP	AGED_MOUSE_HIPPOCAMPUS_ANY_UP	V$_FOXO4_01	SERUM_FIBROBLAST_CORE_DN	CHANG_SERUM_RESPONSE_DN	HSA00051_FRUCTOSE_AND_MANNOSE_METABOLISM	GLYCOLYSIS
Xlr3a	22445	X-linked lymphocyte-regulated 3A	1420357_s_at	0.341	0.000	0	0	0	0	0	0	0	0	0	0	0	0	0	0
FoxO3	56484	forkhead box O3a	1434831_a_at	0.445	0.000	0	0	0	0	0	0	0	0	0	0	0	0	0	0
FoxO3	56484	forkhead box O3a	1434832_at	0.478	0.000	0	0	0	0	0	0	0	0	0	0	0	0	0	0
Slc2a3	20527	solute carrier family 2 (facilitated glucose transporter), member 3	1455898_x_at	0.487	0.000	1	1	0	0	1	0	0	0	0	0	0	0	0	0
Slc2a3	20527	solute carrier family 2 (facilitated glucose transporter), member 3	1437052_s_at	0.488	0.000	1	1	0	0	1	0	0	0	0	0	0	0	0	0
Prss35	244954	protease, serine, 35	1434195_at	0.499	0.000	0	0	0	0	0	0	0	0	0	0	0	0	0	0
Vit	74199	vitrin	1426231_at	0.504	0.001	0	0	0	0	0	0	0	0	0	1	0	0	0	0
Cdh13	12554	cadherin 13	1454015_a_at	0.512	0.000	0	0	0	0	0	0	0	0	0	0	0	0	0	0
Sbsn	282619	suprabasin	1459897_a_at	0.517	0.001	0	0	0	0	0	0	0	0	0	0	0	0	0	0
Six3	20473	sine oculis-related homeobox 3 homolog (Drosophila)	1427523_at	0.519	0.000	0	0	0	0	0	0	0	0	0	0	0	0	0	0
Otx2	18424	orthodenticle homolog 2 (Drosophila)	1425926_a_at	0.525	0.001	0	0	0	0	0	0	0	0	0	1	0	0	0	0
Gad1	14415	glutamic acid decarboxylase 1	1416561_at	0.531	0.000	0	0	0	0	0	0	0	0	0	0	0	0	0	0
Ddit4	74747	DNA-damage-inducible transcript 4	1428306_at	0.536	0.000	0	0	0	1	0	0	1	1	1	1	0	0	0	0
Ndrg1	17988	N-myc downstream regulated gene 1	1423413_at	0.539	0.002	1	0	0	0	0	0	0	1	0	1	0	0	0	0
Selenbp1	20341	selenium binding protein 1	1450699_at	0.544	0.002	0	0	0	0	0	0	0	0	0	1	0	1	0	0
Afap1l2	226250	actin filament associated protein 1-like 2	1436870_s_at	0.546	0.002	0	0	0	0	0	0	0	0	0	0	0	0	0	0
Ndrg1	17988	N-myc downstream regulated gene 1	1456174_x_at	0.547	0.002	1	0	0	0	0	0	0	1	0	1	0	0	0	0
LOC100047339	100047339	similar to lysyl oxidase-like 2	1431004_at	0.549	0.002	0	0	0	0	0	0	0	0	0	0	0	0	0	0
Prelid2	77619	PRELI domain containing 2	1436194_at	0.549	0.003	0	0	0	0	0	0	0	0	0	0	0	0	0	0
Ero1l	50527	ERO1-like (S. cerevisiae)	1419030_at	0.552	0.002	1	0	0	0	0	0	1	0	0	0	0	0	0	0
Eno2	13807	enolase 2, gamma neuronal	1418829_a_at	0.552	0.002	1	0	1	0	0	0	0	0	0	0	0	0	0	1
Npnt	114249	nephronectin	1452106_at	0.556	0.002	0	0	0	0	0	0	0	0	0	0	0	0	0	0
Selenbp2	20342	selenium binding protein 2	1417580_s_at	0.557	0.002	0	0	0	0	0	0	0	0	0	0	0	0	0	0
AI851790	268354	expressed sequence AI851790	1438007_at	0.558	0.002	0	0	0	0	0	0	0	0	0	0	0	0	0	0
2900019G14Rik	72932	RIKEN cDNA 2900019G14 gene	1438194_at	0.559	0.002	0	0	0	0	0	0	0	0	0	0	0	0	0	0
Ero1l	50527	ERO1-like (S. cerevisiae)	1449324_at	0.560	0.002	1	0	0	0	0	0	1	0	0	0	0	0	0	0
Vegfa	22339	vascular endothelial growth factor A	1420909_at	0.561	0.002	0	0	0	0	0	0	0	0	0	0	0	0	0	0
Ppp1r3c	53412	protein phosphatase 1, regulatory (inhibitor) subunit 3C	1425631_at	0.566	0.002	1	0	0	1	0	0	1	0	0	0	0	0	0	0
Gdpd3	68616	glycerophosphodiester phosphodiesterase domain containing 3	1449526_a_at	0.567	0.001	0	0	0	0	0	0	0	0	0	0	0	0	0	0
Lhfpl3	269629	lipoma HMGIC fusion partner-like 3	1433990_at	0.570	0.002	0	0	0	0	0	0	0	0	0	0	0	0	0	0
Ero1l	50527	ERO1-like (S. cerevisiae)	1419029_at	0.574	0.003	1	0	0	0	0	0	1	0	0	0	0	0	0	0
Fosl2	14284	fos-like antigen 2	1437247_at	0.576	0.002	0	0	0	0	0	0	0	0	0	1	0	0	0	0
Mmd2	75104	monocyte to macrophage differentiation-associated 2	1438654_x_at	0.581	0.003	0	0	0	0	0	0	0	0	0	0	0	0	0	0
Nrn1	68404	neuritin 1	1428393_at	0.583	0.002	0	0	0	0	0	0	0	0	0	0	0	0	0	0
Sbsn	282619	suprabasin	1439630_x_at	0.587	0.004	0	0	0	0	0	0	0	0	0	0	0	0	0	0
Pdk1	228026	pyruvate dehydrogenase kinase, isoenzyme 1	1423747_a_at	0.588	0.003	1	0	0	0	0	0	0	0	0	0	0	0	0	0
Pdk4	27273	pyruvate dehydrogenase kinase, isoenzyme 4	1417273_at	0.592	0.004	0	0	0	0	0	0	0	0	0	1	0	0	0	0
NA	NA	NA	1452107_s_at	0.592	0.006	0	0	0	0	0	0	0	0	0	0	0	0	0	0
Ddx3y	26900	DEAD (Asp-Glu-Ala-Asp) box polypeptide 3, Y-linked	1426438_at	0.593	0.002	0	0	0	0	0	0	0	0	0	0	0	0	0	0
3110057O12Rik	269423	RIKEN cDNA 3110057O12 gene	1455475_at	0.594	0.003	0	0	0	0	0	0	0	0	0	0	0	0	0	0
Ankrd37	654824	ankyrin repeat domain 37	1436538_at	0.595	0.003	1	0	0	0	0	0	0	0	0	0	0	0	0	0
Ndrg2	29811	N-myc downstream regulated gene 2	1448154_at	0.596	0.003	0	0	0	0	0	0	0	0	0	0	0	0	0	0
Fgf11	14166	fibroblast growth factor 11	1439959_at	0.598	0.005	0	0	0	0	0	0	1	0	0	0	0	0	0	0
Lgi1	56839	leucine-rich repeat LGI family, member 1	1423183_at	0.599	0.011	0	0	0	0	0	0	0	0	0	0	0	0	0	0
Vegfa	22339	vascular endothelial growth factor A	1451959_a_at	0.600	0.005	0	0	0	0	0	0	0	0	0	0	0	0	0	0
Mmd2	75104	monocyte to macrophage differentiation-associated 2	1424534_at	0.601	0.005	0	0	0	0	0	0	0	0	0	0	0	0	0	0
Clu	12759	clusterin	1437689_x_at	0.601	0.008	0	0	0	0	0	0	0	0	0	0	0	0	0	0
Six3os1	100043902	Six3 opposite strand transcript 1	1431168_at	0.603	0.003	0	0	0	0	0	0	0	0	0	0	0	0	0	0
Ppp1r3c	53412	protein phosphatase 1, regulatory (inhibitor) subunit 3C	1433691_at	0.604	0.002	1	0	0	1	0	0	1	0	0	0	0	0	0	0
Gng2	14702	guanine nucleotide binding protein (G protein), gamma 2	1418452_at	0.604	0.003	0	0	0	0	0	0	0	0	0	0	0	0	0	0
Ndrg1	17988	N-myc downstream regulated gene 1	1420760_s_at	0.605	0.009	1	0	0	0	0	0	0	1	0	1	0	0	0	0
Cdh13	12554	cadherin 13	1434115_at	0.606	0.006	0	0	0	0	0	0	0	0	0	0	0	0	0	0
Pcdh15	11994	protocadherin 15	1444317_at	0.609	0.006	0	0	0	0	0	0	0	0	0	0	0	0	0	0
Slc2a3	20527	solute carrier family 2 (facilitated glucose transporter), member 3	1421924_at	0.609	0.006	1	1	0	0	1	0	0	0	0	0	0	0	0	0
Flt1	14254	FMS-like tyrosine kinase 1	1419300_at	0.613	0.007	0	1	0	0	1	0	0	0	0	1	0	0	0	0
Dbp	13170	D site albumin promoter binding protein	1438211_s_at	0.613	0.006	0	0	0	0	0	0	0	0	1	1	0	0	0	0
Fgf1	14164	fibroblast growth factor 1	1423136_at	0.613	0.004	0	0	0	0	0	0	0	0	0	0	0	0	0	0
Angpt2	11601	angiopoietin 2	1448831_at	0.614	0.009	0	1	0	0	0	0	0	0	0	1	0	0	0	0
Pdlim3	53318	PDZ and LIM domain 3	1449178_at	0.614	0.004	0	0	0	0	0	0	0	1	0	1	0	0	0	0
Nr2f2	11819	nuclear receptor subfamily 2, group F, member 2	1416158_at	0.614	0.011	0	0	0	0	0	0	1	0	0	1	0	0	0	0
Gng2	14702	guanine nucleotide binding protein (G protein), gamma 2	1428156_at	0.620	0.008	0	0	0	0	0	0	0	0	0	0	0	0	0	0
Gpi1	14751	glucose phosphate isomerase 1	1456909_at	0.620	0.003	0	0	0	0	0	0	0	0	0	0	0	0	0	0
Pdlim4	30794	PDZ and LIM domain 4	1417928_at	0.620	0.006	0	0	1	0	0	0	0	0	0	1	0	0	0	0
Bnip3	12176	BCL2/adenovirus E1B interacting protein 3	1422470_at	0.622	0.007	1	1	1	1	1	0	0	0	0	0	0	0	0	0

Car12		76459	carbonic anyhydrase 12	1428485_at	0.624	0.008	0	0	0	0	0	0	0	0	0	0	0	0	0	0	0	0	0
Tmem178		68027	transmembrane protein 178	1429175_at	0.624	0.009	0	0	0	0	0	0	0	0	0	0	0	0	0	0	0	0	0
Cav1		12389	caveolin, caveolae protein 1	1449145_a_at	0.626	0.025	0	0	0	0	0	0	0	1	0	0	0	0	0	0	0	0	0
Itga7		16404	integrin alpha 7	1418393_a_at	0.627	0.008	0	0	0	0	0	0	0	0	0	0	0	0	0	0	0	0	0
E130309F12Rik		272031	RIKEN cDNA E130309F12 gene	1436733_at	0.627	0.003	0	0	0	0	0	0	0	0	0	0	0	0	0	0	0	0	0
Pik3ip1		216505	phosphoinositide-3-kinase interacting protein 1	1428332_at	0.627	0.003	0	0	0	0	0	0	0	0	0	0	0	0	0	0	0	0	0
Slc2a1		20525	solute carrier family 2 (facilitated glucose transporter), member 1	1434773_a_at	0.628	0.006	0	1	1	1	1	0	0	0	0	0	0	0	0	0	0	0	0
Lhfpl3		269629	lipoma HMGIC fusion partner-like 3	1429592_at	0.629	0.008	0	0	0	0	0	0	0	0	0	0	0	0	0	0	0	0	0
Scrg1		20284	scrapie responsive gene 1	1420764_at	0.629	0.008	0	0	0	0	0	0	0	0	0	0	0	0	0	0	0	0	0
Pdgfra		18595	platelet derived growth factor receptor, alpha polypeptide	1421917_at	0.629	0.008	0	0	0	0	0	0	0	0	0	1	0	0	0	0	0	0	0
P4ha2		18452	alpha II polypeptide	1417149_at	0.629	0.021	1	0	0	1	1	0	0	0	0	0	0	0	0	0	0	0	0
Trim9		94090	tripartite motif-containing 9	1434249_s_at	0.630	0.007	0	0	0	0	0	0	0	0	0	0	0	0	0	0	0	0	0
Sesn1		140742	sestrin 1	1438931_s_at	0.631	0.004	0	0	0	0	0	1	0	0	0	0	0	1	0	0	0	0	0
Gpr17		574402	G protein-coupled receptor 17	1456833_at	0.632	0.008	0	0	0	0	0	0	0	0	0	0	0	0	0	0	0	0	0
S100a10		20194	S100 calcium binding protein A10 (calpactin)	1456642_x_at	0.633	0.009	0	0	0	0	0	0	0	0	0	0	0	0	0	0	0	0	0
Gng2		14702	guanine nucleotide binding protein (G protein), gamma 2	1418451_at	0.635	0.006	0	0	0	0	0	0	0	0	0	0	0	0	0	0	0	0	0
3632451O06Rik		67419	RIKEN cDNA 3632451O06 gene	1450770_at	0.635	0.012	0	0	0	0	0	0	0	0	0	0	0	0	0	0	0	0	0
Enpp5		83965	ectonucleotide pyrophosphatase/phosphodiesterase 5	1425702_a_at	0.640	0.011	0	0	0	0	0	0	0	0	0	0	0	0	0	0	0	0	0
Eif2s3y		26908	eukaryotic translation initiation factor 2, subunit 3, structural gene Y-linked	1417210_at	0.640	0.006	0	0	0	0	0	0	0	0	0	0	0	0	0	0	0	0	0
Id2		15902	inhibitor of DNA binding 2	1435176_a_at	0.641	0.008	0	0	0	0	0	0	0	0	0	1	0	0	0	0	0	0	0
Cdh13		12554	cadherin 13	1423551_at	0.641	0.008	0	0	0	0	0	0	0	0	0	0	0	0	0	0	0	0	0
Slc2a1		20525	solute carrier family 2 (facilitated glucose transporter), member 1	1426599_a_at	0.644	0.012	0	1	1	1	1	0	0	0	0	0	0	0	0	0	0	0	0
NA	NA		NA	1437534_at	0.644	0.003	0	0	0	0	0	0	0	0	0	0	0	0	0	0	0	0	0
Acss2		60525	acyl-CoA synthetase short-chain family member 2	1422478_a_at	0.645	0.012	0	0	0	0	0	0	0	0	0	0	1	0	0	0	0	0	0
Gng2		14702	guanine nucleotide binding protein (G protein), gamma 2	1428157_at	0.646	0.006	0	0	0	0	0	0	0	0	0	0	0	0	0	0	0	0	0
Ddo		70503	D-aspartate oxidase	1439096_at	0.648	0.028	0	0	0	0	0	0	0	0	0	0	0	0	0	0	0	0	0
Dscaml1		114873	Down syndrome cell adhesion molecule-like 1	1441706_at	0.650	0.016	0	0	0	0	0	0	1	0	0	0	0	0	0	0	0	0	0
Slc16a3		80879	solute carrier family 16 (monocarboxylic acid transporters), member 3	1449005_at	0.650	0.032	0	0	0	1	0	0	0	0	0	0	0	0	0	0	0	0	0
Ier3		15937	immediate early response 3	1419647_a_at	0.651	0.012	0	0	0	0	0	0	0	0	0	0	0	0	0	0	0	0	0
AI464131		329828	expressed sequence AI464131	1435417_at	0.652	0.013	0	0	0	0	0	0	0	0	0	0	0	0	0	0	0	0	0
Cdc42ep3		260409	CDC42 effector protein (Rho GTPase binding) 3	1450700_at	0.652	0.011	0	0	0	0	0	0	0	0	0	0	0	0	0	0	0	0	0
Lnx1		16924	ligand of numb-protein X 1	1450251_a_at	0.654	0.005	0	0	0	0	0	0	0	0	0	0	0	0	0	0	0	0	0
NA	NA		NA	1457490_at	0.654	0.018	0	0	0	0	0	0	0	0	0	0	0	0	0	0	0	0	0
Klf9		16601	Kruppel-like factor 9	1422264_s_at	0.656	0.017	0	0	0	0	0	0	0	0	0	0	0	0	0	0	0	0	0
Mapt		17762	microtubule-associated protein tau	1424719_a_at	0.658	0.012	0	0	0	0	0	0	0	0	1	0	0	0	0	0	0	0	0
Sorbs1		20411	sorbin and SH3 domain containing 1	1436737_a_at	0.660	0.008	0	0	0	0	0	0	0	0	0	1	0	0	0	0	0	0	0
Skiv2l2		72198	superkiller viralicidic activity 2-like 2 (S. cerevisiae)	1447517_at	0.661	0.012	0	0	0	0	0	0	0	0	0	0	0	0	0	0	0	0	0
NA	NA		NA	1447329_at	0.663	0.002	0	0	0	0	0	0	0	0	0	0	0	0	0	0	0	0	0
Sorbs1		20411	sorbin and SH3 domain containing 1	1428471_at	0.664	0.012	0	0	0	0	0	0	0	0	0	1	0	0	0	0	0	0	0
5830455E04Rik		109026	RIKEN cDNA 5830455E04 gene	1439087_a_at	0.664	0.013	0	0	0	0	0	0	0	0	0	0	0	0	0	0	0	0	0
Txnip		56338	thioredoxin interacting protein	1415996_at	0.664	0.015	0	0	0	0	0	0	0	0	1	1	0	0	0	0	0	0	0
Pfkp		56421	phosphofructokinase, platelet	1416069_at	0.665	0.031	0	1	1	1	0	0	0	0	0	0	0	0	0	0	0	0	1
Slc2a1		20525	solute carrier family 2 (facilitated glucose transporter), member 1	1426600_at	0.666	0.027	0	1	1	1	1	0	0	0	0	0	0	0	0	0	0	0	0
Ntsr2		18217	neurotensin receptor 2	1417151_a_at	0.668	0.025	0	0	0	0	0	0	0	0	0	0	0	0	0	0	0	0	0
Ddx3y		26900	DEAD (Asp-Glu-Ala-Asp) box polypeptide 3, Y-linked	1452077_at	0.668	0.008	0	0	0	0	0	0	0	0	0	0	0	0	0	0	0	0	0
Rps6ka1		20111	ribosomal protein S6 kinase polypeptide 1	1416896_at	0.669	0.023	0	0	0	0	0	0	0	0	0	0	0	0	0	0	0	0	0
NA	NA		NA	1434362_at	0.669	0.018	0	0	0	0	0	0	0	0	0	0	0	0	0	0	0	0	0
Lgr5		14160	leucine rich repeat containing G protein coupled receptor 5	1450988_at	0.669	0.009	0	0	0	0	0	0	0	0	0	0	0	0	0	0	0	0	0
Wipi1		52639	WD repeat domain, phosphoinositide interacting 1	1424917_a_at	0.670	0.017	0	0	0	0	0	1	0	1	0	0	1	0	0	0	0	0	0
S100a10		20194	S100 calcium binding protein A10 (calpactin)	1416762_at	0.671	0.027	0	0	0	0	0	0	0	0	0	0	0	0	0	0	0	0	0
Twist1		22160	twist gene homolog 1 (Drosophila)	1418733_at	0.673	0.034	0	0	0	0	0	0	0	0	0	1	0	0	0	0	0	0	0
Nupr1		56312	nuclear protein 1	1419666_x_at	0.673	0.019	0	0	0	0	0	0	0	0	0	0	0	0	0	0	0	0	0
Slc29a4		243328	solute carrier family 29 (nucleoside transporters), member 4	1424900_at	0.674	0.027	0	0	0	0	0	0	0	0	0	0	0	0	0	0	0	0	0
Sgip1		73094	SH3-domain GRB2-like (endophilin) interacting protein 1	1431300_at	0.675	0.021	0	0	0	0	0	0	0	0	0	0	0	0	0	0	0	0	0
NA	NA		NA	1437987_at	0.676	0.030	0	0	0	0	0	0	0	0	0	0	0	0	0	0	0	0	0
Lnx1		16924	ligand of numb-protein X 1	1455825_s_at	0.677	0.009	0	0	0	0	0	0	0	0	0	0	0	0	0	0	0	0	0
Gbe1		74185	glucan (1,4-alpha-), branching enzyme 1	1420654_a_at	0.678	0.033	1	0	0	0	0	0	1	0	0	0	0	0	0	0	0	0	0
Cspg4		121021	chondroitin sulfate proteoglycan 4	1423341_at	0.678	0.032	0	0	0	0	0	0	0	0	0	0	0	0	0	0	0	0	0
Ndufa4l2		407790	NADH dehydrogenase (ubiquinone) 1 alpha subcomplex, 4-like 2	1434905_at	0.678	0.032	0	0	0	0	0	0	0	0	0	0	0	0	0	0	0	0	0
Prkg2		19092	protein kinase, cGMP-dependent, type II	1435162_at	0.680	0.020	0	0	0	0	0	0	0	0	0	1	0	0	0	0	0	0	0
Pla2g7		27226	plasma)	1430700_a_at	0.681	0.032	0	0	0	0	0	0	0	0	0	0	0	0	0	0	0	0	0
Ddx3y		26900	DEAD (Asp-Glu-Ala-Asp) box polypeptide 3, Y-linked	1426439_at	0.681	0.012	0	0	0	0	0	0	0	0	0	0	0	0	0	0	0	0	0
Cacna1c		12288	calcium channel, voltage-dependent, L type, alpha 1C subunit	1421297_a_at	0.682	0.027	0	0	0	0	0	0	0	0	0	0	0	0	0	0	0	0	0
Cdkn2b		12579	cyclin-dependent kinase inhibitor 2B (p15, inhibits CDK4)	1449152_at	0.683	0.030	0	0	0	0	0	0	0	0	0	0	0	0	0	0	0	0	0
Anks1b		77531	ankyrin repeat and sterile alpha motif domain containing 1B	1460449_at	0.683	0.043	0	0	0	0	0	0	0	0	0	0	0	0	0	0	0	0	0
Adm		11535	adrenomedullin	1447839_x_at	0.684	0.013	1	1	0	1	1	0	0	0	0	0	0	0	0	0	0	0	0
NA	NA		NA	1440527_at	0.684	0.039	0	0	0	0	0	0	0	0	0	0	0	0	0	0	0	0	0
Mxd1		17119	MAX dimerization protein 1	1434830_at	0.684	0.027	0	0	0	0	0	0	0	0	0	0	0	0	0	0	0	0	0
Syt16		238266	synaptotagmin XVI	1434429_at	0.686	0.041	0	0	0	0	0	0	0	0	0	0	0	0	0	0	0	0	0
Fgf1		14164	fibroblast growth factor 1	1450869_at	0.687	0.064	0	0	0	0	0	0	0	0	0	0	0	0	0	0	0	0	0
Rabgap1l		29809	RAB GTPase activating protein 1-like	1434062_at	0.687	0.030	0	0	0	0	0	0	0	0	0	0	0	0	0	0	0	0	0
Scg5		20394	secretogranin V	1423150_at	0.689	0.026	0	0	0	0	0	0	0	0	0	0	0	0	0	0	0	0	0
1700001O22Rik		73598	RIKEN cDNA 1700001O22 gene	1424795_a_at	0.691	0.043	0	0	0	0	0	0	0	0	0	0	0	0	0	0	0	0	0
Rgs20		58175	regulator of G-protein signaling 20	1443694_at	0.691	0.037	0	0	0	0	0	0	0	1	0	1	0	0	0	0	0	0	0
Ndrg1		17988	N-myc downstream regulated gene 1	1450976_at	0.691	0.069	1	0	0	0	0	0	0	1	0	1	0	0	0	0	0	0	0
Gabrb1		14400	gamma-aminobutyric acid (GABA-A) receptor, subunit beta 1	1419719_at	0.692	0.012	0	0	0	0	0	0	0	0	0	0	0	0	0	0	0	0	0
Gats		80909	opposite strand transcription unit to Stag3	1437252_at	0.692	0.027	0	0	0	0	0	0	0	0	0	0	0	0	0	0	0	0	0
Fn1		14268	fibronectin 1	1426642_at	0.692	0.028	0	0	0	0	0	0	0	0	0	1	0	0	0	0	0	0	0
Slc2a3		20527	solute carrier family 2 (facilitated glucose transporter), member 3	1427770_a_at	0.693	0.034	1	1	0	0	1	0	0	0	0	0	0	0	0	0	0	0	0
NA	NA		NA	1440570_at	0.693	0.059	0	0	0	0	0	0	0	0	0	0	0	0	0	0	0	0	0
Vldlr		22359	very low density lipoprotein receptor	1417900_a_at	0.693	0.056	0	0	0	0	0	0	0	0	0	1	0	0	0	0	0	0	0
Egln3		112407	EGL nine homolog 3 (C. elegans)	1418648_at	0.694	0.041	0	0	0	0	0	0	0	0	0	0	0	0	0	0	0	0	0
Hrh1		15465	histamine receptor H1	1438494_at	0.694	0.030	0	0	0	0	0	0	0	0	0	0	0	0	0	0	0	0	0
NA	NA		NA	1435265_at	0.695	0.048	0	0	0	0	0	0	0	0	0	0	0	0	0	0	0	0	0
Rab33a		19337	RAB33A, member of RAS oncogene family	1417529_at	0.695	0.027	0	0	0	0	0	0	1	0	0	1	0	0	0	0	0	0	0
Pvr		52118	poliovirus receptor	1423904_a_at	0.695	0.040	0	0	0	0	0	0	0	0	0	0	0	0	0	0	0	0	0
M6prbp1		66905	mannose-6-phosphate receptor binding protein 1	1416424_at	0.696	0.037	0	0	0	0	0	0	0	0	0	0	0	0	0	0	0	0	0

Pfkfb3	170768	6-phosphofructo-2-kinase/fructose-2,6-biphosphatase 3	1416432_at	0.696	0.061	1	0	0	0	0	0	0	0	0	1	0	0	1	0	0	0	0	0	0	0
1810010H24Rik	69066	RIKEN cDNA 1810010H24 gene	1428809_at	0.696	0.040	0	0	0	0	0	0	0	0	0	0	0	0	0	0	0	0	0	0	0	0
Spon1	233744	spondin 1, (f-spondin) extracellular matrix protein	1424415_s_at	0.696	0.051	0	0	0	0	0	0	0	1	0	1	0	0	0	0	0	0	0	0	0	0
Klf9	16601	Kruppel-like factor 9	1436763_a_at	0.697	0.045	0	0	0	0	0	0	0	0	0	0	0	0	0	0	0	0	0	0	0	0
Gng3	14704	guanine nucleotide binding protein (G protein), gamma 3	1417428_at	0.697	0.039	0	0	0	0	0	0	0	0	0	0	0	0	0	0	0	0	0	0	0	0
Uty	22290	ubiquitously transcribed tetratricopeptide repeat gene, Y chromosome	1426598_at	0.698	0.027	0	0	0	0	0	0	0	0	0	0	0	0	0	0	0	0	0	0	0	0
Qpct	70536	glutaminyl-peptide cyclotransferase (glutaminyl cyclase)	1426622_a_at	0.698	0.043	0	0	0	0	0	0	0	0	0	0	0	0	0	0	0	0	0	0	0	0
3110035E14Rik	76982	RIKEN cDNA 3110035E14 gene	1428184_at	0.699	0.026	0	0	0	0	0	0	0	0	0	0	0	0	0	0	0	0	0	0	0	0
Tmcc3	319880	transmembrane and coiled coil domains 3	1434252_at	0.700	0.043	0	0	0	0	0	0	0	0	0	0	0	0	0	0	0	0	0	0	0	0
A2m	232345	alpha-2-macroglobulin	1434719_at	0.700	0.068	0	0	0	0	0	0	0	0	0	0	0	0	0	0	0	0	0	0	0	0
Pdk1	228026	pyruvate dehydrogenase kinase, isoenzyme 1	1423748_at	0.700	0.080	1	0	0	0	0	0	0	0	0	0	0	0	0	0	0	0	0	0	0	0
1810011O10Rik	69068	RIKEN cDNA 1810011O10 gene	1435595_at	0.702	0.047	0	0	0	0	0	0	0	0	0	0	0	0	0	0	0	0	0	0	0	0
Ifi203	15950	interferon activated gene 203	1448775_at	0.704	0.032	0	0	0	0	0	0	0	0	0	0	0	0	0	0	0	0	0	0	0	0
Mxi1	17859	Max interacting protein 1	1450376_at	0.706	0.043	1	0	0	0	0	1	0	0	0	1	1	1	0	0	0	0	0	0	0	0
Vldlr	22359	very low density lipoprotein receptor	1435893_at	0.706	0.051	0	0	0	0	0	0	0	0	0	1	0	0	0	0	0	0	0	0	0	0
Fxyd6	59095	FXYD domain-containing ion transport regulator 6	1417343_at	0.707	0.030	0	0	0	0	0	0	0	0	0	0	0	0	0	0	0	0	0	0	0	0
Nupr1	56312	nuclear protein 1	1419665_a_at	0.707	0.068	0	0	0	0	0	0	0	0	0	0	0	0	0	0	0	0	0	0	0	0
BC068157	73072	cDNA sequence BC068157	1429269_at	0.707	0.047	0	0	0	0	0	0	0	0	0	0	0	0	0	0	0	0	0	0	0	0
Trim9	94090	tripartite motif-containing 9	1443989_at	0.708	0.056	0	0	0	0	0	0	0	0	0	0	0	0	0	0	0	0	0	0	0	0
Cadm2	239857	cell adhesion molecule 2	1435146_s_at	0.710	0.079	0	0	0	0	0	0	0	0	0	0	0	0	0	0	0	0	0	0	0	0
Cyclin G2	12452	cyclin G2 (Ccng2)	1416488_at	0.710	0.029	0	1	0	1	0	0	0	0	0	1	0	1	0	0	0	0	0	0	0	0
Rnft1	76892	ring finger protein, transmembrane 1	1428078_at	0.711	0.057	0	0	0	0	0	0	0	0	0	0	0	0	0	0	0	0	0	0	0	0
1300014I06Rik	66895	RIKEN cDNA 1300014I06 gene	1428851_at	0.711	0.069	0	0	0	0	0	0	0	0	0	0	0	0	0	0	0	0	0	0	0	0
Cd109	235505	CD109 antigen	1425658_at	0.711	0.086	0	0	0	0	0	0	0	0	0	0	0	0	0	0	0	0	0	0	0	0
Vldlr	22359	very low density lipoprotein receptor	1434465_x_at	0.711	0.069	0	0	0	0	0	0	0	0	0	1	0	0	0	0	0	0	0	0	0	0
C1ql3	227580	C1q-like 3	1451620_at	0.712	0.080	0	0	0	0	0	0	0	0	0	0	0	0	0	0	0	0	0	0	0	0
Cyclin G2	12452	cyclin G2 (Ccng2)	1448364_at	0.712	0.044	0	1	0	1	0	0	0	0	0	1	0	1	0	0	0	0	0	0	0	0
NA	NA	NA	1460061_at	0.713	0.078	0	0	0	0	0	0	0	0	0	0	0	0	0	0	0	0	0	0	0	0
Tnfaip8	106869	tumor necrosis factor, alpha-induced protein 8	1416950_at	0.713	0.078	0	0	0	0	0	0	1	0	0	0	0	1	0	0	0	0	0	0	0	0
Cdc42ep3	260409	CDC42 effector protein (Rho GTPase binding) 3	1422642_at	0.713	0.063	0	0	0	0	0	0	0	0	0	0	0	0	0	0	0	0	0	0	0	0
4833424O15Rik	75769	RIKEN cDNA 4833424O15 gene	1434925_at	0.714	0.091	0	0	0	0	0	0	0	0	0	0	0	0	0	0	0	0	0	0	0	0
Tslp	53603	thymic stromal lymphopoietin	1450004_at	0.714	0.069	1	0	0	0	0	0	0	0	0	0	0	0	0	0	0	0	0	0	0	0
FoxO3	56484	forkhead box O3a	1444226_at	0.715	0.029	0	0	0	0	0	0	0	0	0	0	0	0	0	0	0	0	0	0	0	0
Pcdhb10	93881	protocadherin beta 10	1422729_at	0.716	0.067	0	0	0	0	0	0	0	0	0	0	0	0	0	0	0	0	0	0	0	0
Diras2	68203	DIRAS family, GTP-binding RAS-like 2	1455436_at	0.717	0.087	0	0	0	0	0	0	0	0	0	0	0	0	0	0	0	0	0	0	0	0
Mllt3	70122	translocated to, 3	1453622_s_at	0.718	0.087	0	0	0	0	0	0	0	0	0	1	0	0	0	0	0	0	0	0	0	0
P4ha1	18451	alpha 1 polypeptide	1426519_at	0.718	0.080	1	1	0	0	0	0	0	0	0	0	0	0	0	0	0	0	0	0	0	0
Tagln3	56370	transgelin 3	1450683_at	0.718	0.064	0	0	0	0	0	0	0	0	0	0	0	0	0	0	0	0	0	0	0	0
Bgn	12111	biglycan	1416405_at	0.718	0.049	0	0	0	0	0	0	0	0	0	0	0	0	0	0	0	0	0	0	0	0
Pnrc1	108767	proline-rich nuclear receptor coactivator 1	1433668_at	0.720	0.065	0	0	0	0	0	0	0	0	0	1	0	0	0	0	0	0	0	0	0	0
Mamdc2	71738	MAM domain containing 2	1453152_at	0.720	0.057	0	0	0	0	0	0	0	0	0	0	0	0	0	0	0	0	0	0	0	0
9330159F19Rik	212448	RIKEN cDNA 9330159F19 gene	1438720_at	0.722	0.094	0	0	0	0	0	0	0	0	0	0	0	0	0	0	0	0	0	0	0	0
Igfbp5	16011	insulin-like growth factor binding protein 5	1452114_s_at	0.723	0.043	0	0	0	0	0	0	0	0	0	0	0	0	0	0	0	0	0	0	0	0
Insig2	72999	insulin induced gene 2	1417980_a_at	0.724	0.069	1	0	0	0	0	0	0	0	0	0	0	0	0	0	0	0	0	0	0	0
Gats	80909	opposite strand transcription unit to Stag3	1451589_at	0.724	0.082	0	0	0	0	0	0	0	0	0	0	0	0	0	0	0	0	0	0	0	0
Hebp1	15199	heme binding protein 1	1418172_at	0.726	0.069	0	0	0	0	0	0	0	0	0	0	0	0	0	0	0	0	0	0	0	0
Dbp	13170	D site albumin promoter binding protein	1418174_at	0.727	0.094	0	0	0	0	0	0	0	0	0	1	1	0	0	0	0	0	0	0	0	0
6330512M04Rik	320802	RIKEN cDNA 6330512M04 gene	1455239_at	0.728	0.064	0	0	0	0	0	0	0	0	0	0	0	0	0	0	0	0	0	0	0	0
Jarid1d	20592	jumonji, AT rich interactive domain 1D (Rbp2 like)	1424903_at	0.731	0.020	0	0	0	0	0	0	0	0	0	0	0	0	0	0	0	0	0	0	0	0
Lrrtm2	107065	leucine rich repeat transmembrane neuronal 2	1437787_at	0.731	0.080	0	0	0	0	0	0	0	0	0	0	0	0	0	0	0	0	0	0	0	0
Cdkn1b	12576	cyclin-dependent kinase inhibitor 1B	1434045_at	0.732	0.031	0	1	0	1	0	0	0	0	0	1	0	0	0	0	0	0	0	0	0	0
Lmo1	109594	LIM domain only 1	1418478_at	0.732	0.077	0	0	0	0	0	0	0	0	0	0	0	0	0	0	0	0	0	0	0	0
4933426K21Rik	108653	RIKEN cDNA 4933426K21 gene	1429982_at	0.732	0.064	0	0	0	0	0	0	0	0	0	0	0	0	0	0	0	0	0	0	0	0
Zbtb4	75580	zinc finger and BTB domain containing 4	1453266_at	0.733	0.088	0	0	0	0	0	0	0	0	0	0	0	0	0	0	0	0	0	0	0	0
Cadm4	260299	cell adhesion molecule 4	1426263_at	0.735	0.068	0	0	0	0	0	0	0	0	0	0	0	0	0	0	0	0	0	0	0	0
Mapt	17762	microtubule-associated protein tau	1424718_at	0.735	0.096	0	0	0	0	0	0	0	0	0	1	0	0	0	0	0	0	0	0	0	0
Kcnip3	56461	Kv channel interacting protein 3, calsenilin	1449129_a_at	0.736	0.099	0	0	0	0	0	0	0	0	0	0	0	0	0	0	0	0	0	0	0	0
Brdt	114642	bromodomain, testis-specific	1450178_at	0.736	0.092	0	0	0	0	0	0	0	0	0	0	0	0	0	0	0	0	0	0	0	0
Astx	100113394	amplified spermatogenic transcripts X encoded	1444668_at	0.736	0.013	0	0	0	0	0	0	0	0	0	0	0	0	0	0	0	0	0	0	0	0
Cav2	12390	caveolin 2	1417327_at	0.738	0.092	0	0	0	0	0	0	0	1	0	1	0	0	0	0	0	0	0	0	0	0
Adm	11535	adrenomedullin	1416077_at	0.739	0.078	1	1	0	1	1	0	0	0	0	0	0	0	0	0	0	0	0	0	0	0
LOC100045795	100045795	similar to mKIAA3002 protein	1459981_s_at	0.740	0.067	0	0	0	0	0	0	0	0	0	0	0	0	0	0	0	0	0	0	0	0
Ctsh	13036	cathepsin H	1418365_at	0.741	0.041	0	0	0	0	0	0	0	0	0	0	0	0	0	0	0	0	0	0	0	0
Lgmn	19141	legumain	1448883_at	0.742	0.097	0	0	0	0	0	0	0	0	0	0	0	0	0	0	0	0	0	0	0	0
Klk1b5	16622	kallikrein 1-related peptidase b5	1419010_x_at	0.744	0.009	0	0	0	0	0	0	0	0	0	0	0	0	0	0	0	0	0	0	0	0
Anxa4	11746	annexin A4	1424176_a_at	0.747	0.043	0	0	0	0	0	0	0	0	0	0	0	0	0	0	0	0	0	0	0	0
Uty	22290	ubiquitously transcribed tetratricopeptide repeat gene, Y chromosome	1422247_a_at	0.749	0.056	0	0	0	0	0	0	0	0	0	0	0	0	0	0	0	0	0	0	0	0
Dscam	13508	Down syndrome cell adhesion molecule	1449411_at	0.749	0.096	0	0	0	0	0	0	1	0	0	0	0	0	0	0	0	0	0	0	0	0
Ampd3	11717	adenosine monophosphate deaminase 3	1422573_at	0.750	0.073	0	0	1	0	0	0	0	0	0	0	0	0	0	0	0	0	0	0	0	0
P2rx7	18439	purinergic receptor P2X, ligand-gated ion channel, 7	1419853_a_at	0.753	0.069	0	0	0	0	0	0	0	0	0	0	0	0	0	0	0	0	0	0	0	0
Gdap10	14546	ganglioside-induced differentiation-associated-protein 10	1420342_at	0.754	0.096	0	0	0	0	0	0	0	0	0	0	0	0	0	0	0	0	0	0	0	0
Ssty2	70009	spermiogenesis specific transcript on the Y 2	1417838_at	0.764	0.069	0	0	0	0	0	0	0	0	0	0	0	0	0	0	0	0	0	0	0	0
Agt	11606	angiotensinogen (serpin peptidase inhibitor, clade A, member 8)	1423396_at	0.767	0.061	0	0	0	0	0	0	0	1	0	0	0	0	0	0	0	0	0	0	0	0
NA	NA	NA	1434280_at	0.783	0.041	0	0	0	0	0	0	0	0	0	0	0	0	0	0	0	0	0	0	0	0
NA	NA	NA	1426060_at	0.787	0.083	0	0	0	0	0	0	0	0	0	0	0	0	0	0	0	0	0	0	0	0
Tceal1	237052	transcription elongation factor A (SII)-like 1	1424634_at	0.812	0.047	0	0	0	0	0	0	0	0	0	0	0	0	0	0	0	0	0	0	0	0
Hes5	15208	hairy and enhancer of split 5 (Drosophila)	1456010_x_at	0.816	0.063	0	0	0	0	0	0	0	0	0	0	0	0	0	0	0	0	0	0	0	0
Cd93	17064	CD93 antigen	1456046_at	0.822	0.020	0	0	0	0	0	0	0	0	0	0	0	0	0	0	0	0	0	0	0	0
Actr1b	226977	ARP1 actin-related protein 1 homolog B, centractin beta (yeast)	1447293_x_at	0.826	0.049	0	0	0	0	0	0	0	0	0	0	0	0	0	0	0	0	0	0	0	0
Nudt21	68219	nudix (nucleoside diphosphate linked moiety X)-type motif 21	1455966_s_at	0.838	0.097	0	0	0	0	0	0	0	0	0	0	0	0	0	0	0	0	0	0	0	0
Actr1b	226977	ARP1 actin-related protein 1 homolog B, centractin beta (yeast)	1447292_at	0.893	0.047	0	0	0	0	0	0	0	0	0	0	0	0	0	0	0	0	0	0	0	0
Anxa1	16952	annexin A1	1448213_at	1.077	0.084	0	0	0	0	0	0	0	0	0	1	0	0	0	0	0	0	0	0	0	0
Ugt8a	22239	UDP galactosyltransferase 8A	1419063_at	1.216	0.074	0	0	0	0	0	0	0	0	0	0	0	0	0	0	0	0	0	0	0	0
Spp1	20750	secreted phosphoprotein 1	1449254_at	1.233	0.075	0	1	0	0	0	0	0	0	0	0	0	0	0	0	0	0	0	0	0	0
Gsn	227753	gelsolin	1415812_at	1.266	0.065	0	0	0	0	0	0	0	0	0	0	0	0	1	0	0	0	0	0	0	0
Trf	22041	transferrin	1425546_a_at	1.266	0.017	0	0	0	0	0	0	0	0	0	0	0	0	0	0	0	0	0	0	0	0
Abca1	11303	ATP-binding cassette, sub-family A (ABC1), member 1	1450392_at	1.273	0.093	0	0	0	0	0	0	0	0	0	0	0	0	0	0	0	0	0	0	0	0

Ugt8a		22239	UDP galactosyltransferase 8A	1419064_a_at	1.273	0.067	0	0	0	0	0	0	0	0	0	0	0	0	0	0	0	0	0	0	0	0
Foxa1		15375	forkhead box A1	1418496_at	1.295	0.078	0	0	0	0	0	0	0	0	0	0	0	0	0	0	0	0	0	0	0	0
Mag		17136	myelin-associated glycoprotein	1460219_at	1.300	0.023	0	0	0	0	0	0	0	0	0	0	0	0	0	0	0	0	0	0	0	0
Mobp		17433	myelin-associated oligodendrocytic basic protein	1433785_at	1.303	0.055	0	0	0	0	0	0	0	0	0	0	0	0	0	0	0	0	0	0	0	0
Pdlim2		213019	PDZ and LIM domain 2	1423946_at	1.309	0.051	0	0	0	0	0	0	0	0	0	0	0	0	0	0	0	0	0	0	0	0
Mal		17153	myelin and lymphocyte protein, T-cell differentiation protein	1417275_at	1.310	0.015	0	0	0	0	0	0	0	0	0	0	0	0	0	0	0	0	0	0	0	0
Atm		11920	ataxia telangiectasia mutated homolog (human)	1421205_at	1.315	0.039	0	0	0	0	0	0	0	0	0	0	0	0	0	0	0	0	0	0	0	0
Stag3		50878	stromal antigen 3	1460229_at	1.332	0.073	0	0	0	0	0	0	0	0	0	0	0	0	0	0	0	0	0	0	0	0
Clic5		224796	chloride intracellular channel 5	1458381_at	1.340	0.092	0	0	0	0	0	0	0	0	0	0	0	0	0	0	0	0	0	0	0	0
NA	NA		NA	1445268_at	1.350	0.066	0	0	0	0	0	0	0	0	0	0	0	0	0	0	0	0	0	0	0	0
Kndc1		76484	kinase non-catalytic C-lobe domain (KIND) containing 1	1428599_at	1.354	0.039	0	0	0	0	0	0	0	0	0	0	0	0	0	0	0	0	0	0	0	0
Mbp		17196	myelin basic protein	1454651_x_at	1.356	0.023	0	0	0	0	0	1	0	0	0	0	1	1	0	0	0	0	0	0	0	0
Tsix		22097	X (inactive)-specific transcript, antisense	1436936_s_at	1.358	0.060	0	0	0	0	0	0	0	0	0	0	0	0	0	0	0	0	0	0	0	0
Mbp		17196	myelin basic protein	1433532_a_at	1.359	0.035	0	0	0	0	0	1	0	0	0	0	1	1	0	0	0	0	0	0	0	0
Apod		11815	apolipoprotein D	1416371_at	1.363	0.015	0	0	0	0	0	1	0	1	1	0	1	1	0	0	0	0	0	0	0	0
Plp1		18823	proteolipid protein (myelin) 1	1451718_at	1.368	0.020	0	0	0	0	0	0	0	1	0	1	0	0	0	0	0	0	0	0	0	0
Il33		77125	interleukin 33	1416200_at	1.369	0.005	0	0	0	0	0	0	0	0	0	0	0	0	0	0	0	0	0	0	0	0
Mbp		17196	myelin basic protein	1456228_x_at	1.370	0.028	0	0	0	0	0	1	0	0	0	0	1	1	0	0	0	0	0	0	0	0
Plp1		18823	proteolipid protein (myelin) 1	1425468_at	1.371	0.015	0	0	0	0	0	0	0	1	0	1	0	0	0	0	0	0	0	0	0	0
Bche		12038	butyrylcholinesterase	1437863_at	1.372	0.078	0	0	0	0	0	0	0	0	0	0	0	0	0	0	0	0	0	0	0	0
NA	NA		NA	1440374_at	1.373	0.061	0	0	0	0	0	0	0	0	0	0	0	0	0	0	0	0	0	0	0	0
B130021B11Rik		320860	RIKEN cDNA B130021B11 gene	1438989_s_at	1.376	0.077	0	0	0	0	0	0	0	0	0	0	0	0	0	0	0	0	0	0	0	0
Mbp		17196	myelin basic protein	1451961_a_at	1.377	0.013	0	0	0	0	0	1	0	0	0	0	1	1	0	0	0	0	0	0	0	0
Aspm		12316	asp (abnormal spindle)-like, microcephaly associated (Drosophila)	1441520_at	1.378	0.061	0	0	0	0	0	0	0	0	0	0	0	0	0	0	0	0	0	0	0	0
4933432K03Rik		75793	RIKEN cDNA 4933432K03 gene	1438356_x_at	1.385	0.053	0	0	0	0	0	0	0	0	0	0	0	0	0	0	0	0	0	0	0	0
Dnahc8		13417	dynein, axonemal, heavy chain 8	1424936_a_at	1.385	0.068	0	0	0	0	0	0	0	0	0	0	0	0	0	0	0	0	0	0	0	0
Mbp		17196	myelin basic protein	1419646_a_at	1.386	0.015	0	0	0	0	0	1	0	0	0	0	1	1	0	0	0	0	0	0	0	0
Endod1		71946	endonuclease domain containing 1	1433796_at	1.388	0.084	0	0	0	0	0	0	0	0	0	0	0	0	0	0	0	0	0	0	0	0
Vegfc		22341	vascular endothelial growth factor C	1440739_at	1.392	0.079	0	0	0	0	0	0	0	0	0	0	0	0	0	0	0	0	0	0	0	0
NA	NA		NA	1440862_at	1.399	0.047	0	0	0	0	0	0	0	0	0	0	0	0	0	0	0	0	0	0	0	0
Slc14a2		27411	solute carrier family 14 (urea transporter), member 2	1426109_a_at	1.401	0.081	0	0	0	0	0	0	0	0	0	0	0	0	0	0	0	0	0	0	0	0
Chchd3		66075	coiled-coil-helix-coiled-coil-helix domain containing 3	1431241_at	1.403	0.059	0	0	0	0	0	0	0	0	0	0	0	0	0	0	0	0	0	0	0	0
Sostdc1		66042	sclerostin domain containing 1	1460250_at	1.404	0.046	0	0	0	0	0	0	0	0	0	0	0	0	0	0	0	0	0	0	0	0
Vgll3		73569	vestigial like 3 (Drosophila)	1453593_at	1.404	0.058	0	0	0	0	0	0	0	0	0	0	0	0	0	0	0	0	0	0	0	0
Sostdc1		66042	sclerostin domain containing 1	1449340_at	1.404	0.049	0	0	0	0	0	0	0	0	0	0	0	0	0	0	0	0	0	0	0	0
Nkx2-4		228731	NK2 transcription factor related, locus 4 (Drosophila)	1432863_a_at	1.407	0.058	0	0	0	0	0	0	0	0	0	0	0	0	0	0	0	0	0	0	0	0
Dmrtb1		56296	DMRT-like family B with proline-rich C-terminal, 1	1427252_at	1.407	0.051	0	0	0	0	0	0	0	0	0	0	0	0	0	0	0	0	0	0	0	0
Plp1		18823	proteolipid protein (myelin) 1	1425467_a_at	1.408	0.010	0	0	0	0	0	0	0	1	0	1	0	0	0	0	0	0	0	0	0	0
Mid1		17318	midline 1	1438239_at	1.409	0.049	0	0	0	0	0	0	0	0	0	0	0	0	0	0	0	0	0	0	0	0
6030405A18Rik		329641	RIKEN cDNA 6030405A18 gene	1436444_at	1.411	0.053	0	0	0	0	0	0	0	0	0	0	0	0	0	0	0	0	0	0	0	0
Epb4.1l4a		13824	erythrocyte protein band 4.1-like 4a	1449167_at	1.413	0.055	0	0	0	0	0	0	0	0	0	0	0	0	0	0	0	0	0	0	0	0
Slc4a2		20535	solute carrier family 4 (anion exchanger), member 2	1416637_at	1.416	0.046	0	0	0	0	0	0	0	0	0	0	0	0	0	0	0	0	0	0	0	0
Mbp		17196	myelin basic protein	1436201_x_at	1.420	0.015	0	0	0	0	0	1	0	0	0	0	1	1	0	0	0	0	0	0	0	0
Gh		14599	growth hormone	1460310_a_at	1.421	0.067	0	0	0	0	0	0	0	0	0	0	0	0	0	0	0	0	0	0	0	0
Ermn		77767	ermin, ERM-like protein	1436578_at	1.421	0.009	0	0	0	0	0	0	0	0	0	0	0	0	0	0	0	0	0	0	0	0
2810442I21Rik		72735	RIKEN cDNA 2810442I21 gene	1440541_at	1.421	0.035	0	0	0	0	0	0	0	0	0	0	0	0	0	0	0	0	0	0	0	0
Lor		16939	loricrin	1448745_s_at	1.425	0.045	0	0	0	0	0	0	0	0	0	0	1	0	0	0	0	0	0	0	0	0
Plxna2		18845	plexin A2	1453286_at	1.428	0.039	0	0	0	0	0	0	0	0	0	0	1	0	0	0	0	0	0	0	0	0
Tagln		21345	transgelin	1423505_at	1.430	0.059	0	1	0	0	0	0	0	0	0	0	0	0	0	0	0	0	0	0	0	0
Odz4		23966	odd Oz/ten-m homolog 4 (Drosophila)	1455993_at	1.432	0.085	0	0	0	0	0	0	0	0	0	0	0	0	0	0	0	0	0	0	0	0
2810442I21Rik		72735	RIKEN cDNA 2810442I21 gene	1439112_at	1.436	0.023	0	0	0	0	0	0	0	0	0	0	0	0	0	0	0	0	0	0	0	0
Id4		15904	inhibitor of DNA binding 4	1423260_at	1.437	0.054	0	0	0	0	0	0	0	0	0	0	1	0	0	0	0	0	0	0	0	0
Mgp		17313	matrix Gla protein	1448416_at	1.438	0.093	0	0	0	0	0	0	0	0	0	0	0	0	0	0	0	0	0	0	0	0
Htr3a		15561	5-hydroxytryptamine (serotonin) receptor 3A	1418268_at	1.439	0.049	0	0	0	0	0	0	0	0	0	0	1	0	0	0	0	0	0	0	0	0
NA	NA		NA	1459632_at	1.460	0.046	0	0	0	0	0	0	0	0	0	0	0	0	0	0	0	0	0	0	0	0
Cybrd1		73649	cytochrome b reductase 1	1425040_at	1.461	0.079	0	0	0	0	0	1	0	0	0	0	1	0	0	0	0	0	0	0	0	0
LOC215866		215866	hypothetical protein LOC215866	1426936_at	1.464	0.010	0	0	0	0	0	0	0	0	0	0	0	0	0	0	0	0	0	0	0	0
Anxa6		11749	annexin A6	1429246_a_at	1.464	0.018	0	0	0	0	0	0	0	0	0	0	0	0	0	0	0	0	0	0	0	0
Gpc4		14735	glypican 4	1436514_at	1.465	0.028	0	0	0	0	0	0	0	0	0	0	0	0	0	0	0	0	0	0	0	0
Itga8		241226	integrin alpha 8	1454966_at	1.468	0.071	0	0	0	0	0	0	0	0	0	0	0	0	0	0	0	0	0	0	0	0
Gpc4		14735	glypican 4	1421088_at	1.473	0.024	0	0	0	0	0	0	0	0	0	0	0	0	0	0	0	0	0	0	0	0
Hopx		74318	HOP homeobox	1451776_s_at	1.473	0.028	0	0	0	0	0	0	0	0	0	0	0	0	0	0	0	0	0	0	0	0
Ncoa7		211329	nuclear receptor coactivator 7	1454809_at	1.476	0.038	0	0	0	0	0	0	0	0	0	0	0	0	0	0	0	0	0	0	0	0
Endod1		71946	endonuclease domain containing 1	1426541_a_at	1.479	0.038	0	0	0	0	0	0	0	0	0	0	0	0	0	0	0	0	0	0	0	0
Plcxd3		239318	phosphatidylinositol-specific phospholipase C, X domain containing 3	1436821_at	1.489	0.060	0	0	0	0	0	0	0	0	0	0	0	0	0	0	0	0	0	0	0	0
Anxa6		11749	annexin A6	1415818_at	1.499	0.011	0	0	0	0	0	0	0	0	0	0	0	0	0	0	0	0	0	0	0	0
Socs2		216233	suppressor of cytokine signaling 2	1418507_s_at	1.500	0.052	0	0	0	0	0	0	0	0	0	0	0	0	0	0	0	0	0	0	0	0
NA	NA		NA	1439732_at	1.501	0.066	0	0	0	0	0	0	0	0	0	0	0	0	0	0	0	0	0	0	0	0
Zic3		22773	zinc finger protein of the cerebellum 3	1423424_at	1.517	0.046	0	0	0	0	0	0	0	0	0	0	0	0	0	0	0	0	0	0	0	0
Tpd52l1		21987	tumor protein D52-like 1	1418412_at	1.528	0.016	0	0	0	0	0	0	0	0	0	0	0	0	0	0	0	0	0	0	0	0
Tmem173		72512	transmembrane protein 173	1447621_s_at	1.538	0.015	0	0	0	0	0	0	0	0	0	0	0	0	0	0	0	0	0	0	0	0
Id4		15904	inhibitor of DNA binding 4	1450928_at	1.548	0.019	0	0	0	0	0	0	0	0	0	0	1	0	0	0	0	0	0	0	0	0
Zic1		22771	zinc finger protein of the cerebellum 1	1423477_at	1.578	0.024	0	0	0	0	0	0	0	0	0	0	1	0	0	0	0	0	0	0	0	0
LOC100039795	100039795		similar to C1orf32 putative protein	1436894_at	1.583	0.006	0	0	0	0	0	0	0	0	0	0	0	0	0	0	0	0	0	0	0	0
Cyp1b1		13078	cytochrome P450, family 1, subfamily b, polypeptide 1	1416612_at	1.590	0.010	0	0	0	0	0	0	0	1	0	0	0	0	0	0	0	0	0	0	0	0
Zic1		22771	zinc finger protein of the cerebellum 1	1439627_at	1.593	0.010	0	0	0	0	0	0	0	0	0	0	1	0	0	0	0	0	0	0	0	0
Pkib		18768	protein kinase inhibitor beta, cAMP dependent, testis specific	1421137_a_at	1.598	0.012	0	0	0	0	0	0	0	0	0	0	0	0	0	0	0	0	0	0	0	0
Clic5		224796	chloride intracellular channel 5	1439505_at	1.614	0.006	0	0	0	0	0	0	0	0	0	0	0	0	0	0	0	0	0	0	0	0
Cma1		17228	chymase 1, mast cell	1449456_a_at	1.628	0.039	0	0	0	0	0	0	0	0	0	0	0	0	0	0	0	0	0	0	0	0
Ube1y1		22202	ubiquitin-activating enzyme E1, Chr Y 1	1450285_at	1.637	0.003	0	0	0	0	0	0	0	0	0	0	0	0	0	0	0	0	0	0	0	0
Id4		15904	inhibitor of DNA binding 4	1423259_at	1.656	0.018	0	0	0	0	0	0	0	0	0	0	1	0	0	0	0	0	0	0	0	0
2310076G05Rik		76963	RIKEN cDNA 2310076G05 gene	1442077_at	1.662	0.015	0	0	0	0	0	0	0	0	0	0	0	0	0	0	0	0	0	0	0	0
Dact1		59036	dapper homolog 1, antagonist of beta-catenin (xenopus)	1417937_at	1.675	0.002	0	0	0	0	0	0	0	0	0	0	1	0	0	0	0	0	0	0	0	0
Clic5		224796	chloride intracellular channel 5	1456873_at	1.713	0.002	0	0	0	0	0	0	0	0	0	0	0	0	0	0	0	0	0	0	0	0
Myl9		98932	myosin, light polypeptide 9, regulatory	1452670_at	1.753	0.002	0	0	0	0	0	0	0	0	0	0	0	0	0	0	0	0	0	0	0	0
Cpa3		12873	carboxypeptidase A3, mast cell	1448730_at	1.756	0.023	0	0	0	0	0	0	0	0	0	0	0	0	0	0	0	0	0	0	0	0
Capn6		12338	calpain 6	1421952_at	1.756	0.014	0	0	0	0	0	0	0	0	0	0	0	0	0	0	0	0	0	0	0	0

Frk		14302	fyn-related kinase	1426569_a_at	1.768	0.002	0	0	0	0	0	0	0	0	0	0	0	0	0	0	0	0	0	0	0
Xist		213742	inactive X specific transcripts	1427262_at	1.778	0.003	0	0	0	0	0	0	0	0	0	0	0	0	0	0	0	0	0	0	0
Pitx2		18741	paired-like homeodomain transcription factor 2	1424797_a_at	1.852	0.002	0	0	0	0	0	0	0	0	0	1	0	0	0	0	0	0	0	0	0
6330407J23Rik		67412	RIKEN cDNA 6330407J23 gene	1429628_at	1.865	0.002	0	0	0	0	0	0	0	0	0	0	0	0	0	0	0	0	0	0	0
Prdm1		12142	PR domain containing 1, with ZNF domain	1420425_at	2.002	0.000	0	0	0	0	0	0	0	0	0	1	0	0	0	0	0	0	0	0	0
NA	NA		NA	1427820_at	2.043	0.003	0	0	0	0	0	0	0	0	0	0	0	0	0	0	0	0	0	0	0
Capn6		12338	calpain 6	1450429_at	2.044	0.001	0	0	0	0	0	0	0	0	0	0	0	0	0	0	0	0	0	0	0
Ctgf		14219	connective tissue growth factor	1416953_at	2.082	0.003	0	0	0	0	0	0	0	0	0	0	0	0	0	0	0	0	0	0	0
Prl		19109	prolactin	1429287_a_at	2.237	0.005	0	0	0	0	0	0	0	0	0	0	0	0	0	0	0	0	0	0	0
Pomc		18976	pro-opiomelanocortin-alpha	1433800_a_at	2.587	0.003	0	0	0	0	0	0	0	0	0	0	0	0	0	0	0	0	0	0	0
Tpsab1		17230	tryptase alpha/beta 1	1426175_a_at	2.613	0.002	0	0	0	0	0	0	0	0	0	0	0	0	0	0	0	0	0	0	0
Pomc		18976	pro-opiomelanocortin-alpha	1455858_x_at	2.653	0.001	0	0	0	0	0	0	0	0	0	0	0	0	0	0	0	0	0	0	0